Influence of different subsidence-related drivers on damage to existing buildings

R.P. Meinen

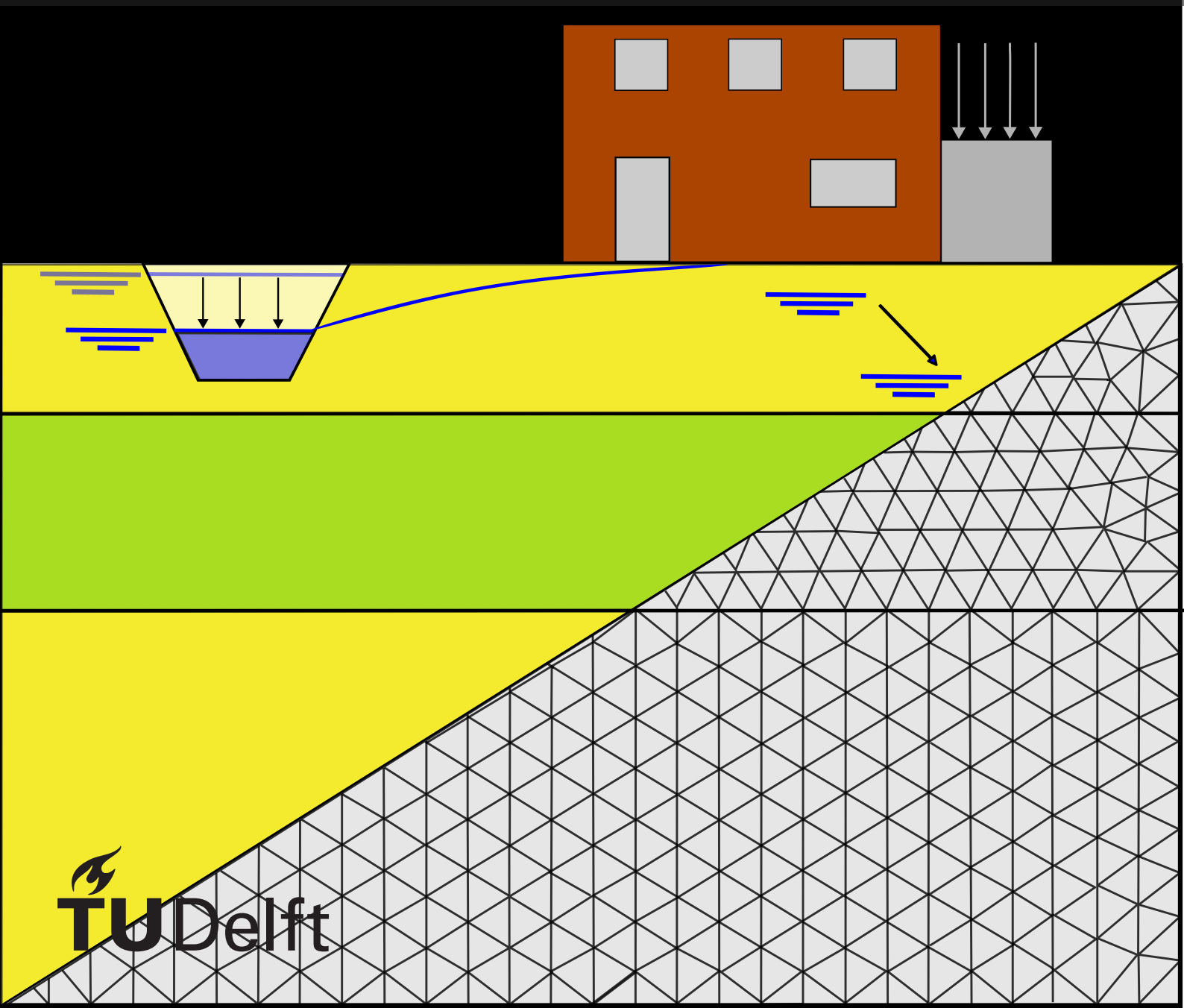

TU Delft

Influence of different subsidence-related drivers on damage to existing buildings

by

R.P. Meinen

Student Name	Student Number
R.P. Meinen	4259920

Committee members:	Dr. ir. M. Korff (chair)
	Dr. ir. R.B.J. Brinkgreve
	Ir. P.A. Korswagen
Supervisor:	A. Prosperi, MSc.
Project Duration:	November, 2023 - July, 2024
Faculty:	Faculty of Civil Engineering and Geosciences, Delft

TU Delft

Preface

With this thesis report, I will complete the master's program in Applied Earth Sciences with a specialization in Geo-Engineering at Delft University of Technology. This thesis bridges the disciplines of structural engineering and geo-engineering. I look forward to applying and further developing the knowledge gained in soil-structure interaction in my future career.

This achievement would not have been possible without assistance. Therefore, I extend my gratitude to my thesis committee for their advice and feedback. The discussions with the committee provided valuable insights that greatly facilitated the writing of my thesis. I am grateful for their willingness to participate on my graduation committee. I would like to express special thanks to Alfonso for the countless hours he dedicated to assisting me.

I would also like to thank my parents, friends and colleagues for their support and care throughout this entire period.

R.P. Meinen
Fluitenberg, July 2024

Summary

Subsidence is a significant geohazard affecting many areas globally, including the western part of the Netherlands. Subsidence is the lowering of the ground relative to the surface level, and it occurs both on the scale of a single structure and larger areas. The shallow subsurface in these areas, characterized by compressible soil, contributes to subsidence, which may be initiated or intensified by additional drivers. Subsidence can cause damage to buildings, leading to increased costs and social concerns.

In the current state of the art, less distinction is made regarding the difference in effects between different subsidence drivers. This study aims to provide insights into the relative influence of different drivers on the damage to existing buildings with a shallow foundation. More specifically, it aims to understand how various conditions and factors influence the damage parameters associated with soil deformation. This approach allows for analysing the interactions between the soil and the structure, ultimately contributing to a better understanding of the relative influence of the different drivers.

Numerical models in PLAXIS 2D have been carried out to compute settlements for various scenarios, involving different soil scenarios, building scenarios, and subsidence drivers. The primary emphasis of the numerical modelling lies on the soil rather than on the structure itself. Various damage parameters have been established based on the numerically calculated settlements. The purpose of this analysis is to determine the impact of settlements on the building based on these damage parameters.

Several aspects related to settlement occurrence and its impact on buildings were investigated. The study provides multiple outcomes regarding the interaction between soil scenarios, different drivers of subsidence, and the presence of an existing building with and without a partial basement. This was achieved by considering the influence of each of these variables on the damage parameters, with emphasis placed on the relative influence of the different drivers. The approach includes a method that compares the influence of the situation with the existing building and the situation without the existing building (greenfield situation). This comparison shows the settlement behaviour caused by the presence of the building load and its interaction with the soil.
Additionally, the combined effects of the soil scenarios, different drivers, and building scenarios on the resulting damage to an existing building are considered.

To conclude, for the soil scenarios considered in this study, the soil scenario with a weak spot (SS3) has the most unfavourable effect on an existing building. For the drivers considered in this study, when evaluating the relative influence of the different drivers, the global groundwater lowering (D2glo) has the most unfavourable effect. Considering the combined effect, the soil scenario exerts the greatest influence on the resulting damage parameters for the evaluated scenarios, followed by the type of driver and the building scenario.

Samenvatting

Bodemdaling is een significant risico dat veel gebieden wereldwijd treft, waaronder het westen van Nederland. Bodemdaling is het zakken van de grond ten opzichte van het maaiveld, en het vindt plaats op zowel de schaal van een enkel gebouw als grotere gebieden. De ondiepe ondergrond in deze gebieden, gekenmerkt door samendrukbare lagen, draagt bij aan bodemdaling, die kan worden geïnitieerd of verergerd door bijkomende factoren. Bodemdaling kan schade aan gebouwen veroorzaken, wat leidt tot hogere kosten en maatschappelijke onrust.

In de huidige stand van de techniek wordt er minder onderscheid gemaakt wat betreft het verschil in effecten tussen verschillende oorzaken van bodemdaling. Deze thesis heeft tot doel inzicht te geven in de relatieve invloed van verschillende verzakkingsoorzaken op de schade aan bestaande gebouwen met een ondiepe fundering. Meer specifiek geeft het inzicht hoe verschillende omstandigheden en factoren de schadeparameters, die verband houden met grondvervorming, beïnvloeden. Deze aanpak maakt het mogelijk de interacties tussen de bodem en het gebouw te analyseren, wat uiteindelijk bijdraagt aan een beter begrip van de relatieve invloed van de verschillende verzakkingsoorzaken.

Numerieke modellen in PLAXIS 2D zijn gebruikt om zettingen te berekenen voor verschillende scenario's, waarbij verschillende grondscenario's, gebouwscenario's en verzakkingsoorzaken van bodemdaling beschouwd zijn. De primaire focus van de numerieke modellering ligt op de grond in plaats van op het gebouw zelf. Op basis van de numeriek berekende zettingen zijn diverse schadeparameters bepaald. Het doel van deze analyse is om de invloed van de zettingen op het gebouw te bepalen op basis van deze schadeparameters.

Verschillende aspecten met betrekking tot het optreden van zettingen en de impact daarvan op gebouwen wordt onderzocht. De studie levert meerdere resultaten op over de interactie tussen grondscenario's, verschillende verzakkingsoorzaken van bodemdaling, en de aanwezigheid van een bestaand gebouw met en zonder een gedeeltelijke kelder. Dit wordt bereikt door de invloed van elk van deze variabelen op de schadeparameters te beschouwen, waarbij de nadruk wordt gelegd op de relatieve invloed van de verschillende verzakkingsoorzaken. De aanpak omvat een methode die de invloed vergelijkt van de situatie met het bestaande gebouw en de situatie zonder het bestaande gebouw. Deze vergelijking laat het zettingsgedrag zien veroorzaakt door de aanwezigheid van de gebouwbelasting en de interactie met de bodem. Daarnaast worden de gecombineerde effecten van de grondscenario's, verschillende verzakkingsoorzaken en gebouwscenario's op de resulterende schade aan een bestaand gebouw beschouwd.

Concluderend, voor de grondcenario's die in deze studie zijn beschouwd, heeft het grondscenario met een zwakke plek (SS3) het meest ongunstige effect op een bestaand gebouw. Voor de verzakkingsoorzaken die in deze studie zijn beschouwd, heeft de verlaging van de globale grondwaterstand (D2glo) het meest ongunstige effect bij het evalueren van de relatieve invloed van de verschillende verzakkingsoorzaken. Gezien het gecombineerde effect, heeft het grondscenario de grootste invloed op de resulterende schadeparameters voor de geëvalueerde scenario's, gevolgd door het type verzakkingsoorzaak en het gebouwscenario.

Contents

List of Figures

List of Tables

1 Introduction

1.1. Background Information

Land subsidence is a geohazard consisting in the lowering of the ground surface that affect many areas worldwide (Bagheri-Gavkosh et al., 2021). An example of an urbanized area subjected to subsidence is the western part of the Netherlands, where the subsurface is mainly characterized by peat and organic clay in the shallow subsurface (Koster et al., 2018). The shallow subsurface is the upper part of the Earth's surface, where most underground activities occur and where the buildings are located (Rosenbaum, 2003). These organic soil layers, mainly formed during the Holocene, are characterized by highly compressible deposits (Dufour and Burrough-Boenisch, 2000).

However, the presence of these highly compressible soil strata is not the only reason for subsidence (Bruna, 2020). For example, since the end of the ice-ages, tectonic subsidence has been occurring as a result of isostasy (Busschers et al., 2007). Another subsidence driver from the past is that peat has been extracted for centuries for fuel purposes (Dufour and Burrough-Boenisch, 2000).

In recent decades urban development, land use, prolonged dry periods, mining, hydrocarbon extraction and water level management have all contributed to past and future subsidence in the Netherlands (Costa et al., 2020). Lowering the groundwater level has been done primarily to protect against floods, cultivating farmland and allowing cattle to graze, which require additional measures such as dike construction and land reclamation, which further contributed to groundwater lowering (Dufour and Burrough-Boenisch, 2000).

At the scale of the single structure, heterogeneity in the soil can also influence the settlement due to subsidence processes (Prosperi, Korswagen, et al., 2023). The potential consequences of subsidence processes include damage to existing buildings. In the Netherlands, masonry is the most common material adopted in structural and non-structural elements of bridges, quay walls and houses (Lourenco, 1997). Particularly, the old masonry buildings hold significant cultural and historical value. Therefore, the damage that slowly accumulates on existing buildings due to subsidence processes leads to increased costs, social unease, and increasing attention (Costa et al., 2020)

A distinction can be made between buildings that are resting on shallow (i.e. strip/raft) and piled foundations (KCAF, 2022). Shallow foundations are directly affected by ground settlements, while piles are indirectly affected by an increase in negative skin friction (Fellenius and Eng, 1984) due to ground settlements and degradation process due to groundwater table lowering (Prosperi, Korswagen, et al., 2023).

It is crucial to understand the mechanisms behind soil subsidence, develop predictive models of subsidence, and formulate effective policies for mitigation and prevention. Armed with this knowledge, strategies can be adapted (Prosperi, Longo, et al., 2023). The current models for predicting damage are mainly based on the consequences of settlements. In the current state of the art, less distinction is made regarding the effects of different subsidence drivers.

In this study, a numerical comparative study of different subsidence drivers and their effect on existing buildings is carried out. In this study, the primary focus of the numerical modelling is on the soil rather than on the structure itself. The aim of this research is to provide insight into the relative influence of different subsidence drivers on the damage of existing buildings.

1.2. Problem statement

This study addresses the challenge of understanding the effects of soil subsidence on buildings. Due to different subsidence drivers, damage can occur to existing buildings. In the current state of the art, there has been less focus so far on comparing these different subsidence drivers.

Another issue is implementing these drivers in a numerical model that also include the presence of the structure. Including this soil-structure-interaction is necessary to analyse the damage response of the buildings.

1.3. Research objective and questions

This study aims to provide insights into the relative influence of different drivers on the damage to existing buildings with a shallow foundation. More specifically, it aims to understand how various conditions and factors influence the damage parameters associated with soil deformation. This approach allows for analysing the interactions between the soil and the structure, ultimately contributing to a better understanding of the relative influence of the different drivers.

1.3.1. Main Research Question

What is the relative influence of different subsidence-related drivers on damage to existing buildings on shallow foundations?

1.3.2. Research sub-questions

1. *What are the existing modelling strategies to compare the influence of different subsidence drivers?*
2. *Which are the most relevant subsidence drivers for urban areas in the Netherlands?*
3. *What are the causes of differential settlement?*
4. *Which are the most suitable modelling strategies to compute the settlement due to different subsidence drivers and their effect on existing buildings?*
5. *How can the damage response of existing buildings due to differential settlements be determined?*
6. *What is the impact of a partial basement under a building on the occurrence of differential settlement and the resulting damage?*

1.4. Research approach

In this section, a research approach is presented, aiming to ultimately address the research questions. The research aims to determine the relative influence of different subsidence drivers and their effects on existing buildings.

The methodology of this research consists of the following steps, see figure 1.1

- Literature review: Literature review of the different drivers of subsidence in the Netherlands. Besides that, literature of existing modelling strategies for these different subsidence drivers must be reviewed. In this regard, it is important to consider the advantages and disadvantages of the various strategies. Subsequently, a selection will be made of the different scenarios that will be further examined in the subsequent steps of the research.
- Modelling methodology: In this research, the numerical models will be built with PLAXIS. The different selected scenarios are applied in the numerical models. For the structure, a masonry building, a simplified representation will be modelled. In this regard, different modelling strategies are employed.
- Results/analysis: The calculated settlements are used to determine the damage parameters. Based on these damage parameters, the damage to the building for the different scenarios is assessed. Subsequently, the relative influence of the damage parameters is determined. The results are compared with the findings from the literature.
- Discussion: Discussion/evaluation of the research, including the limitations of the adopted procedure
- Conclusion: Conclusions are formulated.

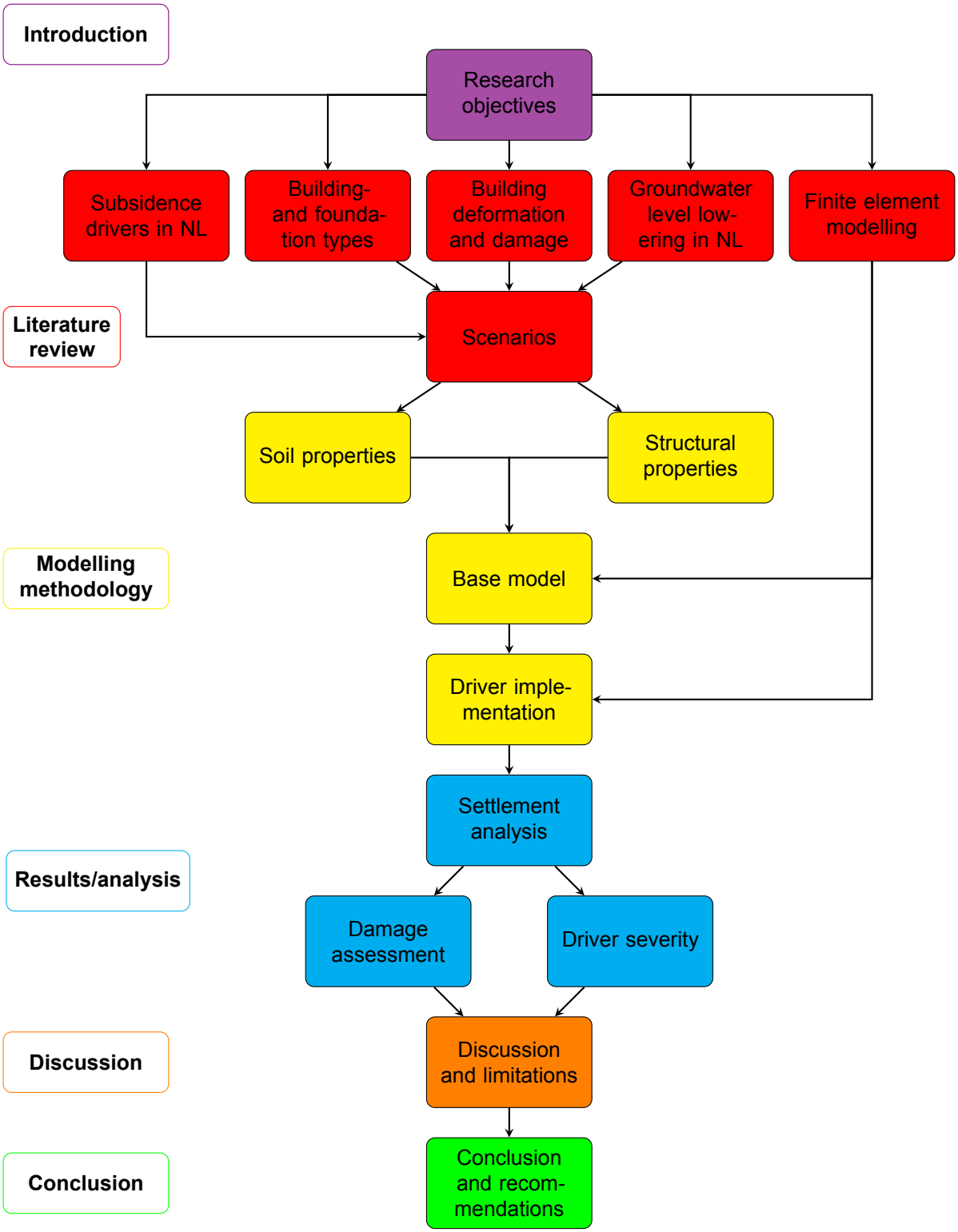

Figure 1.1: Flow diagram of the adopted procedure

2

Literature/Theoretical Framework

2.1. Subsidence drivers in the Netherlands

In figure 2.1, an overview of various natural and anthropogenic subsidence drivers is shown (Minderhoud et al., 2015). Numerous studies have already been conducted on structural damage resulting from subsidence in the Netherlands. A distinction can be made between studies that focus on the effect of deep (Rots et al., 2021; Figueroa-Miranda et al., 2018) and shallow subsidence sources (Giardina et al., 2013; Peduto et al., 2022; Zhou et al., 2011). However, not many of them have taken into account the effect of multiple overlapping drivers.

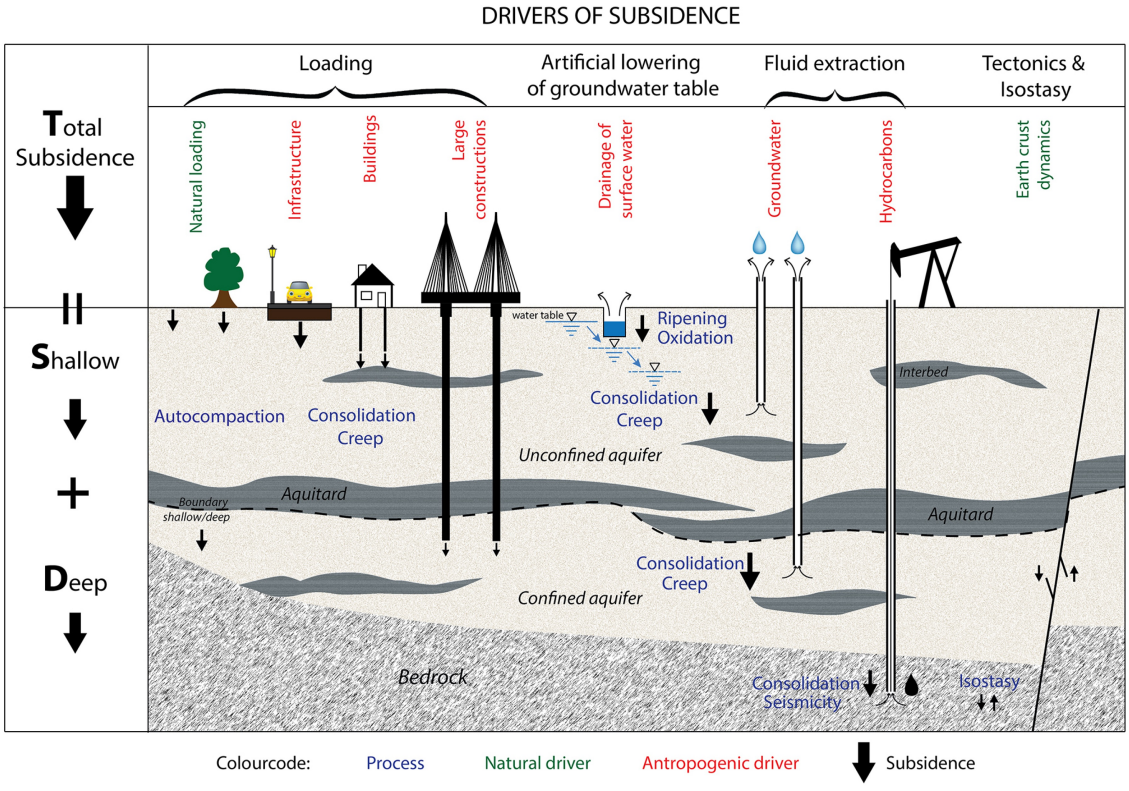

Figure 2.1: Illustration of subsidence drivers (Minderhoud et al., 2015)

In geotechnical engineering, the term subsidence generally refers to settlements resulting from one or multiple causes, such as indicated in figure 2.1 (Prosperi, Korswagen, et al., 2023).

Table 2.1 shows a list of all natural and anthropogenic drivers of subsidence, along with the scale, urban or rural, depth and their effect. In the following subsections, a brief description of each driver, and its effect is reported.

Driver	Scale	Area	Type	Depth	Effect
Groundwater absorption by tree roots	local	urban/ rural	natural	shallow	oxidation, consolidation, creep
Broken sewer system	local	urban/	anthropogenic	shallow	oxidation, consolidation, creep
Tunneling/Excavation (underground)	local	urban	anthropogenic	shallow	consolidation, creep, soil removal
Load of new infra/structures	local/ regional	urban	anthropogenic	shallow	consolidation, creep
Additional load due to renovation	local/ regional	urban	anthropogenic	shallow	consolidation, creep
Mining (salt/coal)	local/ regional	rural	anthropogenic	deep	removal of material/soil
Water level management	regional	urban/ rural	anthropogenic	shallow	oxidation, consolidation, creep
Seasonal groundwater level fluctuations	regional	urban/ rural	natural	shallow	consolidation, creep swell/shrink
Extraction of resources hydrocarbons/fluids	regional	urban/ rural	anthropogenic	deep	consolidation, creep, vibrations
Tectonics	national/ regional	urban/ rural	natural	deep	vibrations, isostasy
Climate change	national	urban/ rural	anthropogenic (natural)	shallow	oxidation, consolidation, creep

Scale: 'local' means at the location of a house or neighbourhood, 'regional' means an area with the size of a major Dutch city or province and in this case 'national' refers to the Netherlands
Depth: Shallow $<$ 50 m and Deep $>$ 50 m
(Busschers et al., 2007; Dufour and Burrough-Boenisch, 2000; Figueroa-Miranda et al., 2018; Minderhoud et al., 2015; Zhou et al., 2011)

Table 2.1: List of the natural and human drivers, sorted by their scale

Drivers

Different natural and anthropogenic drivers contribute to the overall subsidence, as described in the first section. Below a list is given of the main different drivers along with their corresponding explanations:

- **Groundwater absorption by tree roots:** In the Netherlands, detached houses are typically characterized by the presence of back gardens with trees. The roots of the trees can alter the water content of the soil significantly and then cause localized subsidence (Zhou et al., 2011).

- **Broken sewer system** Sewer pipes are rarely full of water. When a sewer pipe breaks, and it is below the groundwater level, groundwater can flow into the sewer pipe. This can result in a local drop in the groundwater level, which can lead to subsidence (KCAF, 2022)

- **Tunnel/excavation (underground)** During the drilling phase of the construction of tunnels, usually, more soil has been removed, which results that the volume of the final tunnel is less than the volume of the excavated area. Of course, measures are taken, however, it is unavoidable to prevent stress redistributions and movements in the soil due to the tunnel construction process. (Plaxis, 2023b).

- **Load of new infra/structures and/or additional load due to renovation/new stories** The applying of weight or additional weight can lead to various effects that cause subsidence (Lambe and Whitman, 1969).

- **Mining (salt/coal)** Subsidence due to mining is primarily caused by the underground removal of materials such as salt and coal. This can result in local subsidence with sinkholes and differential settlements (Bruna, 2020).

- **Water level management** Water level management in the Netherlands falls under the responsibility of the water boards (ten Brinke, 2016). Lowering the groundwater level has been done primarily to protect against water- related hazards, which required additional measures such as dike construction and land reclamation, which further contributed to groundwater lowering (Dufour and Burrough-Boenisch, 2000).

- **Seasonal groundwater level fluctuations** Due to seasonal groundwater fluctuations, it can dry out and then re-saturated again. This can result in the shrinking and swelling of expansive soil types (Blom et al., 2022).

- **Extraction of resources of hydrocarbons/fluids** When the cause of subsidence occurs at a depth of more than 400 meters, it is referred to as deep subsidence. This mainly concerns the extraction of gas and the mining of salt or coal. The extraction of hydrocarbons reduces the fluid pressure in rock formations, with subsidence as a result (Bruna, 2020).

- **Tectonics** Another form of deep subsidence is natural subsidence due to tectonic movements. Tectonic subsidence is primarily caused by extension. The Earth's crust stretches, resulting in various faulting systems, which in turn lead to subsidence (Bruna, 2020). Another form of natural subsidence is glacio-isostasy.

- **Climate change** Due to climate change, the Netherlands is experiencing more and more dry periods. This results in a declining groundwater level (Blom et al., 2022).

Effects

Below a list is given of various effects along with their corresponding explanations:

- **Consolidation:** As can be seen in table 2.1, there are several drivers leading to consolidation. In the case of a change in load in undrained soil (clay and peat), excess pore pressure occurs. This happens in a time period that is short compared to the dissipation time. When the loading is complete, water starts to flow by the consolidation and the soil will decrease in volume (Lambe and Whitman, 1969). Consolidation occurs not only under influence of a change in load but also due to other changing boundary conditions, such as groundwater table lowering (Verruijt, 2018) and water extraction from an aquifer (Figueroa-Miranda et al., 2018).

- **Creep:** Soft soil often undergoes deformations even when the load remains constant. This phenomenon is called creep. This shows ever-increasing settlements on buildings, even when all conditions remain the same (Verruijt, 2018).

- **Oxidation:** Soil containing organic matter, such as peat and humic clay, is susceptible to oxidation when it comes into contact with oxygen. When the groundwater level drops and oxygen reaches the organic material, this process begins. Oxidation results in disappearing of the soil, which can lead to subsidence (Zain, 2019; Koster et al., 2018).

- **Vibrations and isostasy:** In the context of tectonic movements and extraction of resources, vibrations can occur, which can lead to compaction and, consequently, subsidence (Bruna, 2020). In the Netherlands, the earth's crust is still adjusting the effects of last glacial cycle. During this period, the earth's crust in Scandinavia was compressed by the weight of the ice, causing a rise of the surface. Now that the ice is gone, Scandinavia is rising and the surface of the Netherlands is subsiding (Busschers et al., 2007).

- **Swell/shrink:** Soils absorbs water and loses water depending on the circumstances. Soils, which are susceptible to swelling and shrinking, compact as they dry and expand as they absorb water. This process occurs primarily in clayey soil types (Stewart et al., 2016). In many cases, this often results in a differential setting (Zhang and Briaud, 2015)

2.2. Groundwater

A change in the groundwater level is a significant driver of subsidence of the surface. In the Netherlands, the average groundwater level is relatively close to the surface level. However, there are several reasons that can cause a change in the water level (Dufour and Burrough-Boenisch, 2000). The groundwater situation in the Netherlands relies on factors like groundwater recharge, seepage, and extraction. The primary driver for recharge is the surplus precipitation, which is the difference between rainfall and evaporation. This means that the annual recharge is not only determined by precipitation but also by meteorological conditions such as temperature, wind, soil type, vegetation and the amount of sunshine. Besides this, the recharge is also, although to a lesser extent, influenced by infiltration of the rivers and (sub)surface underground drainage (Dufour and Burrough-Boenisch, 2000). The quantity of precipitation remains relatively consistent throughout the year, indicating a minimal seasonal precipitation pattern in the Netherlands. Nevertheless, local variations can lead to significant differences, resulting in local wet or dry conditions (Dufour and Burrough-Boenisch, 2000).

2.2.1. Seasonal fluctuation

Throughout the year, there is a seasonal variation in the groundwater level. Generally, there is a precipitation surplus during the winter months, September to March, and a precipitation deficit during the summer months, April to August (Dufour and Burrough-Boenisch, 2000).

Due to climate change, winters are becoming wetter while summers are getting drier, resulting in an increase in groundwater levels in wet periods and lower groundwater levels in dry periods. The lowering of the groundwater level in the summer is additionally intensified by the increase in average temperature (Dufour and Burrough-Boenisch, 2000).

2.2.2. Water level management

Some of the precipitation either flows off into surface water and eventually reaches the sea or evaporates. The rest penetrates into the ground, but a considerable portion ultimately finds its way into surface water through upward seepage, drainage, and water management to maintain the water levels at desired levels. There are numerous governmental organizations involved in regulating the groundwater levels, each with their own interests. Lowering the groundwater level has been done primarily to protect against floods, cultivating farmland and allowing cattle to graze, which require additional measures such as dike construction and land reclamation, which further contributed to groundwater lowering (Dufour and Burrough-Boenisch, 2000).

2.2.3. Local groundwater level lowering

In addition to the overall groundwater level, there can be a change in the groundwater level at a local level. For example, the rainfall in the summer will become briefer and more concentrated in specific areas, leading to an increase in localized heavy downpours, while others areas will stay relatively dry (Dufour and Burrough-Boenisch, 2000).

Besides this, the fluctuations of water levels of the main rivers, especially the Rhine, will increase. The reason for this is a decrease in the flow of meltwater from the Alps into the rivers, with as result that the contribution of rainfall become larger. This also results in lower river water levels during the summer. These changes in water levels affect the groundwater level, particularly impacting the areas around the major rivers (Dufour and Burrough-Boenisch, 2000).

Another factor that influence the local groundwater level is the absorption of water by tree roots. Quantifying the amount of groundwater that natural vegetation requires is challenging because most vegetation do not obtain water directly from an aquifer, but instead, they absorb water that seeps into the unsaturated zone (Dufour and Burrough-Boenisch, 2000). This does not mean that the absorption of water by the roots of trees has no effect on the subsurface. Especially in swelling and shrinking-sensitive clay layers, a change in moisture content can have significant consequences (Mercer et al., 2011)

2.3. Building- and foundation types

There are various foundation types in the Netherlands which are susceptible to settlement. A distinction can be made between wooden pile foundations and shallow foundations (KCAF, 2022), see figure 2.2.

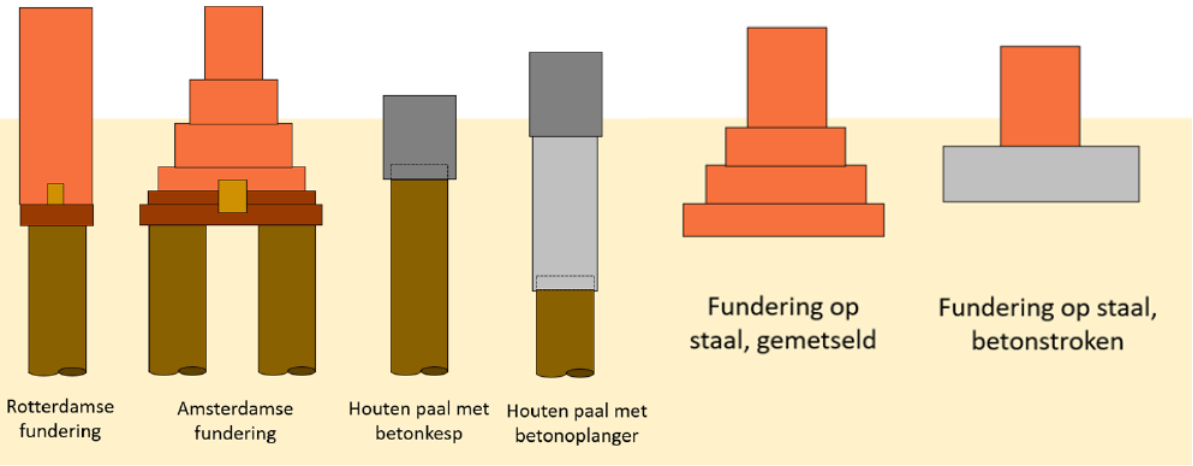

Figure 2.2: Foundation types in the Netherlands (KCAF, 2022)

The mechanism causing damage to a building differs between a wooden pile foundation and a shallow foundation. Wooden piles will decay when they are above the water level. This results in a reduction of the load-bearing capacity of the piles, potentially leading to damage.

Damage to shallow foundations occurs because weaker layers beneath the foundation may subside, causing differential settlement.

2.4. Building deformation and damage

Ground movements linked to subsidence can cause movements of structures. Various types of movements can occur that result in different forms of deformation of a building. In this case, various types of movements can occur that result in different forms of deformation of a building (Burland and Wroth, 1974; Prosperi, Korswagen, et al., 2023) In the list below and in figure 2.3, several definitions and symbols are provided for the deformation of foundations (Burland and Wroth, 1974; Prosperi, Korswagen, et al., 2023).

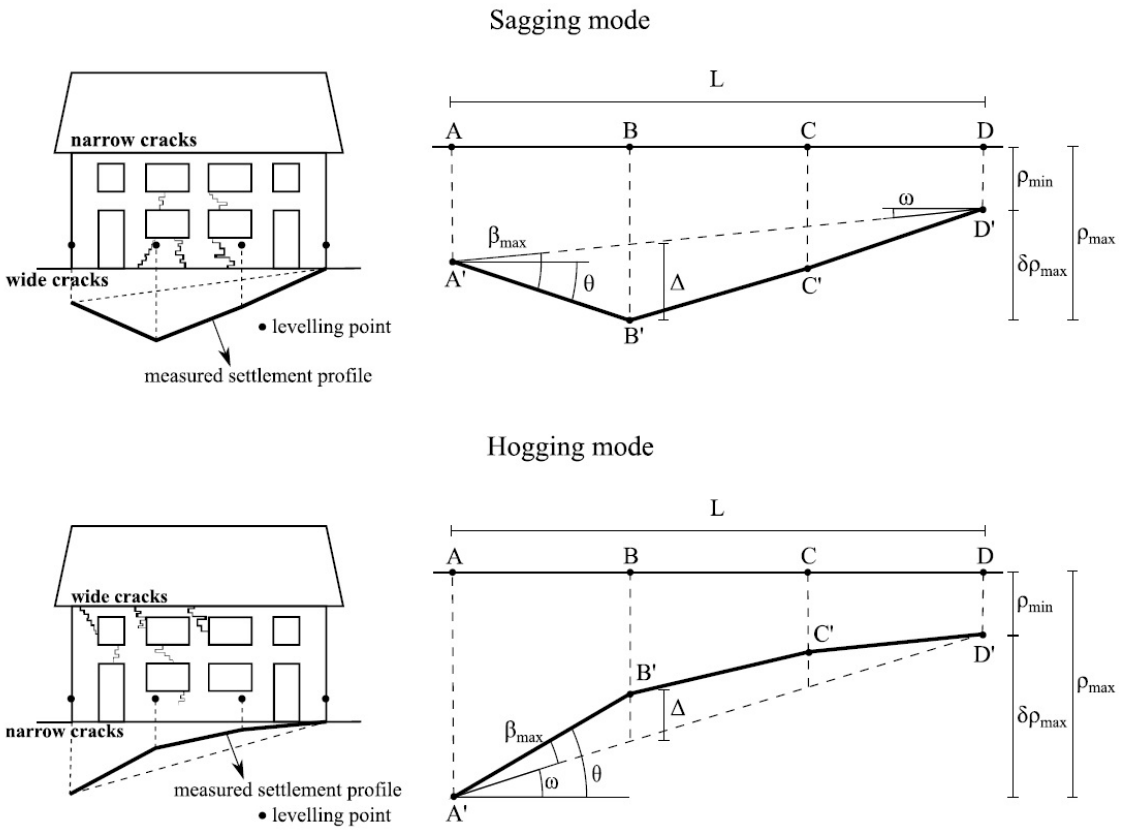

Figure 2.3: Definitions for the deformation of foundations
(Prosperi, Korswagen, et al., 2023)

Where the symbols can be described as follows according to Burland and Wroth, 1974; Prosperi, Korswagen, et al., 2023.

1. Settlement (ρ), heave (ρh).
2. Differential settlement ($\delta\rho$) and/or differential heave ($\delta\rho h$).
3. Rotation (θ) is the difference in the slope of the straight line of two reference points.
4. Tilt (ω) is the rotation of the whole structure.
5. Angular distortion (β) can be explained as the rotation of the straight line connecting two reference points relative to the tilt.
6. Deflection ratio (Δ/L) is defined as the relationship between the maximum relative deflection and the length of this.

Rotation and angular distortion have been identified as the most reliable predictors of building damage, followed by the deflection ratio and differential settlement. (Prosperi, Korswagen, et al., 2023).

These different movements can cause aesthetic or structural damage of varying severity. The damage response of masonry buildings is often classified according to the width of cracks in the brickwork (Prosperi, Korswagen, et al., 2023). The extent of damage to the building caused by settlement can be assessed using a damage classification (Boscardin and Cording, 1989), see figure 2.4.

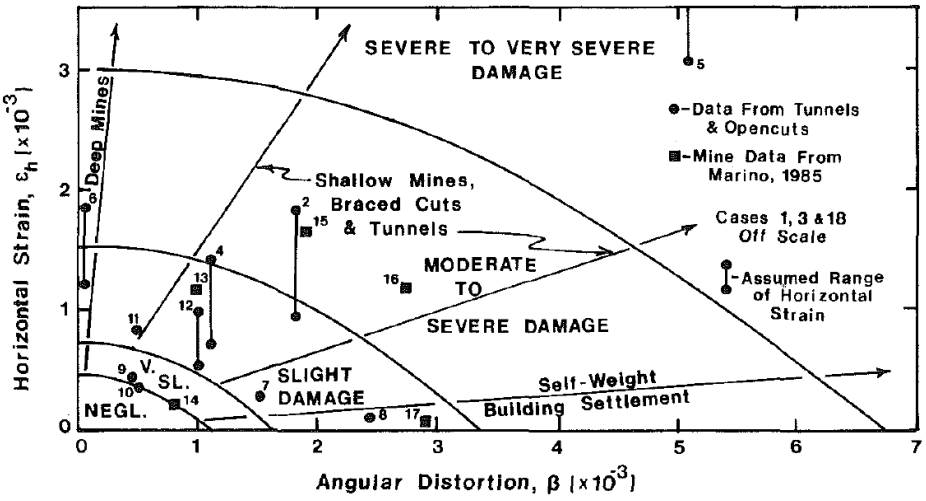

Figure 2.4: Angular distortion vs Horizontal strain (Boscardin and Cording, 1989)

Damage limits can be defined in terms of angular distortion as well as maximum and differential settlements. These allowable settlements and distortions can be used for design (Skempton and MacDonald, 1956).

2.5. Monitoring and predicting subsidence

The term 'settlement' refers to the vertical component of ground displacement, while deformation refers to movement of or within structures (Gaba et al., 2003) and is often used, in geotechnical jargon, as a synonym for 'subsidence'. In the Dutch context, several monitoring techniques and inspection methods are used to assess whenever a building is undergoing settlement and, in turn, to assess its deformation and the induced damage (KCAF, 2022).

2.5.1. Monitoring

The following list gives an overview of some monitoring methods:

- **Visual inspection:** A visual inspection provides an initial general indication of building deformation. During this inspection, visible aspects can be inventoried that indicate reduced foundation performance. An example is the presence of cracks in the walls and crooked window and door frames (KCAF, 2022).
- **Bed joint levelling measurements 'Lintvoegwaterpassing' in Dutch:** Bed joint leveling measurements enable tracking of the deformations of masonry buildings throughout their lifespan by measuring the horizontal displacement of points along the brickwork layers. This method allows reproduction of the settlement shape of a structure along its length due to settlements (Prosperi, Korswagen, et al., 2023; KCAF, 2022).
- **Floor levelling measurements 'Vloerwaterpassing' in Dutch:** Floor levelling measurements determine which floors reflect the original deformations. The measurement of floors should be carried out near the beam supports in a foundation wall with respect to a horizontal plane. This determines the established inclination of foundation walls (KCAF, 2022).
- **Plump levelling measurements 'Loodmeting' in Dutch:** The method determines the forward or backward tilting of the facade, measuring the inclination of a facade relative to the vertical (KCAF, 2022).
- **Traditional and innovative elevation measurements:** One way to determine the settlement of a building is to compare the historical construction level with the current construction level. If the historical construction level with respect to the NAP height is known, a global absolute settlement can be determined (KCAF, 2022). Fixed measurement points (such as stainless steel

measuring bolts bonded into facades) are surveyed in relation to reference measurement points (for example in nearby non-subsiding structures). Another way to monitor the elevation is through synthetic aperture radar (SAR). However, because this method has been relatively short-lived, the amount of available data is often limited to use for determining settlement over an extended period (Prosperi, Korswagen, et al., 2023).

2.5.2. Predicting subsidence

Cone penetration tests

As mentioned earlier, the soil composition is an important factor in predicting subsidence. For the most soils, cone penetration tests (CPT's) are the most convenient method to determine the soil stratigraphy at a specific location. It offers a continuous and precise digital cone resistance (q_s) and sleeve friction (f_s) profile. Based on this CPT data, an interpretation of soil type and its behavior can be determined (Robertson, 2009).

DINOloket is a database of the Dutch Geological Survey (Geologische Dienst Nederland). DINOloket provides data and data models of the subsurface of the Netherlands. Requesting and downloading this data, such as CPT data, is publicly accessible ("Geologische Dienst Nederland", 2024).

Hydrological data

Due to the significant diversity in underground characteristics, an extensive network of monitoring points is essential to collect the required groundwater data in the Netherlands. These networks contain data such as water table depth or groundwater hydraulic head and are recorded regularly. The geological survey of the Netherlands also manages these databases (Dufour and Burrough-Boenisch, 2000).

2.6. Finite element modelling

There are several ways to model the interaction between a structure and the soil in a numerical model. In this section, several methods are considered, with their advantages and disadvantages highlighted. Based on this, a modelling strategy can be selected.

2.6.1. Soil

Finite element modelling (FEM) can be used to create a numerical representation of the soil and its properties. By dividing the soil into a finite number of discrete elements, each with its own set of mechanical properties, FEM can simulate how the soil will respond to different loads and conditions. The model incorporates various soil parameters, such as elasticity, plasticity, and consolidation characteristics, to provide a realistic analysis of the soil behaviour (Plaxis, 2023a).

PLAXIS is a specialized finite element software designed to conduct deformation, stability, and flow analyses for a variety of geotechnical applications (Plaxis, 2023a).

The finite elements are usually composed of rectangles or triangles, with intersections called nodes. These different sections are known as elements, that divided the soil into small parts. These elements create a mesh, where the movement of the nodes in relation to each other defines the stress and strain conditions within each element based on the material properties. The soil's behaviour is nonlinear and can be characterized by selecting from various constitutive models, see section 2.7 (Plaxis, 2024).

2.6.2. Structure/building

The finite element method can also be used to model structures. Within PLAXIS 2D, there are two possibilities for this: using plate elements, when it is assumed that a beam represents the structure and using polygons (Plaxis, 2023a). Both methods are briefly explained below.

Plate elements

Plate elements are line elements that represent a beam. When the ratio between the bending stiffness and the axial stiffness changes, the thickness of the beam is automatically adjusted. An advantage of using plate elements in PLAXIS is the ease of generating results for the structural element. (Plaxis, 2023a).

Polygons

Another way to model a structure is by using polygons. A material model is then assigned to these polygons. The advantage of this approach is that it allows for the selection of more advanced material models, where the nonlinearity of the material is taken into consideration (Plaxis, 2024).

2.6.3. Soil Structure Interaction

In general, two methods can be distinguished in modelling the soil-structure interaction (SSI): the direct approach and the sub-structure approach (Longo et al., 2021, Bapir et al., 2023).

Substructure approach

In the substructure approach, the complete model consists of multiple submodels. Usually, this involves two models: a so-called superstructure (building) and the substructure (soil) (Longo et al., 2021). For the soil model, a linear material model is often assumed, which is a disadvantage. However, compared to the direct approach, the advantage of this method is that it requires relatively little computation time. Additionally, it has the practical benefit of being easily applicable (Longo et al., 2021, Bapir et al., 2023).

Direct approach

In the direct approach, both the soil and the building are integrated into a one model. The advantage of this is that non-linear soil models and more complex structures can be modelled together. The disadvantage is that more computation time is required (Bapir et al., 2023).

2.7. Constitutive models for soil

In the following subsections, the most common soil material models that can be used in PLAXIS 2D are described.

2.7.1. Soft Soil Model (SSM)

The Soft Soil Model (SSM) can be explained as a material model that is suitable for normally-consolidated soft soils. Figure 2.5 shows the failure envelope of the Soft Soil model. To avoid overestimation of the soil strength, because of a higher M-value, the Mohr-Coulomb failure envelope is added so that it can model dilatancy at failure. To give the model a minimum strength, the cohesion term is relatively small, which result in a small threshold ellipse (Brinkgreve, 2020).

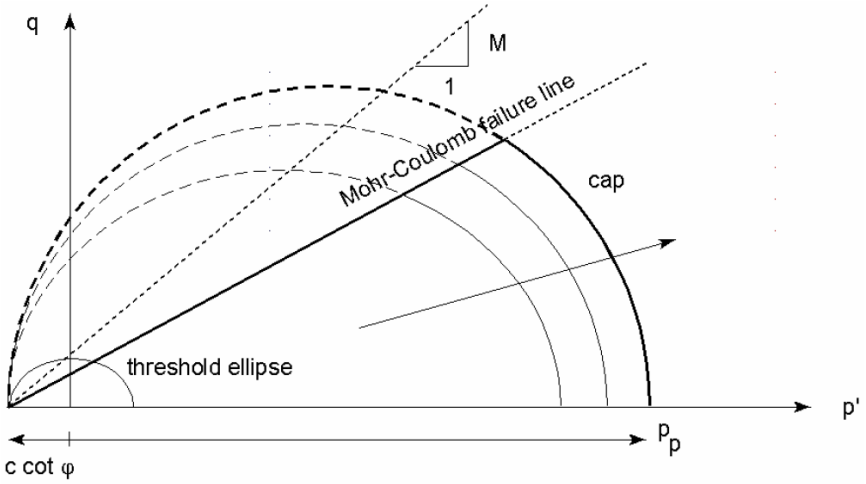

Figure 2.5: Visualisation of the failure envelope of the Soft Soil model (Brinkgreve, n.d.)

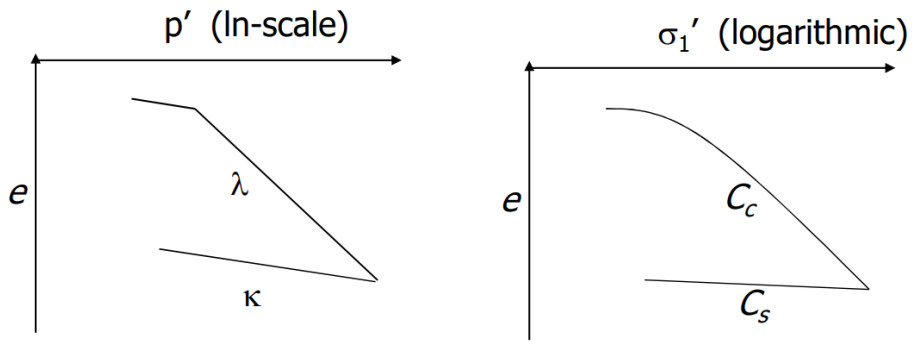

Figure 2.6: Difference between isotropic compression parameters of the Soft Soil Model (left) and compression parameters from consolidation test results (right) (Brinkgreve, 2020)

In table 2.2 the most important parameters are given for the Soft Soil Model. The compression parameters can be derived from consolidation tests, see figure 2.6.

Formulas 2.1 and 2.2 illustrates how the compression parameters (Bjerrum) from the NEN 9997-1 table 2b can be converted into the parameters λ^* and κ^*.

$$\lambda^* \approx \frac{C_c}{2.3(1+e)} \tag{2.1}$$

$$\kappa^* \approx \frac{C_s}{2.3(1+e)} \tag{2.2}$$

φ'	Friction angle
c'	Cohesion
Ψ	Dilatancy angle
λ^*	Modified compression index
κ^*	Modified swelling index
v_{ur}	Poisson's ratio for unloading / reloading
K_0^{NC}	Horizontal/vertical stress ratio in 1D compression
M	K_0^{NC} parameter

Table 2.2: SSM parameters

The following list outlines some possibilities and limitations (Brinkgreve, 2020).

Possibilities

- Better non-linear formulation of soft soil behaviour than the Mohr Coulomb model
- A distinction is made between primary loading and unloading / reloading
- Remembers the pre-consolidation stresses
- Stiffness parameters derived from consolidation tests
- Can be used for compressive stress paths

Limitations

- Only suitable for soft soils
- Creep is not considered
- Anisotropic behaviour is not considered
- Less suitable for non-compressive stress paths

2.7.2. Hardening Soil Model (HS)

The Hardening Soil model can be used as a non-linear model for both soft and stiff soils, and is depth-dependent. Two types of hardening are included in the model, namely compaction hardening, during primary compression, and shear hardening, during deviatoric loading.

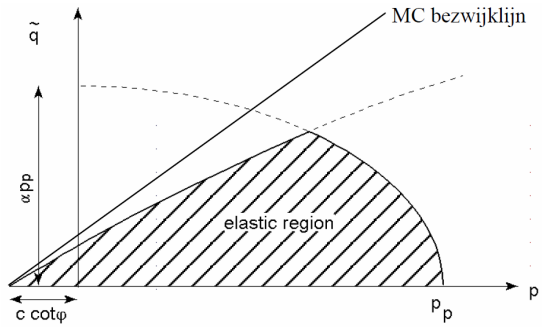

Figure 2.7: Visualisation of the failure envelope of the Hardening Soil model (Brinkgreve, n.d.)

Figures 2.8 and 2.9 shows how the Hardening Soil model stiffness parameters will be derived.

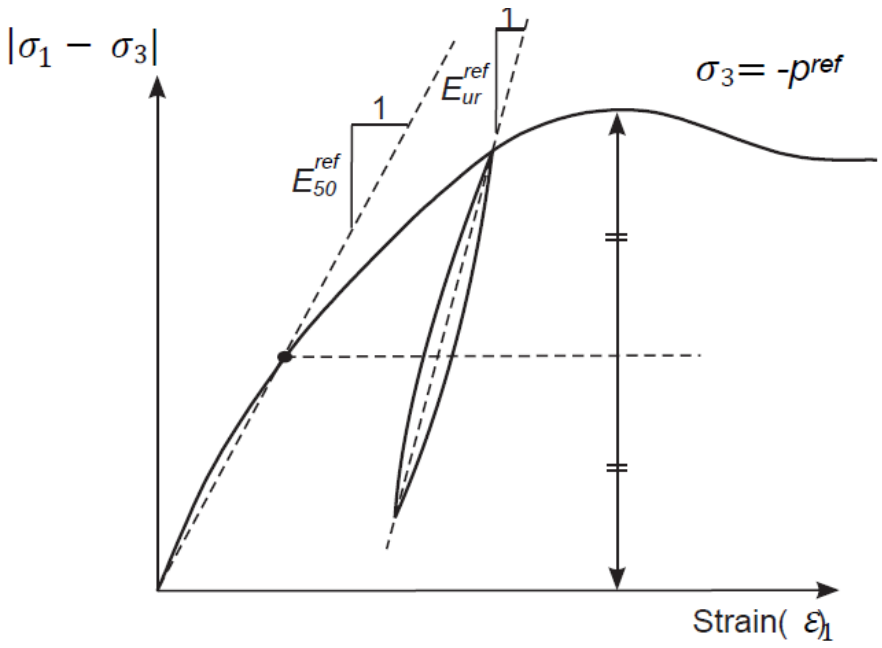

Figure 2.8: Definitions of HS parameters, triaxial test (Plaxis, 2024)

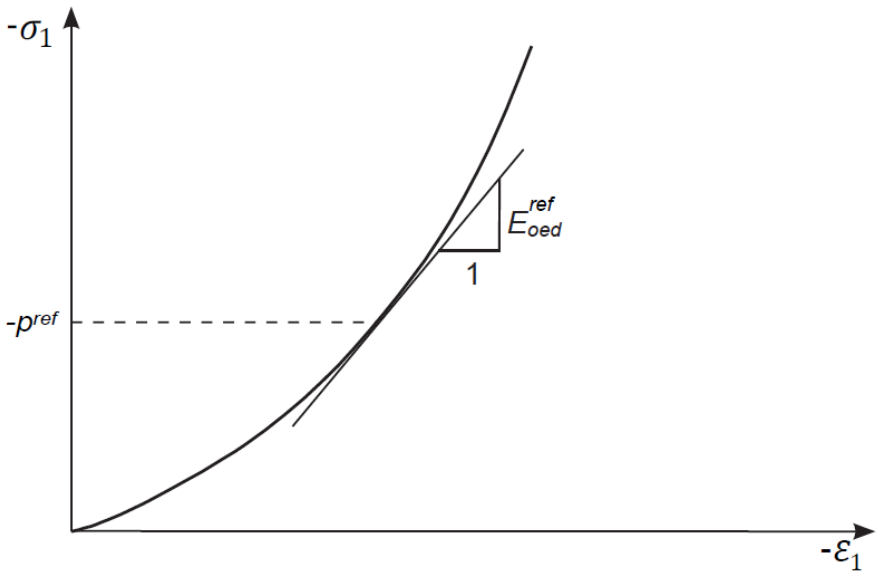

Figure 2.9: Definitions of HS parameters, oedometer test (Plaxis, 2024)

In table 2.3 the most important parameters are given for the Hardening Soil model.

φ'	Friction angle
c'	Cohesion
Ψ	Dilatancy angle
v_{ur}	Poisson's ratio in unloading / reloading
m	Rate of stress dependency in stiffness behaviour
p^{ref}	Reference pressure (100 kPa)
E_{50}^{ref}	Secant stiffness from triaxial test at reference pressure
E_{oed}^{ref}	Tangent stiffness from oedometer test at p^{ref}
E_{ur}^{ref}	Reference stiffness in unloading / reloading
K_0^{NC}	Horizontal/vertical stress ratio in 1D compression
R_f	Failure ratio q_f /$q_a$like in Duncan-Chang model

Table 2.3: HS parameters

The following list outlines some possibilities and limitations (Brinkgreve, 2020).

Possibilities

- Better non-linear formulation of soil behaviour than the Mohr Coulomb model
- A distinction is made between primary loading and unloading / reloading
- Remembers the pre-consolidation stress
- Other stiffnesses for other stress paths
- Well suited for excavations

Limitations

- No peak strength and softening
- Does not consider creep behaviour
- Anisotropic behaviour is not considered
- No accumulation of strain or pore pressure in cyclic loading
- Not suitable for very soft soils

2.7.3. Hardening Soil Small Strain Stiffness Model (HSS)

The main difference between the HS model and the HSS model is that the HSS model considers that at very small strains, the soil behaves very stiff.

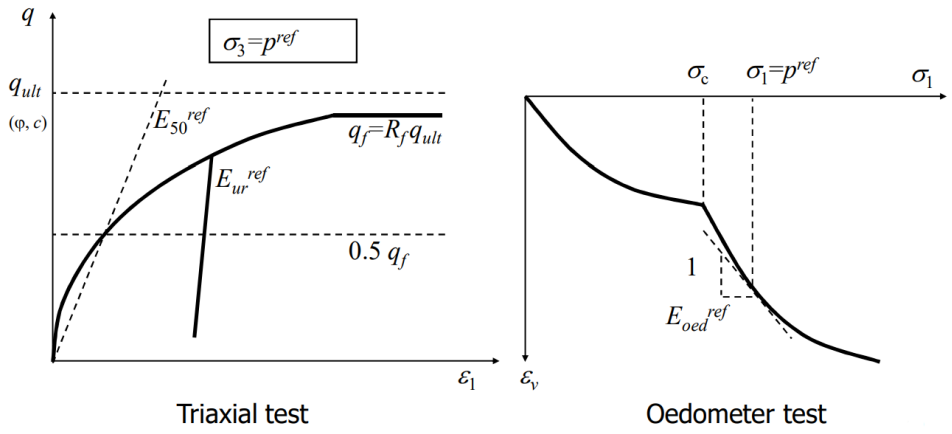

Figure 2.10: HSS stiffness parameters from a triaxial test (left) and a consolidation test (right) (Brinkgreve, 2020)

In table 2.4 the most important parameters are given for the Hardening Soil Small Strain Stiffness. It involves the Hardening Soil model except the additional small strain parameters G_0^{ref} and $\gamma_{0.7}$, see figure 2.11.

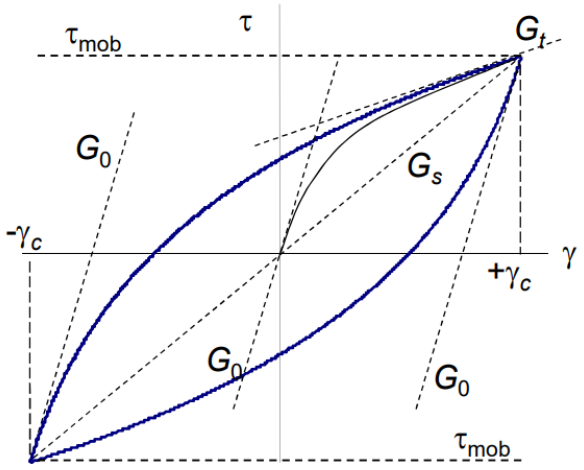

Figure 2.11: HSS stiffness parameters from a cyclic shear test (Brinkgreve, 2020)

φ'	Friction angle
c'	Cohesion
Ψ	Angle of dilatancy
v_{ur}	Poisson's ratio in unloading / reloading
m	Rate of stress dependency in stiffness behaviour
p^{ref}	Reference pressure (100 kPa)
E_{50}^{ref}	Secant stiffness from triaxial test at reference pressure
E_{oed}^{ref}	Tangent stiffness from oedometer test at p^{ref}
E_{ur}^{ref}	Reference stiffness in unloading / reloading
K_0^{NC}	Horizontal/vertical stress ratio in 1D compression
R_f	Failure ratio q_f /$q_a$like in Duncan-Chang model
G_0^{ref}	Reference shear stiffness at small strains
$\gamma_{0.7}$	Shear strain at which G has reduced to 0.7

Table 2.4: HSS parameters

The following list outlines some possibilities and limitations of HSS model (Brinkgreve, 2020).

Possibilities

- See HS model
- Large stiffness at small strain levels

Limitations

- No peak strength and softening
- Does not consider creep behaviour
- Anisotropic behaviour is not considered
- Not suitable for very soft soils

3

Modelling Methodology

This chapter focuses on all modelling aspects and how the different scenarios are represented in the model, including geotechnical properties, structural properties, and model setup.

3.1. Scenarios

This section describes how, based on chapter 2, various scenarios have been defined. First, an overview of several possible scenarios is provided. Then, a selection is made, supported by reasoning, of the scenarios considered in this study. This chapter is divided into the following sections:

- Soil scenarios
- Building scenarios
- Groundwater level scenarios
- Selected scenarios

The names for the different scenarios are indicated by a code name. The first part of the code name indicates the soil scenario, the second part the building scenario, and the last part indicates the driver that occurs. Example: SS1-B1-D1 means soil scenario 1, building scenario 1 and driver 1. The different scenarios with their corresponding code names are specified in upcoming subsections.

3.1.1. Soil scenarios

An initial analysis has been made of various soil profiles that commonly occur in areas affected by subsidence, resulting in damage to buildings. Soil profiles are available at DINOloket (https://www.dinoloket.nl/), which is a database of the Dutch geological institute (TNO Geologische Dienst Nederland).

Of course, the soil composition can consist of an infinite variety in the composition of the materials, but for the purpose of the model, the soil profile only distinguishes between weak soil, susceptible to settling, and strong soil, less susceptible to settling.

The soil profiles are divided in the following soil scenarios with:

- Horizontally oriented layers
- Inclined oriented layers
- Weak spots

A sketch of the different soil scenarios is depicted in figure 3.1

Left: horizontally oriented layers (SS1), Middle: inclined oriented layers (SS2), Right: weak spot (SS3), Green: weak soil, Yellow: strong soil

Figure 3.1: Soil scenarios: SS1, SS2 and SS3

Soil scenarios SS2 and SS3 are selected due to the contrast between the weak and strong soil layers when mirrored across the vertical axis. The expectation is that these soil scenarios are susceptible to differential settlement and the accompanying deformation of buildings under uniformly distributed loading. Scenario SS1 serves as a check where differential settlement is not expected to occur under uniformly distributed loading.

In reality, the composition of the soil consists of an infinite number of possibilities. The selected soil scenarios are a simplified representation of reality. The aim here is to reflect extreme situations, where both no differential settlement (SS1) and a relatively large amount of differential settlements (SS2) are expected. Additionally, a scenario has been selected in which a relatively high amount of distortion (SS3) is expected.

3.1.2. Building scenarios

It is expected that approximately 70 percent of all houses in the Netherlands have shallow foundations (Raad voor de leefomgeving en infrastructuur, 2024). So damage to buildings due to subsidence most commonly occurs at buildings with shallow foundations (Kok and Angelova, 2020), this study focuses on shallow foundations.

Two different building scenarios are considered in the initial situation in the models, namely a building without a basement and a building with a basement. Additionally, a building scenario is considered as a driver, which will be implemented as subsidence driver, see figure 3.2.

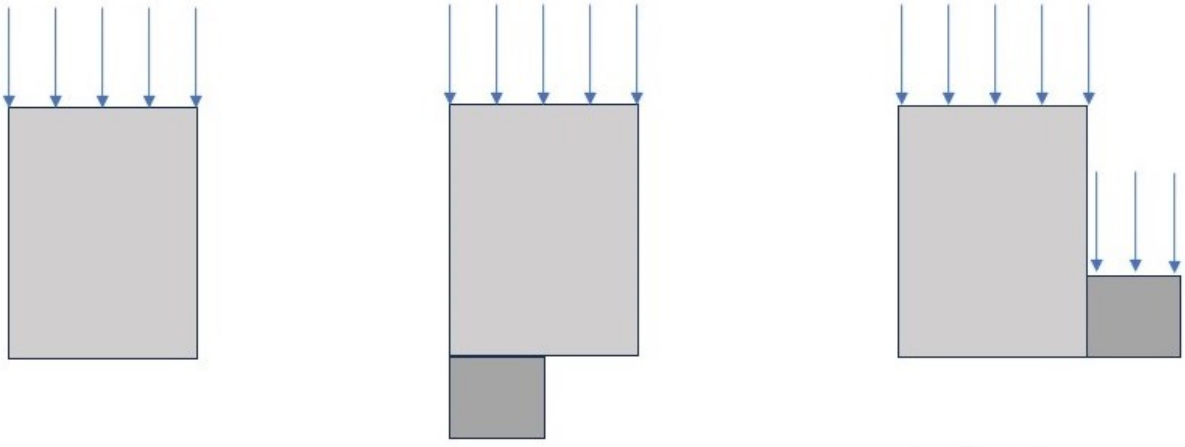

Left: existing building scenario (B1), Middle: existing building scenario with a basement (B2), Right: Scenario with an additional load next to an existing building as driver (D1)

Figure 3.2: Building scenarios: BS1, BS2 and D1

Building scenario B1 serves as an existing detached building. Additionally, an existing building with a basement has also been selected as a building scenario. The expectation is that the presence of a basement will influence the occurrence of differential settlement. Building scenario D1 serves as a subsidence driver. This driver is selected due to the frequent occurrence of adding an annex to an

existing building.

Most homes in the Netherlands consist of low-rise buildings (CBS, 2023), with masonry being a widely used building material for centuries (KNB, 2021). In this study, the modelled buildings aim to simulate low-rise, two-story masonry houses.

3.1.3. Groundwater level scenarios

Due to the increasing trend of dry periods in the Netherlands, (Dufour and Burrough-Boenisch, 2000), and the consequent rise in the number of subsidence-related damage cases, (Costa et al., 2020), various groundwater level scenarios have been considered in this study. The different groundwater level situations can be divided into the following scenarios:

- Global groundwater level lowering
- Local groundwater level lowering
- Groundwater level fluctuation

The effect of groundwater fluctuation is not considered in this study.

Water level management

Figure 3.3 and 3.4 shows the different groundwater level scenarios which are considered as drivers. The different water levels indicate the intensity of the driver. The lower the groundwater level, the higher the intensity of the respective driver.

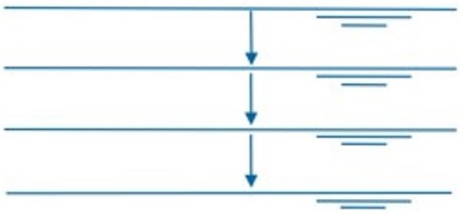

Figure 3.3: Groundwater level lowering D2glo

Driver D2glo has been selected due to the progressively lowering groundwater levels during dry periods in the Netherlands. Due to climate change, winters are becoming wetter while summers are getting drier, resulting in an increase in groundwater levels in wet periods and lower groundwater levels in dry periods. The lowering of the groundwater level in the summer is additionally intensified by the increase in average temperature (Dufour and Burrough-Boenisch, 2000). In settlement calculations, the lower the groundwater level, the more critical it is. The reduced groundwater level thus reflects the groundwater level after a dry summer.

Figure 3.4: Local groundwater level lowering D2loc

Additionally, a local groundwater level has been selected as a driver due to the local variations in groundwater levels. For example, the rainfall in the summer will become briefer and more concentrated in specific areas, leading to an increase in localized heavy downpours, while others areas will stay relatively dry (Dufour and Burrough-Boenisch, 2000). Besides this, the fluctuations of water levels of the main rivers, especially the Rhine, will increase. The reason for this is a decrease in the flow of meltwater from the Alps into the rivers, with as result that the contribution of rainfall become larger. This also results in lower river water levels during the summer. These changes in water levels affect

the groundwater level, particularly impacting the areas around the major rivers (Dufour and Burrough-Boenisch, 2000).

A local groundwater level decrease can also be caused by water absorption by tree roots. Figure 3.5 shows an example of groundwater level lowering due to the absorption of tree roots. Most vegetation do not obtain water directly from an aquifer, but instead, they absorb water that seeps into the unsaturated zone (Dufour and Burrough-Boenisch, 2000). This does not mean that the absorption of water by the roots of trees has no effect on the subsurface. Especially in swelling and shrinking sensitive clay layers, a change in moisture content can have significant consequences (Mercer et al., 2011).

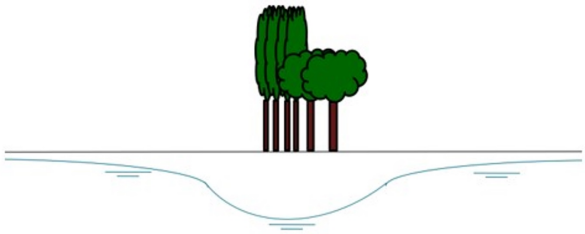

Figure 3.5: Local groundwater level lowering due to tree root absorption (D3t)

In this study, the local water level lowering caused by a waterway and by water absorption from tree roots is considered the same. Henceforth, this driver will be referred to as local groundwater level lowering (D2loc) in the remainder of this report.

3.1.4. Selected Scenarios

This section gives an overview of the selected scenarios. The illustrations below provide a general overview of how the scenarios are modeled and are not drawn to scale. Specific dimensions will be provided later in this chapter.

Base Models

Figure 3.6 illustrates the combination of the soil scenarios and the building scenarios that serve as base models. The basic models consist of soil models with horizontal layering (SS1), inclined layering (SS2), and a weak spot (SS3). Variations include a building without a basement (B1) and a building with a basement (B2).

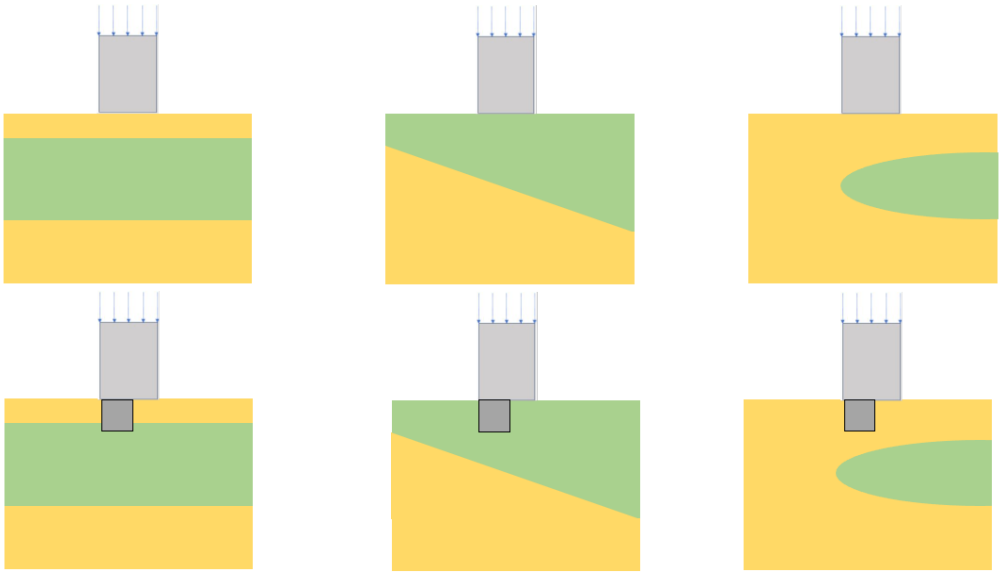

Figure 3.6: Base model for the different scenarios, the building and the soil model, are not drawn to scale.

Driver implementation

Figures 3.7, 3.8 and 3.9 represent the implementation of the different drivers in the base model. Table 3.1.4 gives an overview of combinations of the different scenarios with the corresponding names.

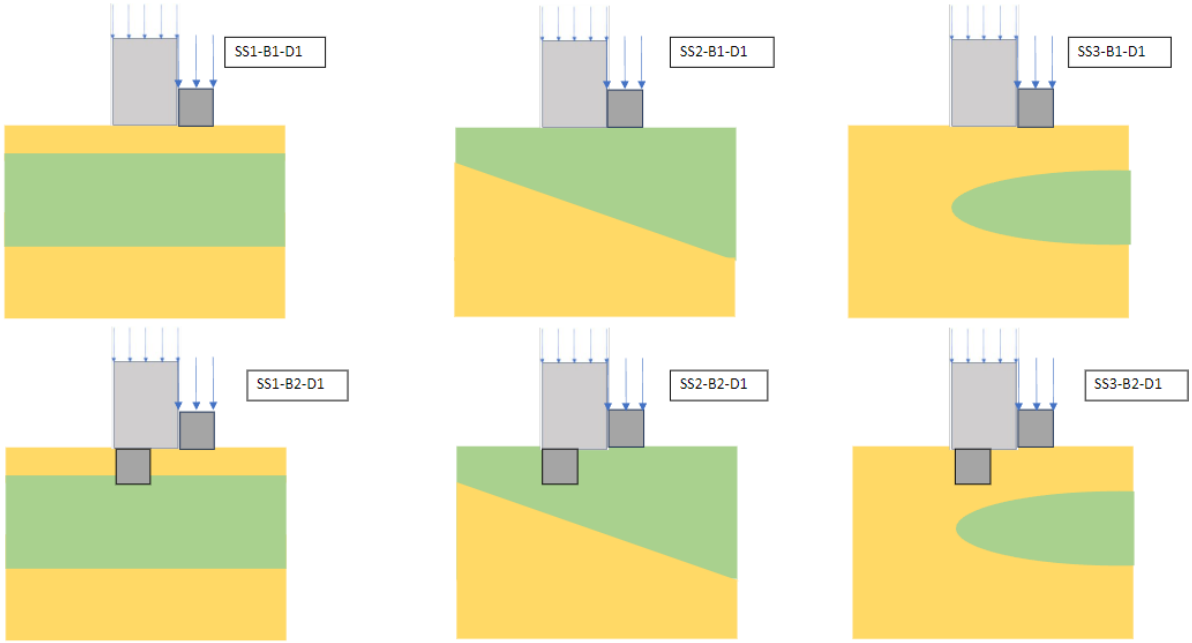

Figure 3.7: Scenarios with an additional load as driver, the building, the driver and the soil model are not drawn to scale.

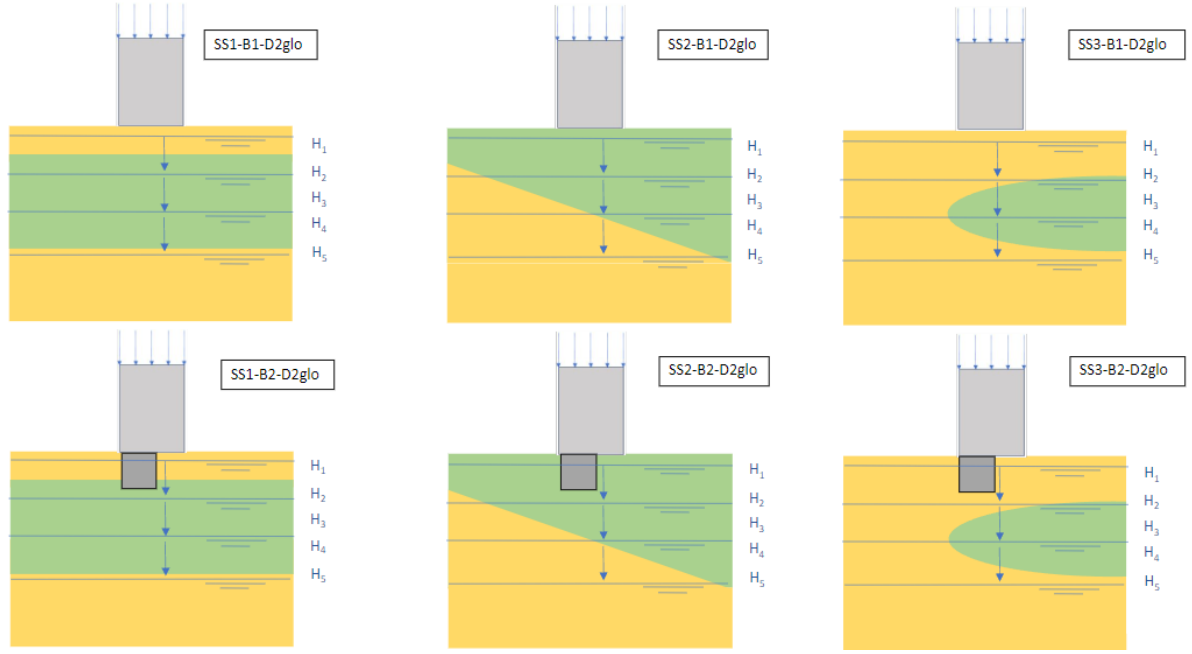

Figure 3.8: Scenarios with water level management as driver: groundwater level lowering. The building, the driver and the soil model are not drawn to scale.

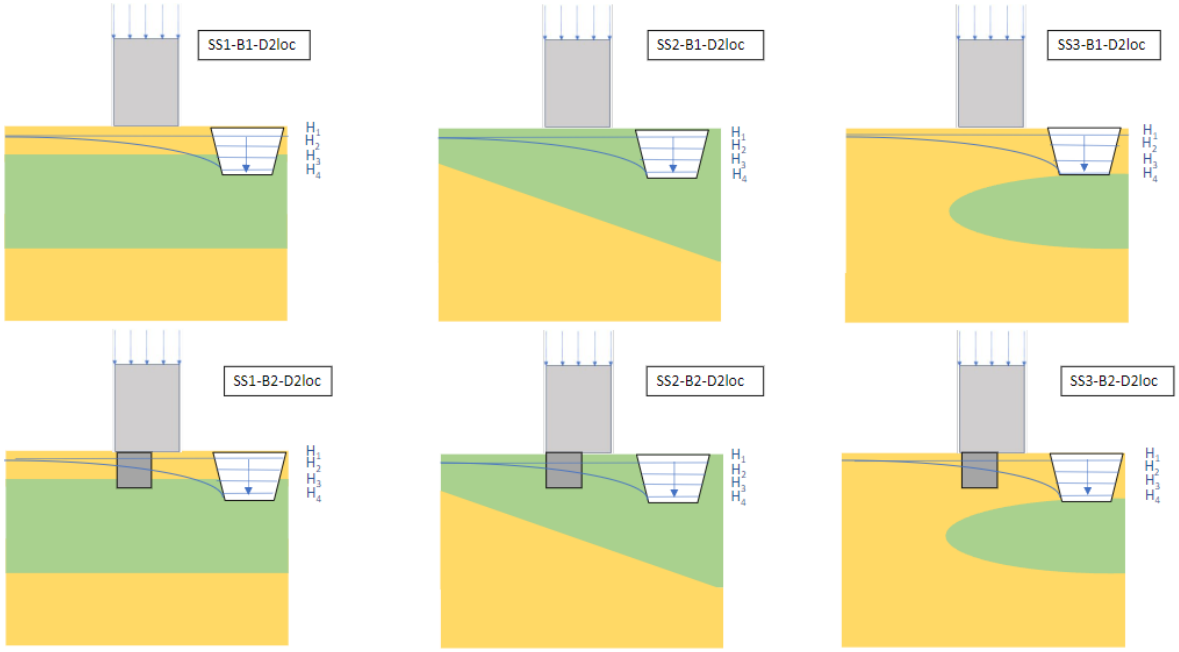

Figure 3.9: Scenarios with water level management as driver: local groundwater level lowering. The building, the driver and the soil model are not drawn to scale.

Table 3.1: An overview of the selected scenarios

Soil scenario	Building scenario	Driver
SS1	B1	D1
SS2		
SS3		
SS1	B2	
SS2		
SS3		
SS1	B1	D2glo
SS2		
SS3		
SS1	B2	
SS2		
SS3		
SS1	B1	D2loc
SS2		
SS3		
SS1	B2	
SS2		
SS3		

3.1.5. Settlement response hypotheses

In this section, expectations regarding the settlements of various variables that may influence differential settlements are discussed. Figure 3.10 presents the expectations based on the soil scenarios, figure 3.11 presents the expectations based on the different implemented drivers, and figure 3.12 presents the expectations of the various building scenarios.

The expectations for the soil scenarios are based on a uniformly distributed load. For soil scenario SS1, only uniform settlement of the building is expected. The most differential settlement is expected for soil scenario SS2, but the most distortion is expected for soil scenario SS3 due to the soil's heterogeneous nature. For soil scenario SS2, less distortion is expected than in soil scenario SS3 because the building in the case of soil scenario SS2 is relatively stiff compared to the soil.

The existing building in figure 3.11 is shown to clarify the nature of the different drivers. For drivers D1 and D2loc, distortion of the existing building is expected due to the nature of the driver. For driver D2glo, no differential settlement of the existing building is expected.

Based on the building scenarios, differential settlement and distortion are expected only in the case of the presence of a partial basement (B2).

When the different variables that can cause differential settlement are combined, the most differential settlement is expected in scenario SS2-B2-D2loc. The most distortion is expected in scenario SS3-B2-D2loc. Additionally, it is expected that the influence of the soil is the greatest in the occurrence of differential settlements, followed by the driver and the building scenario.

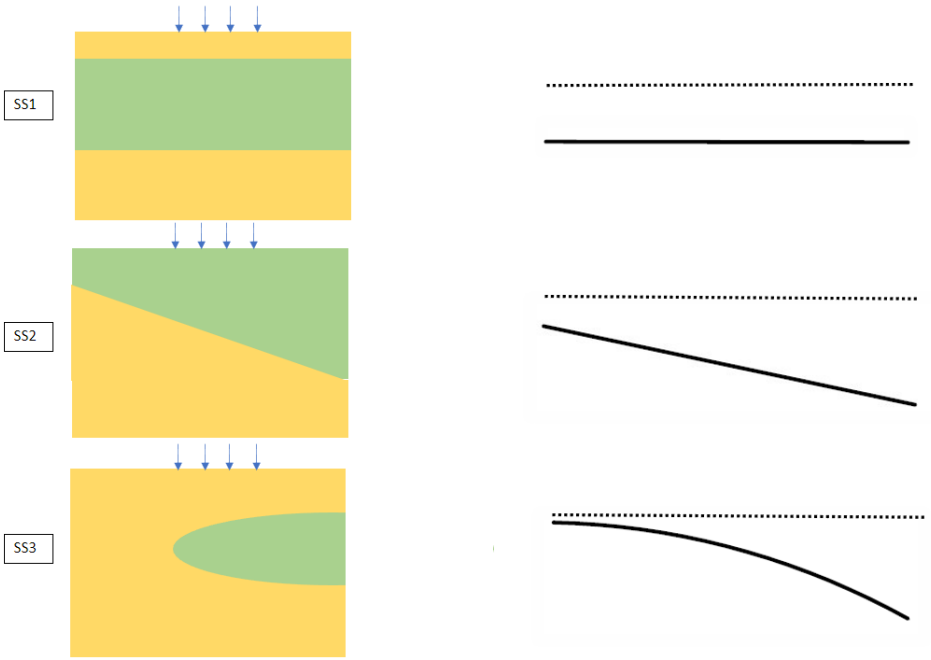

Figure 3.10: The expected deformation of the existing building based on the different soil scenarios under a uniform load. The black dotted line represents the original shape of the bottom edge of the building, and the thick solid black line represents the expect deformation of the building

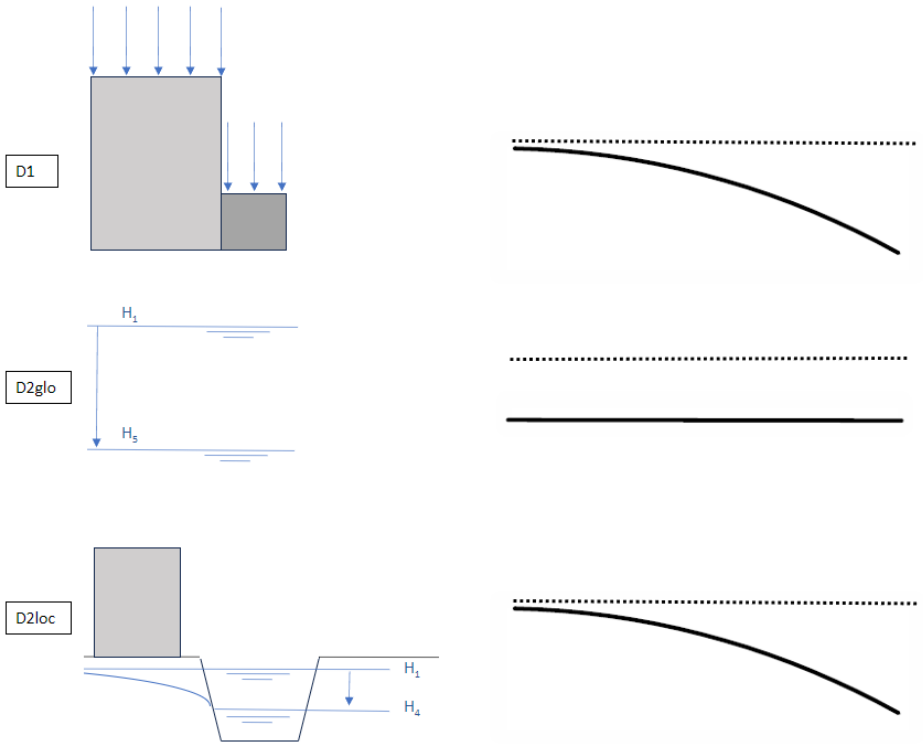

Figure 3.11: The expected deformation of the existing building as a result of implementing the different drivers. The black dotted line represents the original shape of the bottom edge of the building, and the thick solid black line represents the expect deformation of the building.

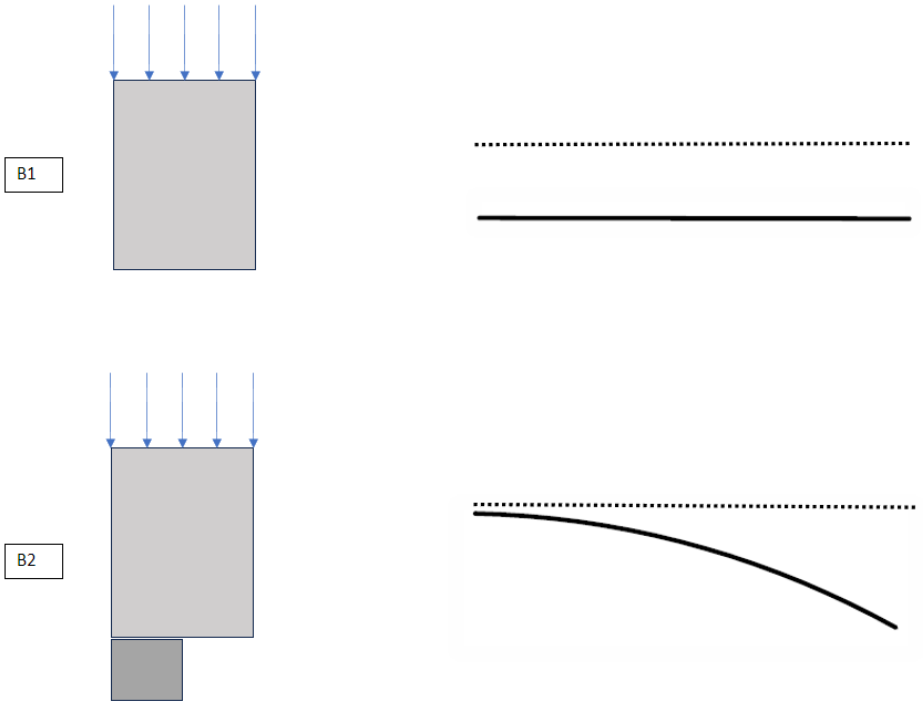

Figure 3.12: The expected deformation of the existing building based on the different building scenarios. The black dotted line represents the original shape of the bottom edge of the building, and the thick solid black line represents the expect deformation of the building

3.2. Geotechnical Properties

This section focuses on all soil properties, and it will show which parameters are used in the PLAXIS models. In the PLAXIS models, a distinction is made between strong soil and weak soil. Here, sand is considered as strong soil and clay is considered as weak soil.

In this study, it has been chosen to use the Hardening Soil Small Strain Stiffness model model for a strong soil and Soft Soil model for a weak soil.

3.2.1. Soil properties

The tables below show the parameters used in the models. Moderate clay and moderate sand have been selected as the basis for soil properties to use an average value.

Soil	γ_{dry}	γ_{sat}	E'	φ'	c'	c_u	k	$C_c/(1+e_0$	$C_{sw}/(1+e_0$	C_α
	[kN/m^3]	[kN/m^3]	[MPa]	[°]	[kPa]	[kPa]	[m/s]	[-]	[-]	[-]
Moderate clay	17	17	2	17.5	5	50	0.0001	0.1533	0.0511	0.0061
Moderate sand	18	20	45	32.5	0	-	1.0	0.0038	0.0013	0

Table 3.2: Physical and mechanical (model) parameters from Dutch standards, NEN 9997-1+C2

The Soft Soil model has been chosen as the material model for the weak soil. The Soft Soil model is considered a suitable model for simulating normally consolidated soft soil (Plaxis, 2024).

Soil	λ^*	κ^*	Ψ	OCR
	[-]	[-]	[°]	[-]
Moderate clay	0.1069	0.02911	0	1.3

Table 3.3: Additional model parameters: Soft Soil model

The Hardening Soil Small Strain Stiffness model has been selected as the material model for the strong soil. The HSSmall is considered a suitable model for strong soils like sand (Plaxis, 2024).

Soil	E_{50}^{ref}	E_{oed}^{ref}	E_{ur}^{ref}	$\gamma_{0.7}$	G_0^{ref}	Ψ	OCR
	[kPa]	[kPa]	[kPa]	[-]	[kPa]	[°]	[-]
Moderate sand	35000	35000	100000	0.00013	122600	2.5	1.0

Table 3.4: Additional model parameters: HSSmall model

3.2.2. Water levels

Initial groundwater level

In most parts of the Netherlands, the groundwater level is relatively close to the surface, < 4 m below surface (Dufour and Burrough-Boenisch, 2000). The initial groundwater level is set at 0.8 meters below the ground surface. This is at the same level as the bottom of the foundation and is considered a realistic level. This initial groundwater level is applied to all modelled scenarios.

Groundwater level variations

To consider the effect of groundwater level lowering, the level was gradually lowered step by step.

	Surface level [m + NAP]	**Water level [m + NAP]**
H1 (initial)	0	-0.8
H2	0	-2.8
H3	0	-3.8
H4	0	-4.8
H5	0	-5.8

Table 3.5: Water levels driver D2glo

	Surface level [m + NAP]	Water level [m + NAP]	Distance from building [m]]
H1 (initial)	0	-0.8	5
H2	0	-3.8	5
H3	0	-4.8	5
H4	0	-5.8	5

Table 3.6: Water levels driver D2loc

These variations have been applied to the scenarios with global groundwater level lowering, driver D2glo and a local groundwater level lowering, driver D2loc. For driver D1, only the initial groundwater level is applied.

3.3. Structural Properties

This section describes the material properties of the building and how it is implemented in the numerical models. The structural elements consist of a building, with and without a basement, an annex and the interfaces. It is considered that these elements are situated on shallow foundations. The building, annex and basement are modelled as plate elements in PLAXIS. The used properties are described in the following subsections.

3.3.1. Building dimensions

In figures 3.13-3.16, the dimensions of the different used structural elements of the building for the various scenarios are presented.

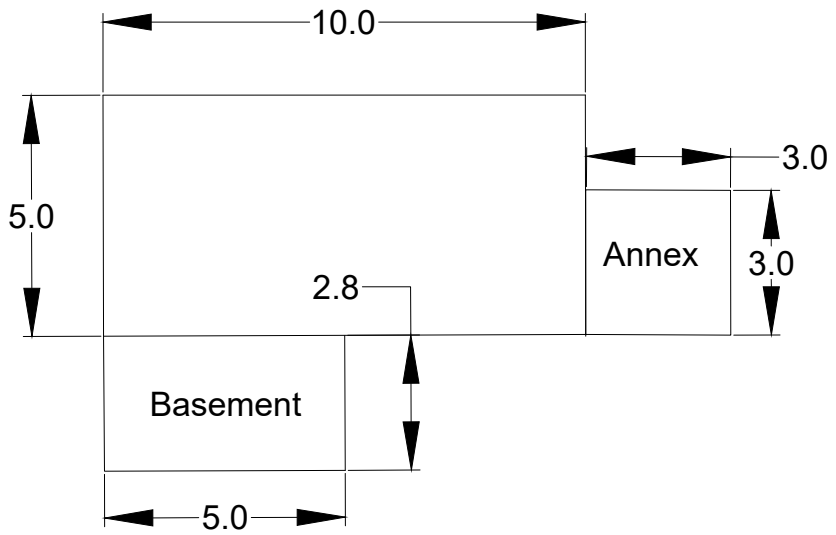

Figure 3.13: Building dimensions in [m]

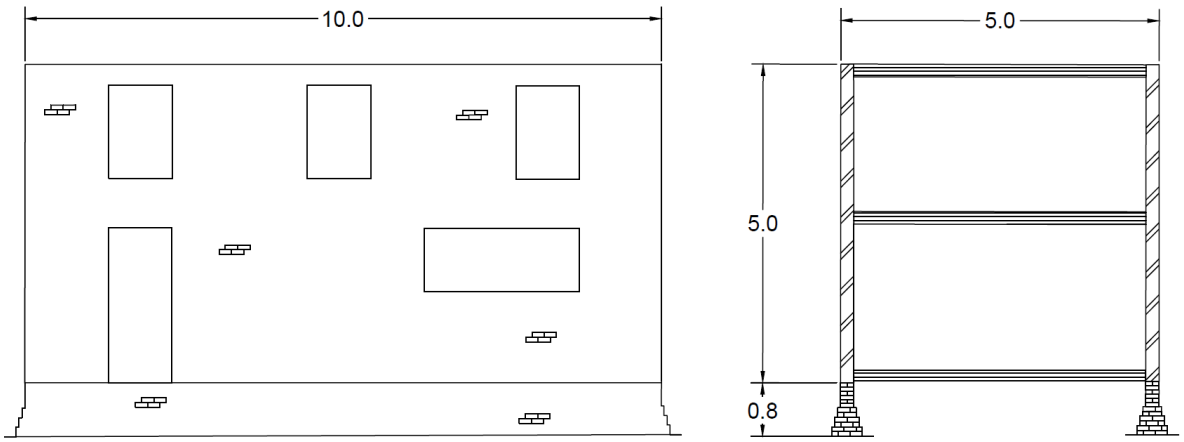

Figure 3.14: Geometry of the different elements of the existing building in [m]

The walls of the existing building consist of masonry and have a thickness of 0.21 meters, which are resting on a masonry strip foundation. The assumption has been made that the modelled building has a stepped brick footing as foundation base, see figure 3.16. Besides this, the building has three wooden floors. It is assumed that the facade contains a relatively large number of openings(> 25%), see figure 3.14.

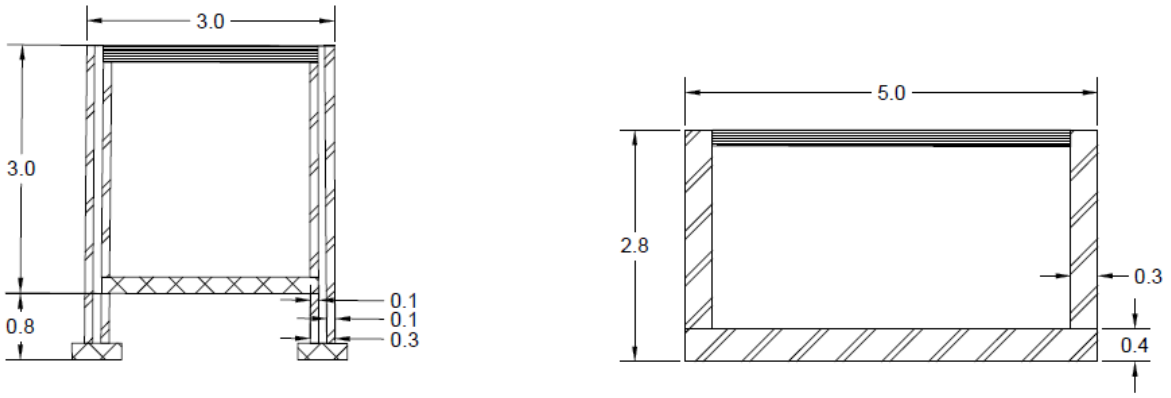

Figure 3.15: Geometry of the annex (left) and the basement (right) in [m]

The annex consists of cavity walls with a thickness 0,3 m (two times a wall with a thickness of 0.1 m and a cavity of also 0.1 m). In contrast to the existing building, the annex is founded on a concrete strip foundation. The annex is relatively new compared to the existing building, and therefore it has a concrete foundation base (0,6 m x 0.2 m), see figure 3.15. The first floor is made of concrete, and the flat roof is made of wood, see figure 3.15.

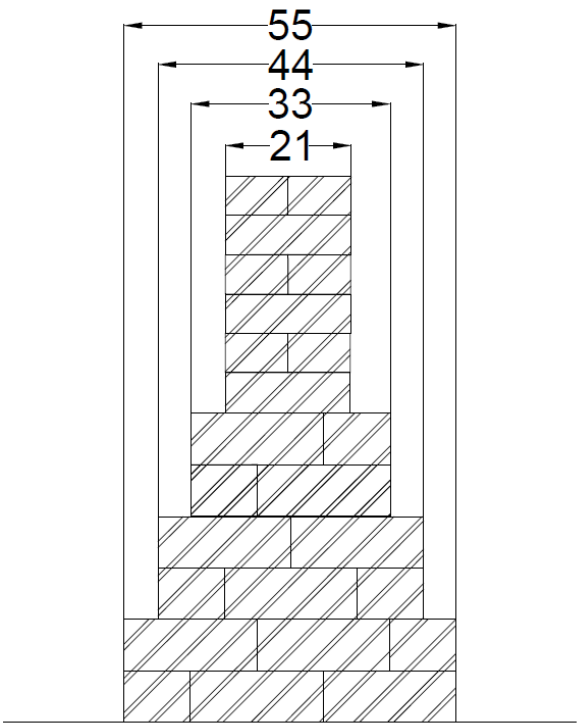

Figure 3.16: Stepped brick footing, dimensions in [cm]

3.3.2. Material properties for the building

The used material properties for the building are shown in table 3.7.

Material properties	**Young's modulus**, E $[MPa]$	**Mass density**, ρ $[kg/m^3]$
Masonry	6000	19
Concrete	32000	24
Wood	11000	6

Table 3.7: Material properties for the building

3.3.3. Building weight

The weight of the building is modelled by applying a line load on the plate elements. The different elements of the building are presented in figures 3.14-3.16 and the total weight of the building is presented in table 3.8. The calculation is shown in Appendix A.2.1.

Description	**Value**
Height building	5.0 m
Width building	10.0 m
No. of storeys	1 masonry strip foundation, 3 wooden floors/roof
Foundation	Masonry strip foundation 0.80 m high
Walls	Masonry walls with a thickness of 0.21 m
Weight building	22.6 $kN/m/m$

Table 3.8: Calculated weight of the building without basement

The different elements of the annex and the total weight of the annex are presented in table 3.9

Description	Value
Height building	3 m
Width building	3 m
No. of storeys	1 concrete strip foundation,1 concrete floor, 1 wooden floor/roof
Foundation	Concrete strip with a thickness of 0.20 m and a width of 0.60 m
Walls	Masonry cavity(0,1 m) walls (2 times 0.10 m) with a thickness of 0.30 m
Weight building	20.0 $kN/m/m$

Table 3.9: Calculated weight of the annex

To consider the influence of the driver, variations in the intensity of the driver need to be made, as was also done for drivers D2glo and D2loc by varying the water level, see table 3.5 and 3.6. Table 3.10 shows the variations in the amount of load applied to the annex.

Variation	Weight of the annex, driver D1 [$kN/m/m$]
Construction phase 1 (load 1)	16.4
Construction phase 2 (load 2)	18.2
Final phase (load 3)	20.0

Table 3.10: Annex weight, driver D1, variation

The weight of the basement is not considered. The weight of the removed material exceeds that of the basement.

3.3.4. Building stiffness

The bending stiffness EI for a foundation can be calculated using formula A.1 in which the Young's modulus (E) is multiplied by the moment of inertia (I)

$$EI = E \cdot \frac{b \cdot h^3}{12} \tag{3.1}$$

The structural elements in the PLAXIS model are divided in three different parts, namely the existing building, a basement and an annex (driver D1) next to the existing building. When each of these elements is applied depends on the different scenarios, see subsection 3.1.4. The calculation is shown in Appendix A.2.2.

Structural Element	EA [kN/m]	EI [kNm^2/m]
Existing building	$2.4 \cdot 10^7$	$3.2 \cdot 10^5$
Basement (footing)	$2.4 \cdot 10^7$	$3.2 \cdot 10^5$
Basement (walls)	$7.1 \cdot 10^6$	$2.3 \cdot 10^7$
Annex	$6.4 \cdot 10^6$	$2.1 \cdot 10^4$

Table 3.11: Stiffnesses of the different structural elements

Condition of the building

To examine the impact of the building's quality, different stiffness variants for the existing building have been considered. A sensitivity analysis has been conducted for the stiffness of the existing building by considering various variants of stiffnesses. The different variations for the stiffnesses are presented in table 3.12

Stiffness	Factor		
Axial stiffness, EA	0.1	1.0 (ref.)	10
Bending stiffness, EI	0.1	1.0 (ref.)	10

Table 3.12: Stiffness variations

3.3.5. Soil-Structure Interfaces

Interfaces are employed to simulate the soil-structure interaction. This interface enables the transfer of forces and displacements between the relatively stiff structure and the relatively soft soil. These soil-structure interfaces are placed between the soil and the plate elements.

3.4. Model-Setup

In this section, it is described how the numerical model in PLAXIS 2D is built. All the different scenarios, see 3.1.4, are modelled as a plane strain model with 15-Noded elements.

To visualize the various modelling aspects, some images of scenario SS3-B2-D1 are provided, see figure 3.17 and 3.19. This scenario includes not only the existing building but also a basement and an annex as structural elements. As shown in figure 3.17, the far left and far right sides are situated at a considerable distance from the structural element, minimizing the influence of the edges of the soil contour.

The PLAXIS 2D program is employed for the fully automatic generation of finite element meshes. Hence, careful consideration is given to obtain an appropriate balance between accuracy and computational time, while also monitoring mesh quality.

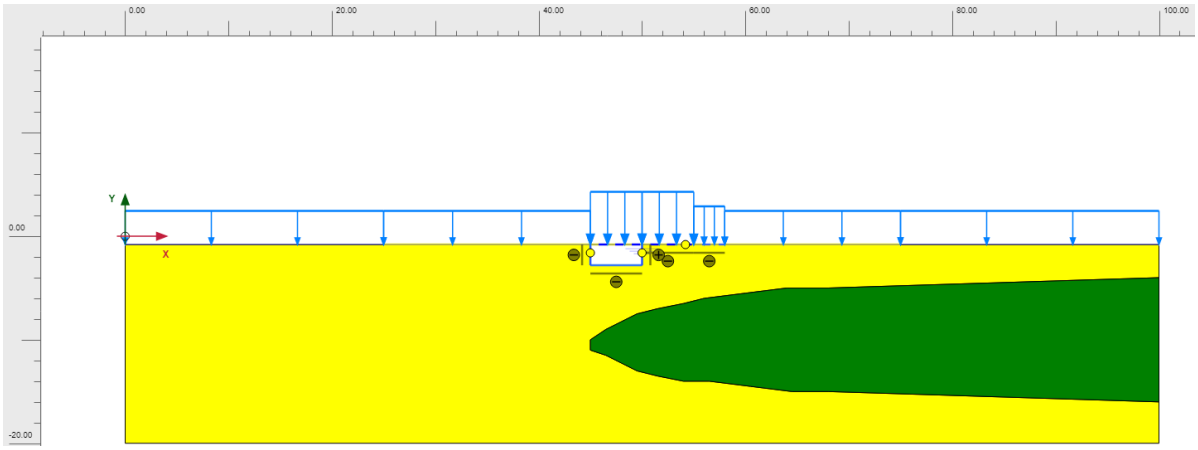

Figure 3.17: Geometry-model SS3-B2-D1

3.4.1. Structures

The structural elements of the models are modelled as plate elements. The structural elements should have properties that are representative of the reality. The properties assigned to the different structural elements are given in section 3.3.

3.4.2. Staged construction

The model consists of different phases with varying time intervals and calculation methods. The different phases are present in table 3.13, followed by a brief explanation below.

	Calculation type	Pore pressure	Time interval [day]	End time [day]	Ignore undrained behaviour [Yes/No]	Reset displ. to zero [Yes/No]
Initial phase A	K0 procedure	Phreatic	0	0	Y	N
Initial phase B	Plastic	Phreatic	1	1	Y	Y
Construction phase	Plastic	Phreatic	10	11	Y	Y
Consolidation phase 1*	Plastic	Phreatic	25550	25561	Y	Y
Driver Implementation	Plastic	Phreatic	10	25571	N	N
Consolidation phase 2	Consolidation	Phreatic	365	25936	N	N
Consolidation phase 3	Consolidation	Phreatic	18250	44186	N	N

Table 3.13: The different phases with the main settings

- **Initial phase A:** The initial stresses in this phase are generated by using the K0 procedure. This calculation method aims to establish the initial stresses for the model, considering the soil's loading history.
- **Initial phase B:** To avoid numerical difficulties, the structural elements have been placed on top of the soil body. To simulate an embedded foundation, the top 0,8 m of the soil is modelled as a line load. Initiating this line load occurs in this phase. This phase is part of generating the initial stress and is therefore an addition to 'Initial phase A'. In this phase, a plastic calculation type is used, undrained behaviour is ignored, and the displacements are reset to zero. Since this phase occurred far in the past, prior to the construction of the existing building, it is not relevant to consider undrained behaviour and the displacements.
- **Construction phase:** This phase serves as the implementation phase of the structural elements with the corresponding load of the existing building. The line load of the top 0.8 m of the ground has been replaced by the line load of the existing building to simulate an excavation first and then the placement of the building. The line load of the top 0.8 m of the ground has been replaced by the line load of the existing building to simulate excavation first and then the placement of the building. In this construction phase, a plastic calculation method has been applied as well. Since this phase occurred far in the past, it is not relevant to consider undrained behaviour. Besides that the displacements are reset to zero, because of the scope, it is not relevant to consider the deformations of the building during the construction phase.
- **Consolidation phase 1*:** After the construction phase, a phase of 25,550 days (70 years) follows to simulate the age of the existing building. Since the scope of this study mainly involves assessing the influence of the different drivers, the displacements are also set to zero in this phase and undrained behaviour is considered. So in this phase where no consolidation occurs, the process is time independent. That means that in fact no settlements occur in this phase. Nonetheless, it was decided to include a time interval for these phases as well, to get a total picture of the timeline.
- **Driver Implementation:** In this phase, the different drivers are implemented, see section 3.1.4. A plastic calculation type is used in this phase to conduct an elastic-plastic deformation analysis.
- **Consolidation phase 2:** Consolidation period of 1 year, with the consolidation calculation type, to determine the effect of the different drivers after 365 days (1 year).
- **Consolidation phase 3:** Consolidation period of 50 years, with the consolidation calculation type, to determine the effect of the different drivers after 18250 days (50 years). The aim of this phase is to predict the settlements that will occur after the implementation of the different drivers.

Applied modelling procedure to consider the relative influence of different drivers.

To consider the relative influence of different drivers, the procedure shown in figure 3.18 has been followed. For all scenarios, the models were executed for the situation with the existing building and

for the situation without the existing building, the greenfield situation.

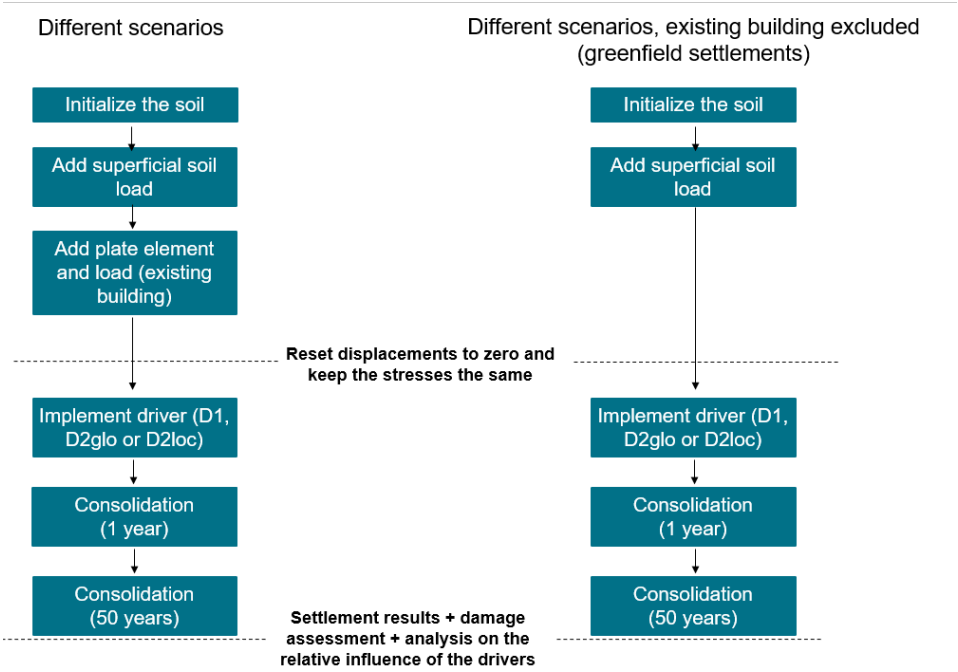

Figure 3.18: Flowchart for the applied procedure where the model is executed for the different scenarios for the situation with the existing building and for the greenfield situation in order to analyse the relative influence of different drivers

3.4.3. Groundwater flow model conditions

In table 3.14 the model conditions for the consolidation boundaries in the PLAXIS model are given.

Boundary	Closed/Open
BoundaryXMin	Closed
BoundaryXMax	Closed
BoundaryYMin	Open
BoundaryYMax	Open

Table 3.14: Model conditions of consolidation boundaries

BoundaryXMin and BoundaryXMax are set to closed and BoundaryYMin and BoundaryYMax are set to open. Drainage through the boundaries is only possible at the top and bottom of the soil model. Drainage through the boundaries is therefore not possible at the extreme left and right sides, in order to simulate the reality where the soil extends continuously.

3.4.4. Soil-Structure Interfaces

Interfaces are employed to simulate the interaction between the soil and the structure. In this case, scenario SS1-B2-D1 serves as an example. In this scenario, the existing building, a basement, and an annex are modelled as structural elements. Figure 3.19 shows the used interface elements. The purpose of assigning a sign to an interface is solely to differentiate interfaces on either side of a line, with no impact on its behaviour (Plaxis, 2023a). The model simulates the roughness of the interaction by selecting an appropriate value assigned to the strength reduction factor (R_{inter}) (Plaxis, 2023a). In all models, the default option 'From adjacent soil' is select for the material mode parameter. The interfaces are set as rigid, corresponding to R_{inter} = 1.0 (Plaxis, 2023a).

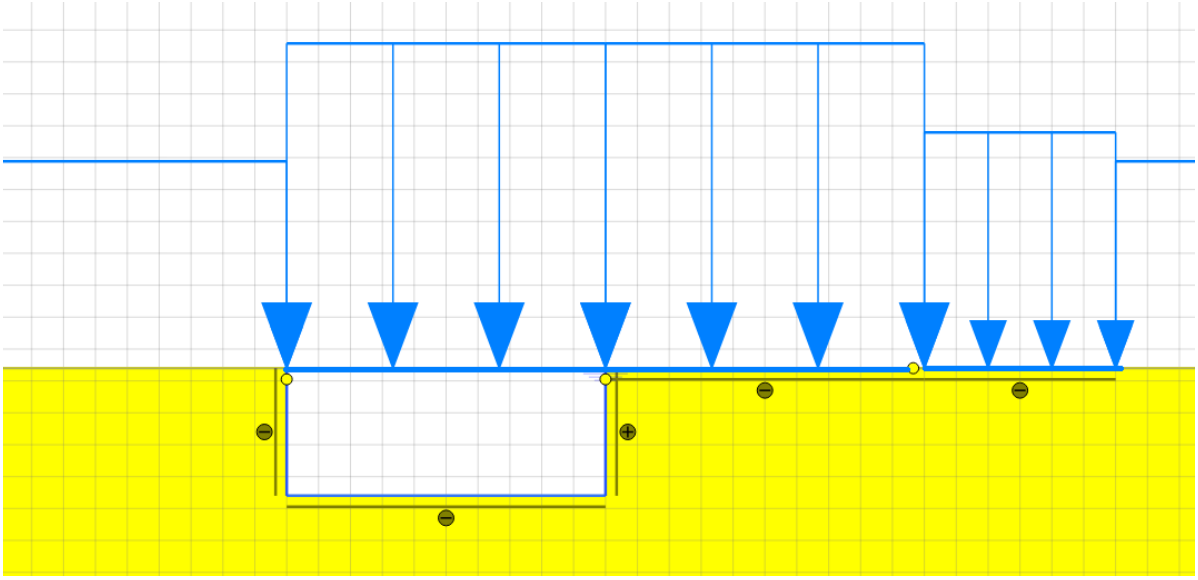

Figure 3.19: An example of the used interface elements PLAXIS with building scenario B2 (existing building with a basement) and driver D1 (annex, applying an additional load). The hinge points are indicated by small yellow dots. The yellow dot shown on the right represents the hinge point between the existing building and the annex. The yellow dots between the vertical elements and the horizontal element represent the hinge points between the basement and the existing building.

3.4.5. Embedment depth foundation

The embedment depth of the foundation of the existing building is assumed to be 0.8 meters below ground level (NAP -0.8 m), see figure 3.17. To prevent numerical difficulties, the foundation level is set at -0.8 m and the surrounding soil is modelled as a line load with a corresponding soil weight, see table 3.15.

Soil lithology	Unit weight of soil (unsat.)	Load with a height of 0.8 m
	$[kN/m^3]$	$[kN/m/m]$
Sand (SS1 and SS3)	18.0	14.4
Clay (SS2)	17.0	13.6

Table 3.15: Corresponding load with a height of 0.8 m to simulate an embedded foundation

3.4.6. Connection between existing building and annex

An attempt has been made to generate the most realistic connection possible between the existing building and the annex (driver D1). It is common for an annex not to be attached to the existing building. Therefore, the extension must be freestanding. However, the foundation footings will overlap, affecting each other both vertically, and horizontally. It has been chosen to apply a hinge point as a connection, allowing rotation. The hinge points are indicated by small yellow dots. The yellow dot shown on the right represents the hinge point between the existing building and the annex, see figure 3.19. As an alternative, a small gap, for example 0.01m, could be applied to simulate a dilatation. However, this results in a less well-fitting mesh generation; therefore, a hinge point has been chosen.

3.4.7. Connection between existing building and basement

Hinge points have been placed between vertical structural elements and the horizontal structural element, representing the basement walls and the existing building, respectively. The hinge points are indicated by small yellow dots. The yellow dots between the vertical elements and the horizontal element represent the hinge points between the basement and the existing building, see figure 3.19. Here, the vertical plates are designated as custom parts ('child objects'), and the horizontal plate is designated as a reference part ('parent object'). The hinge points can rotate freely. The idea behind this is that it allows the horizontal plate (the existing building) to bend more freely, creating a more representative situation of reality. Using moment-fixed points results in a too conservative approach.

3.4.8. Gathering results

To maintain consistency in collecting the calculated settlement results for each scenario, especially across various building scenarios, it has been decided to gather them using a geogrid. It should be noted that no tensile strength (0.1 kN/m) has been assigned to this geogrid, and it is solely used for result collection purposes. Because no tensile strength has been assigned to the geogrid, it follows the deformations of the structural elements and the soil entirely.

4

Results/Analysis

This chapter presents the results of the analysis of the relative influence of different subsidence drivers on the damage of existing buildings. The first part of this chapter considers the analysis of the settlement computations for all scenarios, followed by a section in which the impact of the settlements of the different scenarios on the existing building is assessed. Subsequently, there is a section focusing on the relative influence of the different subsidence drivers

4.1. Settlement computation

This section presents the results of settlement analysis at the end of phase 6. It has been chosen to apply 'Load 3' (D1), 'H5' (D2glo) and 'H4' (D2loc) for this calculations. So the situations with the highest intensity of the drivers.

For scenarios SS1-B1-D2glo (4.1.1), SS2-B1-D2glo (4.1.2), SS3-B1-D2loc (4.1.3), and SS2-B2-D1 (4.1.4) the results from the finite element model are presented in more detail as examples. This includes the impact on the deformed mesh, the influence of the drivers on the stress for a node in the middle of the weak layer over time, and the progression of the water pressure from the moment the driver is implemented.

For each scenario, the depth is plotted against the distance within the corresponding soil model. This has been done for the different scenarios, including the situation where the load from the existing building is omitted, thus only applying the driver. What is referred to as a greenfield situation. These figures provide a general overview of the influence of the different drivers on the settlements at the ground surface. This will be further investigated in the subsequent sections. In figures 4.10, 4.20 and 4.30 the settlements at ground level for the different drivers are combined in one figure for soil scenario SS1, SS2 and SS3.

4.1.1. Scenario SS1-B1

In the next figures the settlement of surface for the drivers D1 (4.8), D2glo (4.7), and D2loc (4.9) for soil scenario SS1 are presented. Figure 4.7 illustrates the reference model, where both the soil and the load are uniformly distributed.

Reference model: SS1-B1-D2glo

The reference model and the resulting calculation outcomes serves as verification of the assumed procedure. The selected scenario, SS1-B1-D2glo, consists of horizontal soil layers, with the applied loads from both the existing building and the driver evenly distributed over the subsurface. In a homogeneous soil structure with uniformly distributed load, it is expected that no differential settlements will occur.

For the purpose of analysing the reference model, soil deformations, deformation of the structural element, settlements over time and the excess pore pressure over time have been considered.

Figures 4.1 and 4.2 shows the deformed mesh for a situation with the existing building and the greenfield situation at the end of phase 6. Both figures show uniform settlements without differential settlements and deformations.

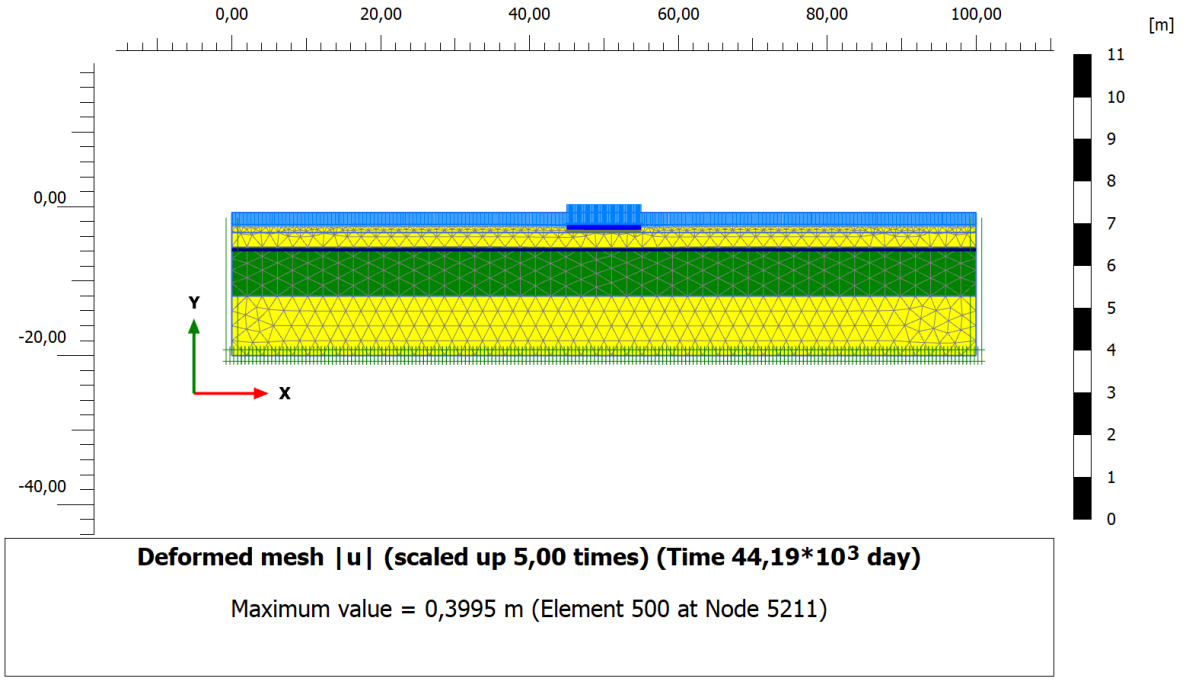

Figure 4.1: Deformed mesh scenario: SS1-B1-D2glo (reference model)

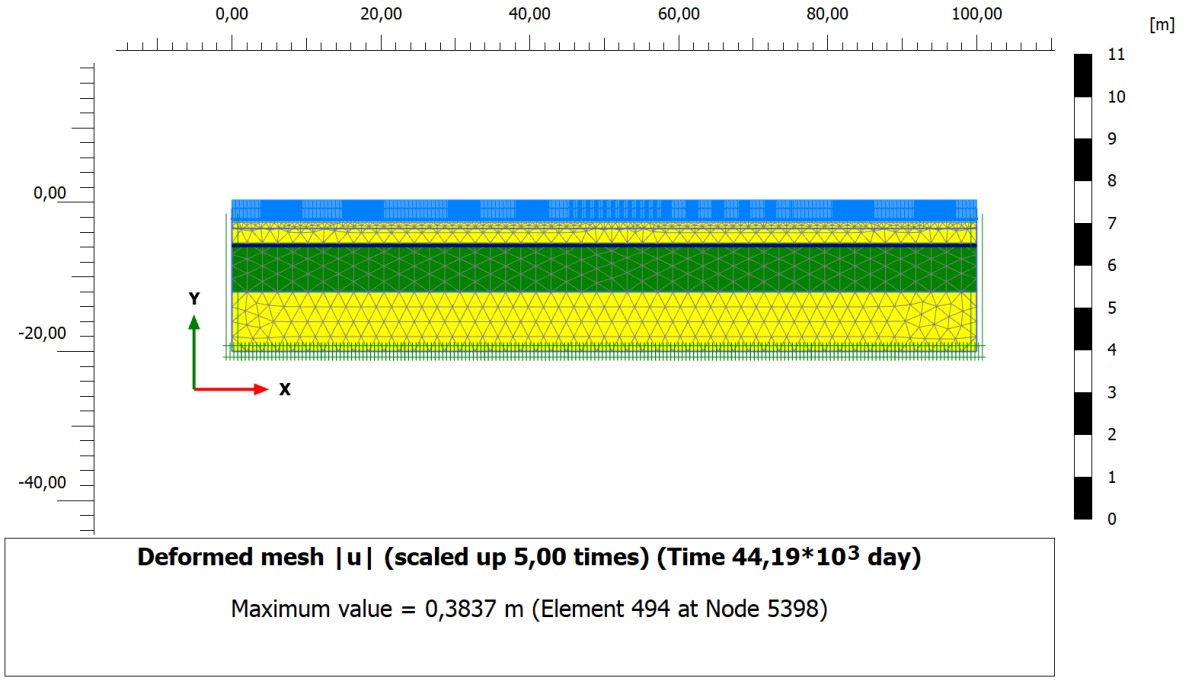

Figure 4.2: Deformed mesh scenario: SS1-D2glo (greenfield situation)

Almost all deformations occur in the soft layer, indicated by the green colour. These results align with the hypotheses. The mesh is automatically generated by PLAXIS and shows a finer mesh size at the top of the ground contour.

Figure 4.3 shows the impact on the stresses of a node in the middle of the weak layer over time. The total stress, effective stress, and water pressure are plotted in a graph. The graph on the right shows the settlement of the same node. In both graphs, the moment of implementing the driver is indicated

with a dashed orange line.

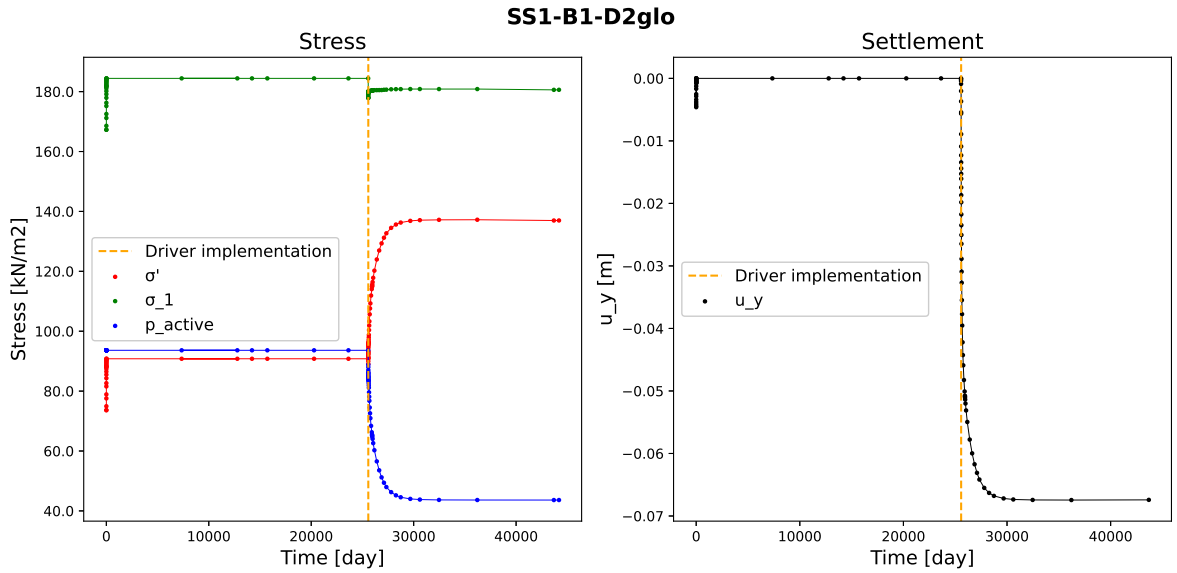

Figure 4.3: Left: Total stress, effective stress and the pore pressure over time for a node in the middle of the weak layer, Right: Settlement over time for the same the node in the middle of the weak layer. In both graphs, the moment of implementing the driver is indicated with a dashed orange line

The vertical line at t=0 in the time-settlement graph is caused by the initiation of soil stresses in the initial phase. Immediately afterward, this settlement is reset to zero, so it does not affect the final result.

Figures 4.4, 4.5 and 4.6 shows the excess pore pressure for phase 4, phase 5 and phase 6.These are the phases from the moment of implementing the driver to the final phase. The amount of excess pore pressure is a good indicator of the extent of consolidation that has already occurred. So this can serve as an indicator for the amount of settlement that may still occur under constant loads.

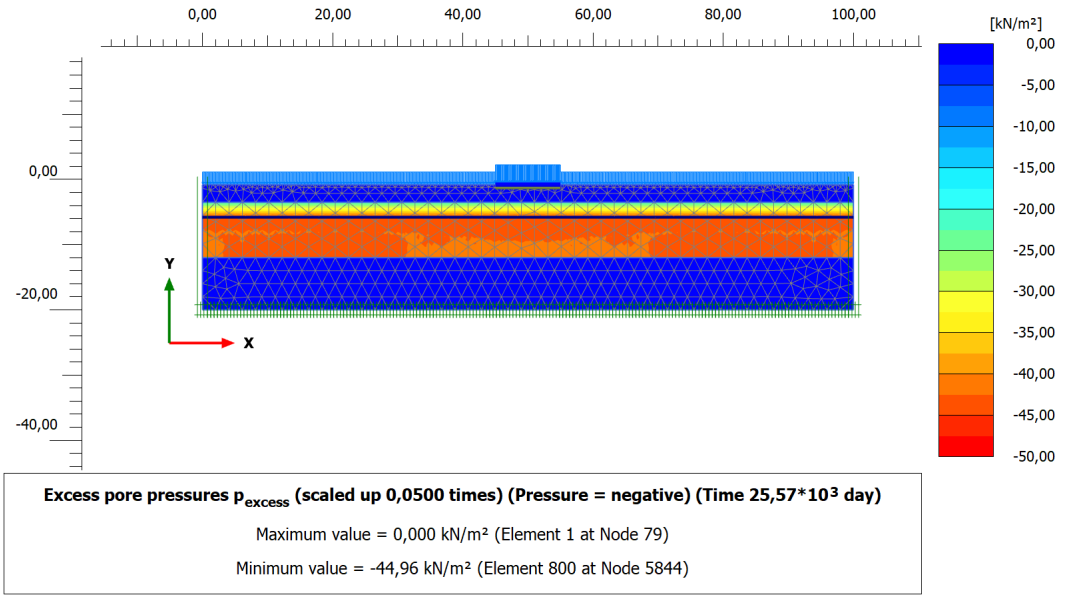

Figure 4.4: SS1-B1-D2glo: Excess pore pressure in phase 4, at the moment of implementing the driver, global water level lowering

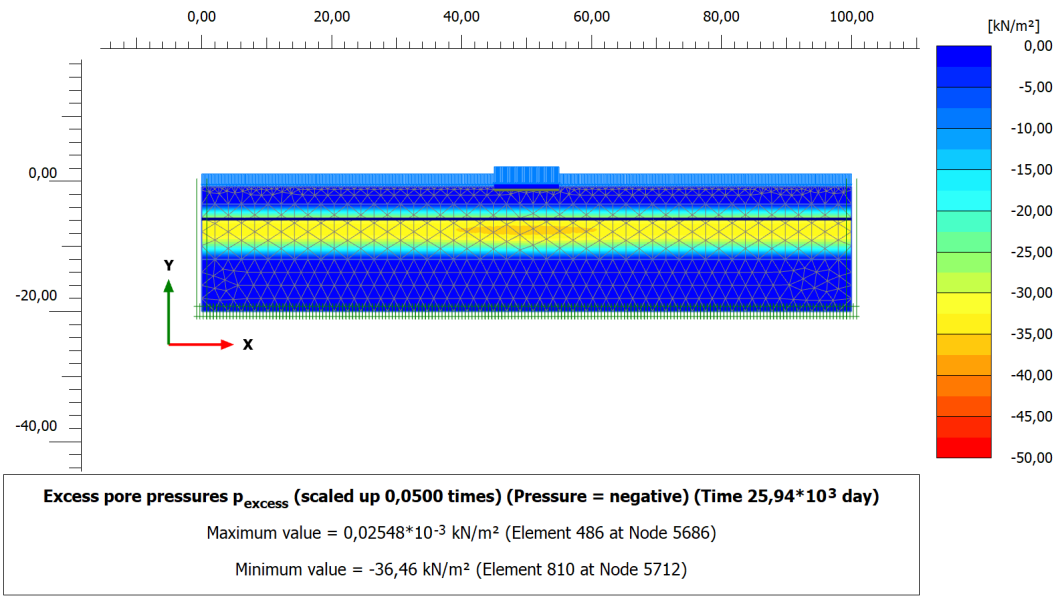

Figure 4.5: SS1-B1-D2glo: Excess pore pressure in phase 5, with a consolidation period of 1 year

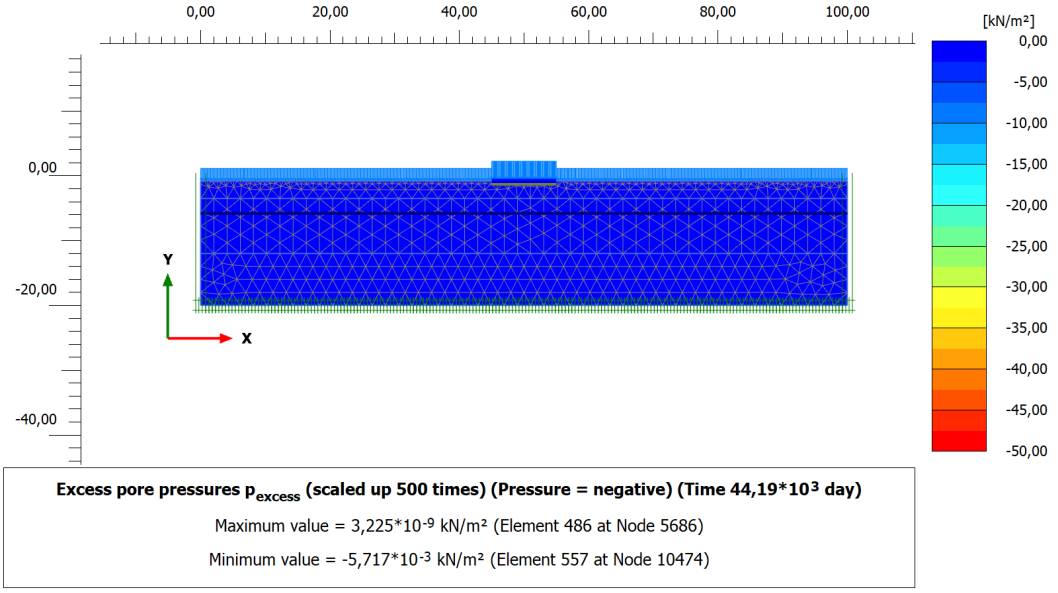

Figure 4.6: SS1-B1-D2glo: Excess pore pressure in phase 6, with a consolidation period of 50 years

The dissipation of excess pore pressure occurs, as expected, in the weak soil (clay layer). A uniform decrease in excess pore pressures is visible over time.

In figure 4.7, both the settlements in the situation with the building and the settlements in the greenfield situation are depicted from the reference model. The vertical dashed lines indicate the boundaries of where the building is located. A uniform settlement across the entire length of the profile is visible in the greenfield situation (orange line). The impact of the existing building's presence is clearly evident from the green line.

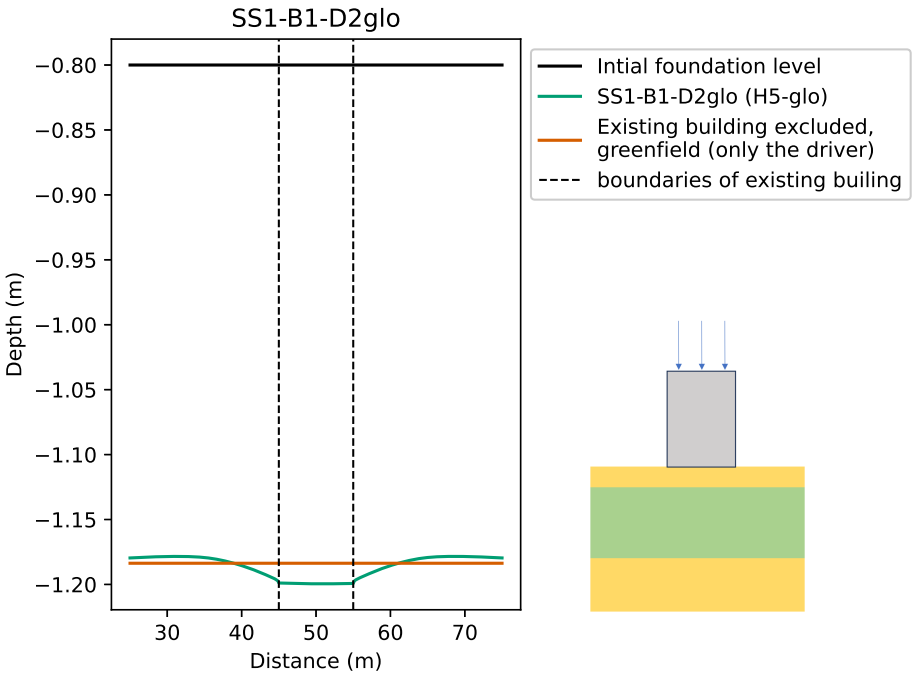

Figure 4.7: Settlement of the surface of scenario SS1-B1-D2glo

SS1-B1-D1

In the following two figures, the other drivers for this ground scenario are depicted. Figure 4.8 shows the settlements resulting from applying an additional load directly adjacent to the existing building. What stands out here is that the absolute settlements are lower than those in the situation with a water level lowering.

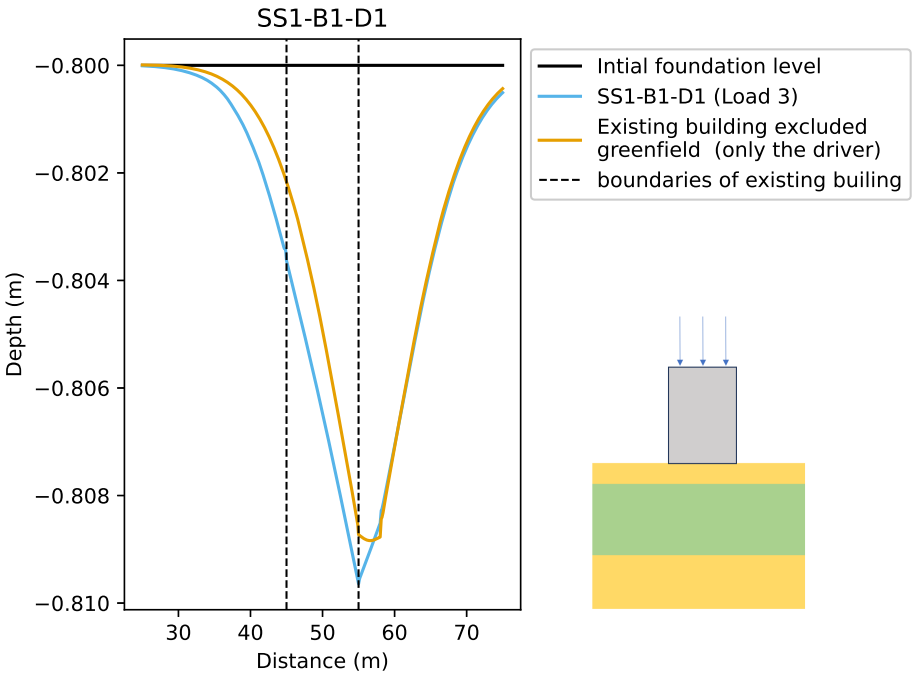

Figure 4.8: Settlement of the surface of scenario SS1-B1-D1

SS1-B1-D2loc

Figure 4.9 shows the settlement of soil scenario SS1 with a local water level lowering as driver (D2loc). Here, the influence of the non-uniform nature of the applied load from the driver is clearly visible.

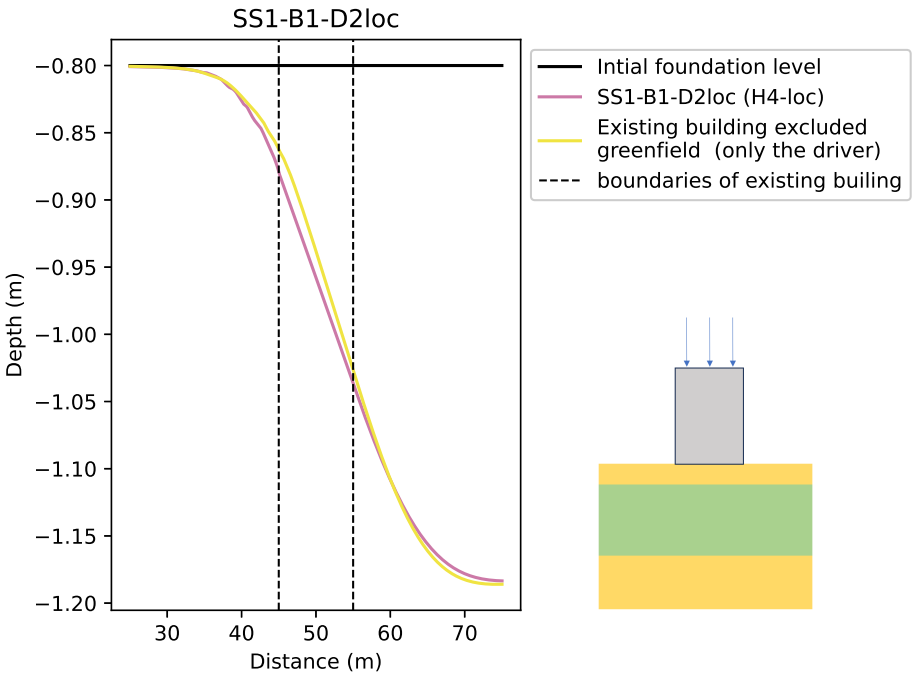

Figure 4.9: Settlement of the surface of scenario SS1-B1-D2loc

SS1-B1-D1-D2glo-D2loc

In figure 4.10 the settlement for the situation with the existing building, caused by the different drivers, are combined in one figure.

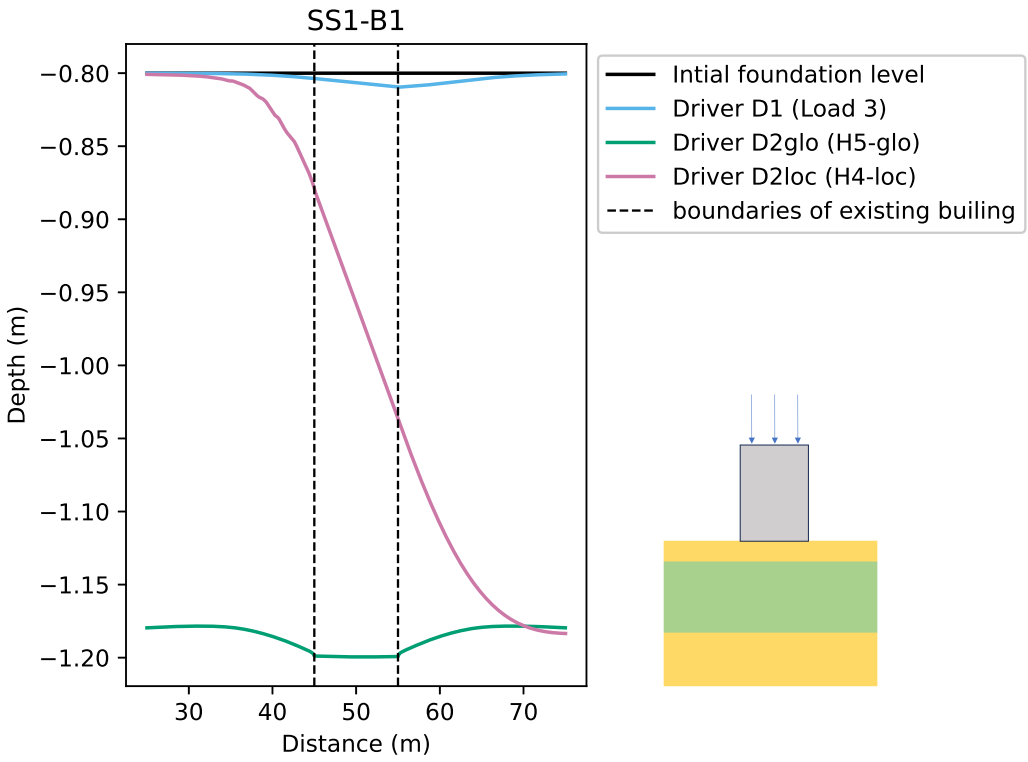

Figure 4.10: Surface settlement of Soil Scenario 1 (SS1)

The difference in absolute settlements between driver D1 and D2glo is remarkable. Additionally, it is evident that driver D2loc induces the most differential settlement for ground scenario SS1.

4.1.2. Scenario SS2-B1

In this section, the results of the settlements for the various drivers for ground scenario SS2 are presented. The same procedure as for the previous ground scenario has been applied. In the next figures the settlement of surface for the drivers D1 (4.11), D2glo (4.18), and D2loc (4.19) are presented.

SS2-B1-D1

In the figure below 4.11, the settlement of scenario SS2-B1-D1 is shown.

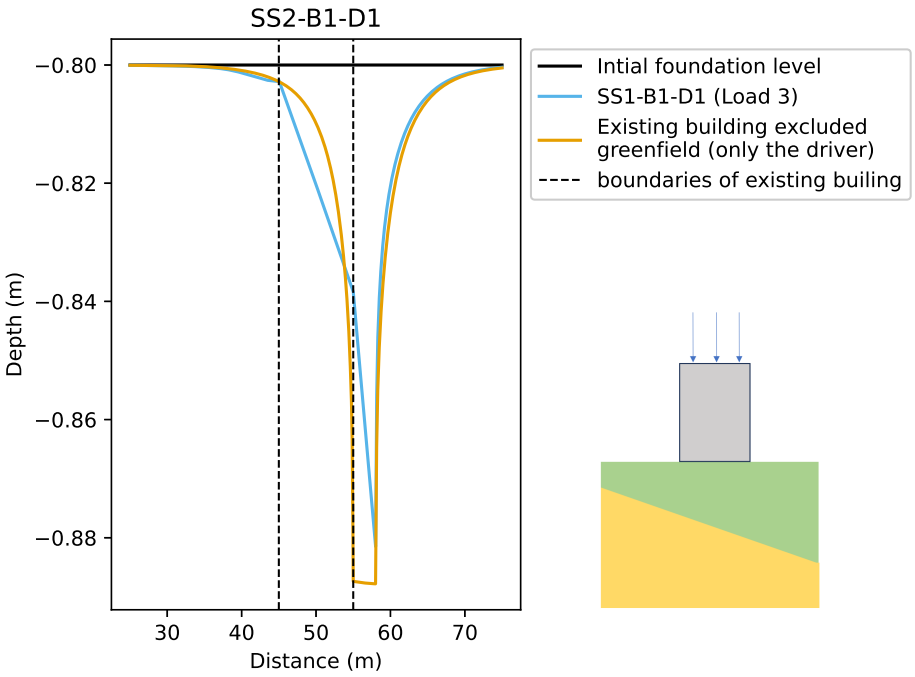

Figure 4.11: Settlement of the surface of scenario SS2-B1-D1

What stands out about the settlement of the annex is that, in this ground scenario (SS2), it exhibits differential settlement in the opposite direction compared to soil scenario SS1.

SS2-B1-D2glo

This scenario also serves as an example where a more comprehensive presentation of the results of the finite element model is provided. This includes the impact on the deformed mesh, the influence of the drivers on the stress for a node in the middle of the weak layer over time, and the progression of the water pressure from the moment the driver is implemented.

Figures 4.12 and 4.13 shows the deformed mesh for a situation with the existing building and the greenfield situation at the end of phase 6. The deformations are on an exaggerated scale, to make them more visible.

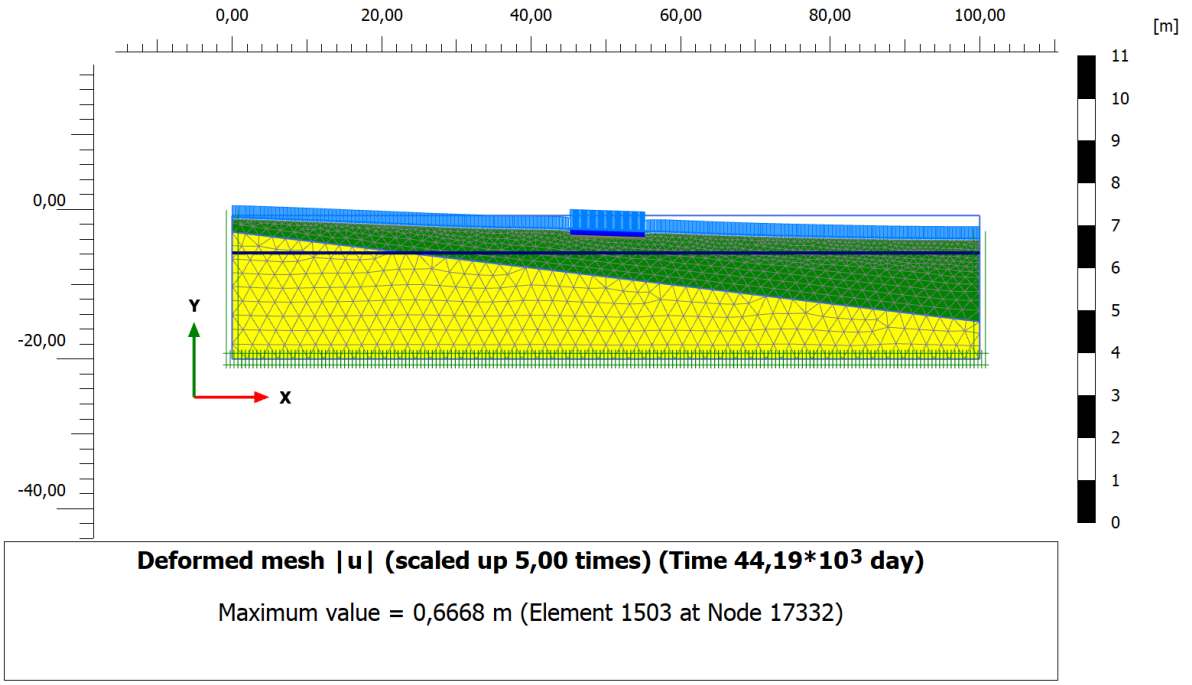

Figure 4.12: Deformed mesh scenario: SS2-B1-D2glo

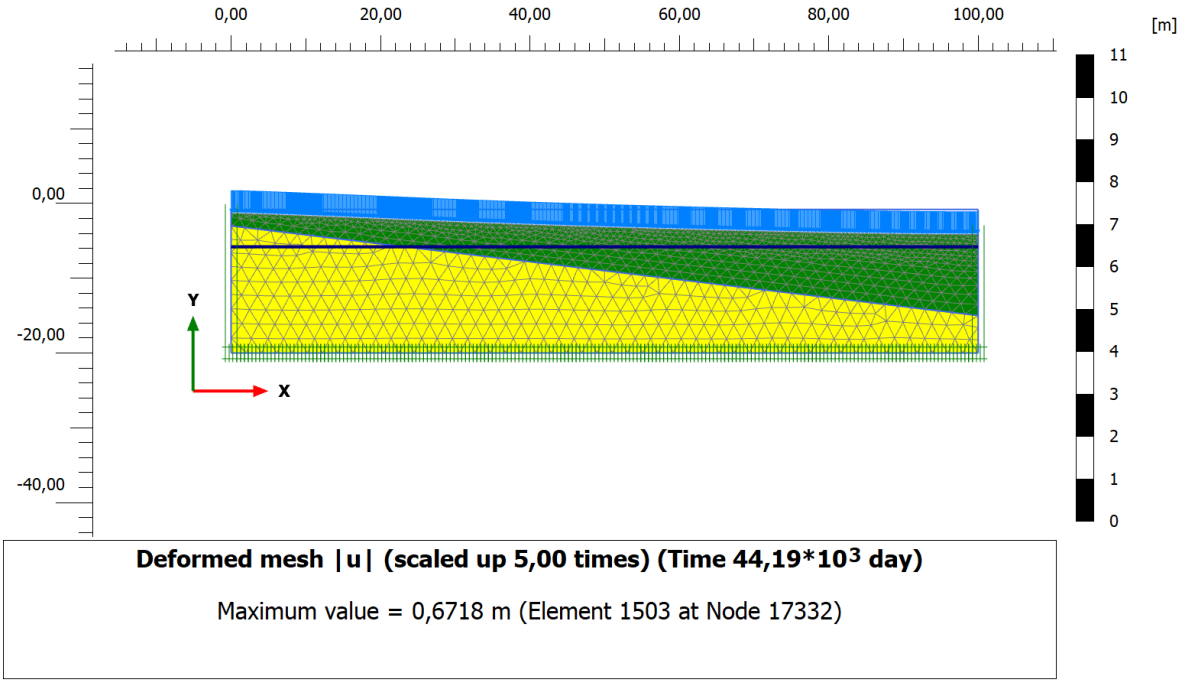

Figure 4.13: Deformed mesh scenario: SS2-D2glo (greenfield situation)

Figure 4.14 shows the impact on the stresses of a node in the middle of the weak layer over time. The total stress, effective stress, and water pressure are plotted in a graph. The graph on the right shows the settlement of the same node. In both graphs, the moment of implementing the driver is indicated with a dashed orange line.

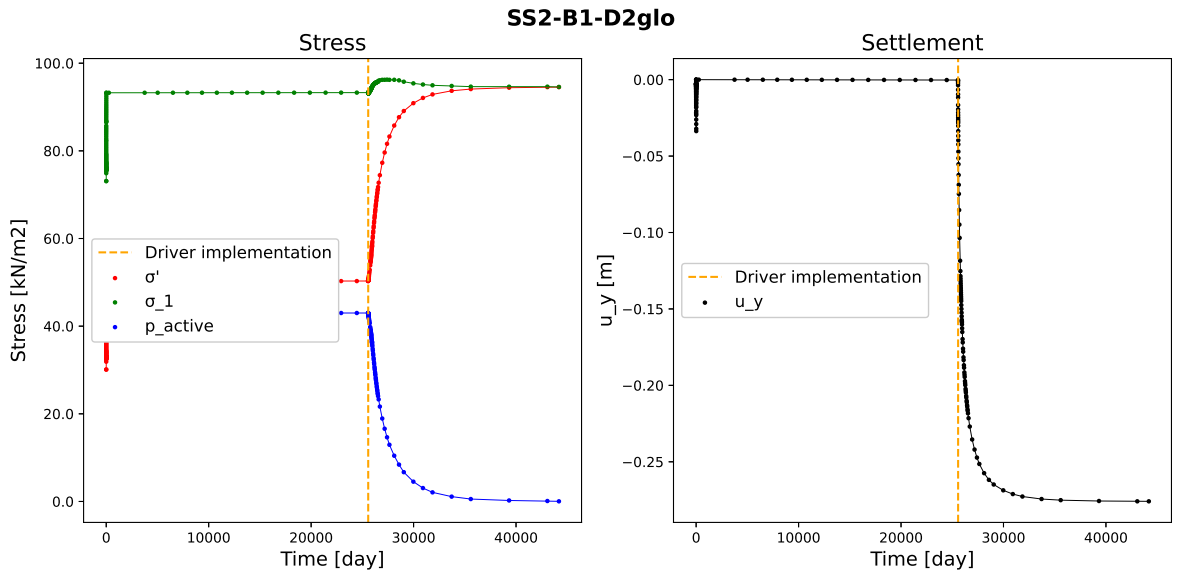

Figure 4.14: Left: Total stress, effective stress and the pore pressure over time for a node in the middle of the weak layer, Right: Settlement over time for the same the node in the middle of the weak layer. In both graphs, the moment of implementing the driver is indicated with a dashed orange line

The vertical line at t=0 in the time-settlement graph is caused by the initiation of soil stresses in the initial phase. Immediately afterward, this settlement is reset to zero, so it does not affect the final result.

Figures 4.15,4.16 and 4.17 shows the excess pore pressure or phase 4, phase 5 and phase 6.

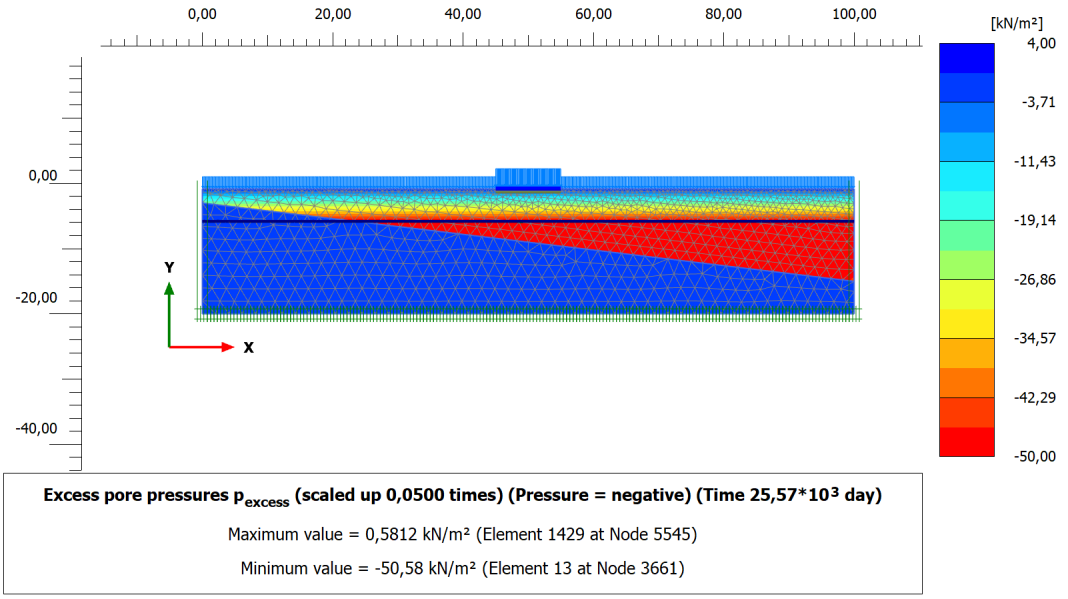

Figure 4.15: SS2-B1-D2glo: Excess pore pressure in phase 4, at the moment of implementing the driver, global water level lowering

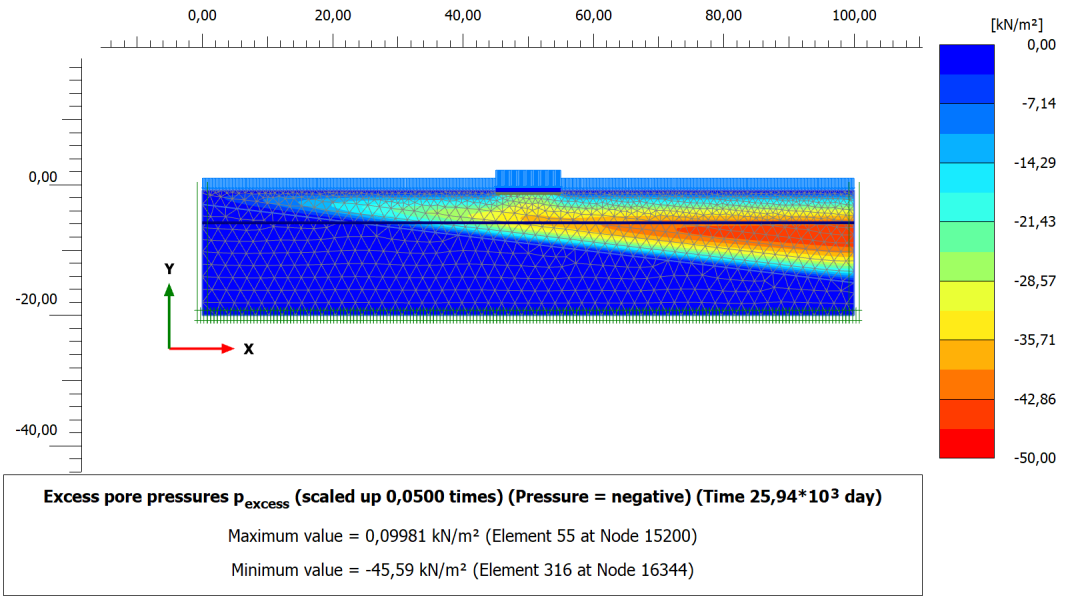

Figure 4.16: SS2-B1-D2glo: Excess pore pressure in phase 5, with a consolidation period of 1 year

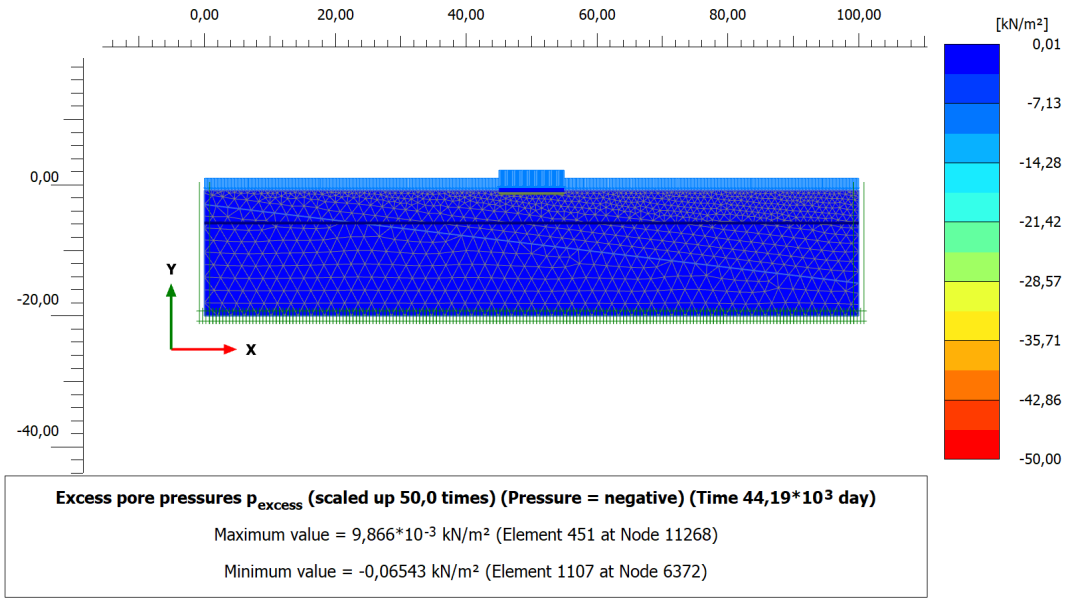

Figure 4.17: SS2-B1-D2glo: Excess pore pressure in phase 6, with a consolidation period of 50 years

The dissipation of excess pore pressure occurs, as expected, in the weak soil (clay layer). And again, a clear decrease in excess pore pressures is observed from the moment of implementing the driver until the final phase.

In the figure below 4.18, the settlement of scenario SS2-B1-D2glo is shown.

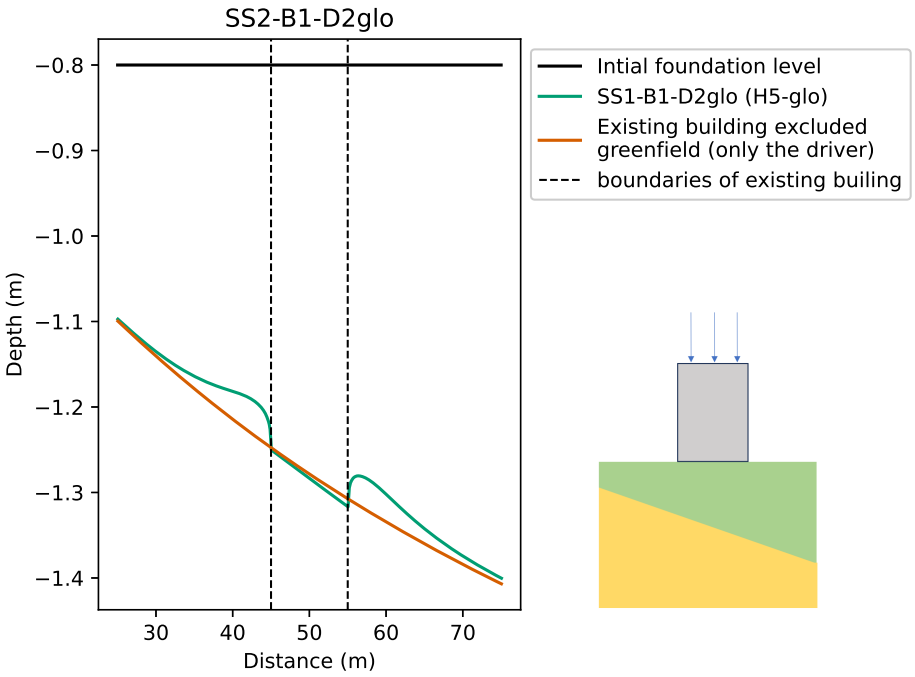

Figure 4.18: Settlement of the surface of scenario SS2-B1-D2glo

Unlike the reference model, there is now a non-uniform applied load, resulting in differential settlement. Additionally, it is clearly visible that the presence of the building restricts the settlement directly adjacent to it.

SS2-B1-D2loc
In the figure below 4.19, the settlement of scenario SS2-B1-D2loc is shown.

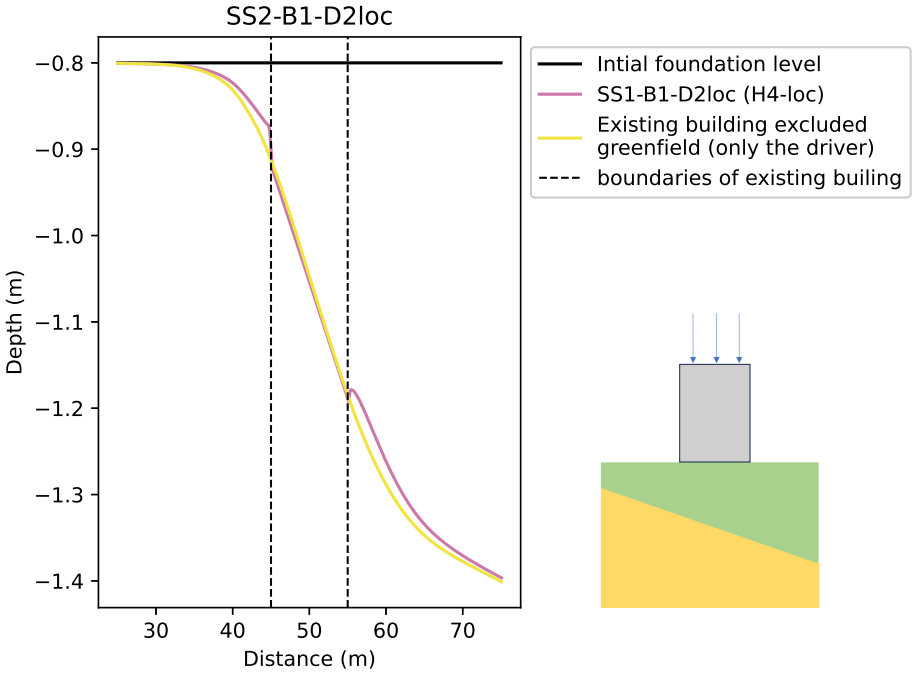

Figure 4.19: Settlement of the surface of scenario SS2-B1-D2loc

SS2-B1-D1-D2glo-D2loc
In figure 4.20 the settlement for the situation with the existing building, caused by the different drivers, are again combined in one figure.

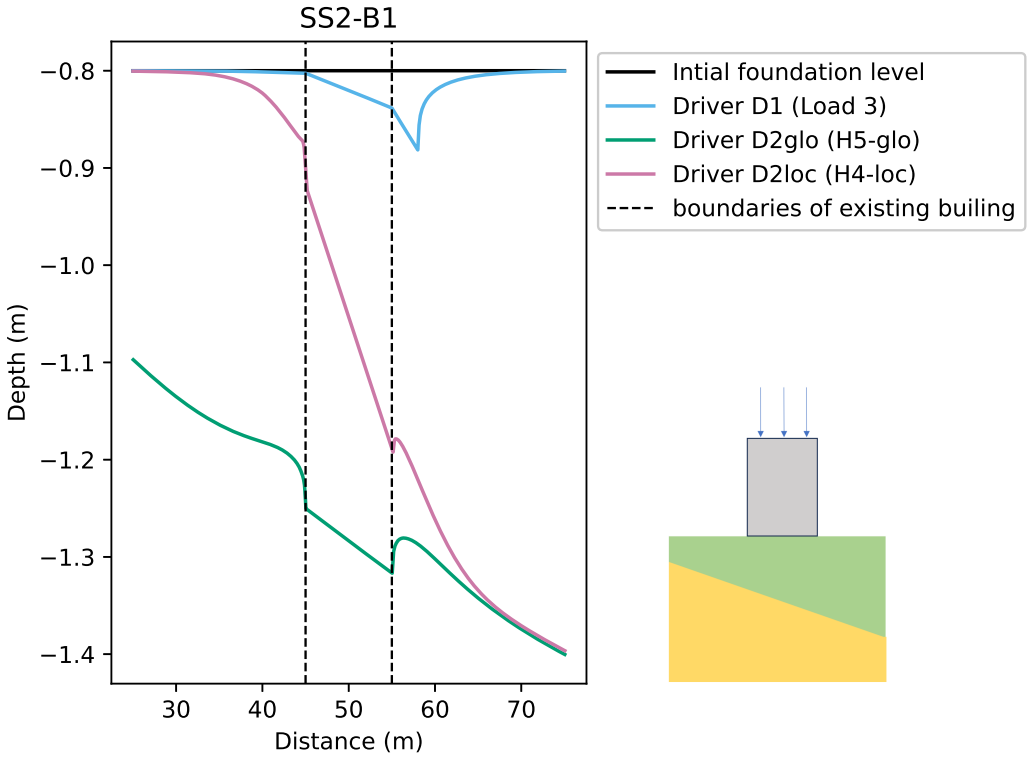

Figure 4.20: Surface settlement of Soil Scenario 2 (SS2)

What is notable for all drivers is the significant bending of the ground surface directly adjacent to the building.

4.1.3. Scenario SS3-B1

In this section, the results of the settlements for the various drivers for ground scenario SS2 are presented. The same procedure as for the previous ground scenario has been applied. In the next figures the settlement of surface for the drivers D1 (4.28), D2glo (4.29), and D2loc (4.27) are presented.

SS3-B1-D2loc
This scenario also serves as an example where a more comprehensive presentation of the results of the finite element model is provided. This includes the impact on the deformed mesh, the influence of the drivers on the stress for a node in the middle of the weak layer over time, and the progression of the water pressure from the moment the driver is implemented.

Figures 4.21 and 4.22 shows the deformed mesh for a situation with the existing building and the greenfield situation at the end of phase 6. The deformations are on an exaggerated scale, to make them more visible.

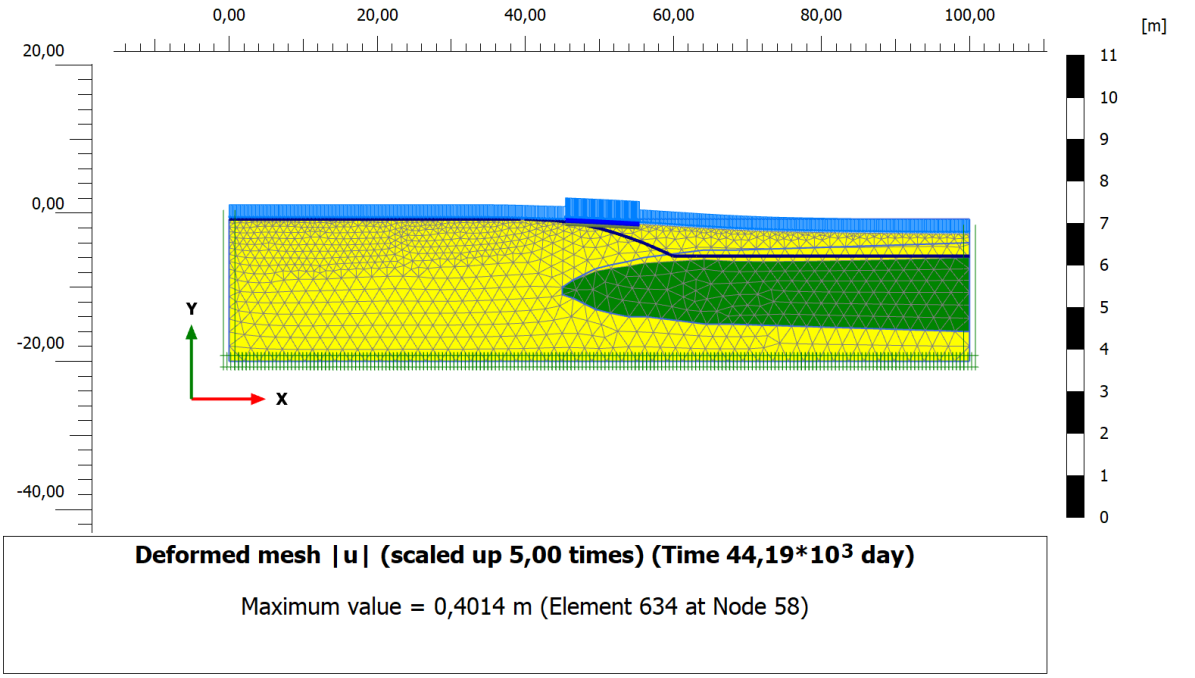

Figure 4.21: Deformed mesh scenario SS3-B1-D2loc

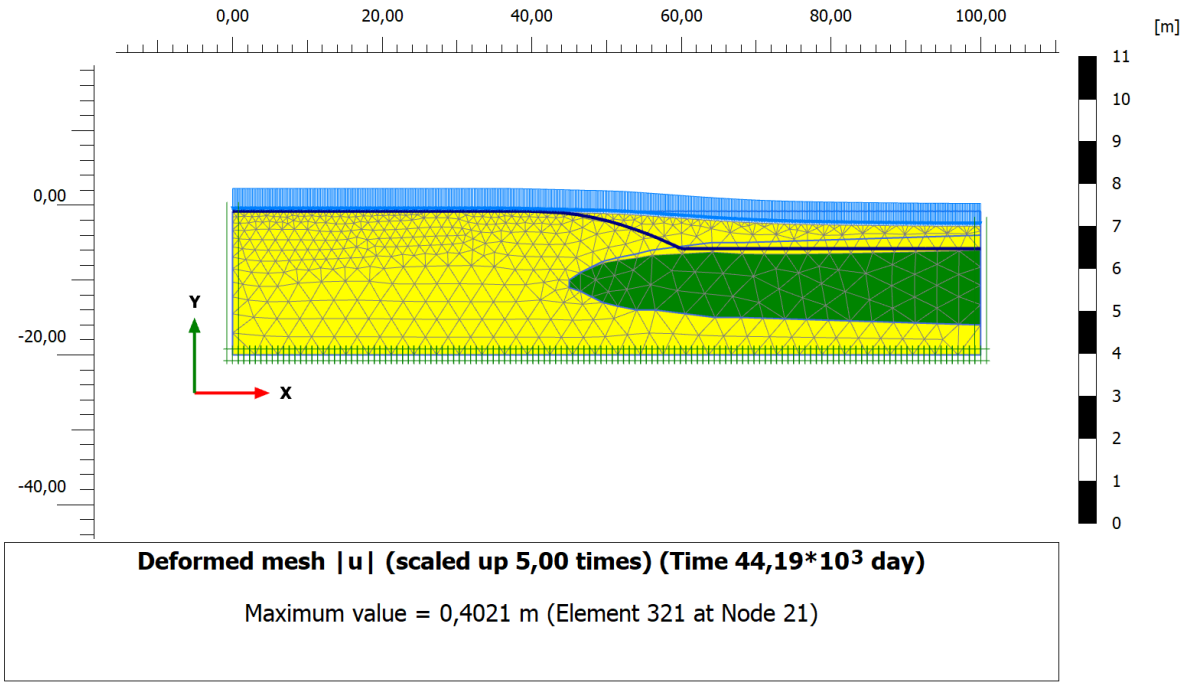

Figure 4.22: Deformed mesh scenario SS3-D2loc (greenfield situation)

The mesh is automatically generated by PLAXIS. The figures show that the mesh becomes finer towards the top of the soil contour. What is also noticeable is that the mesh adopts a finer pattern on the left side of the ground model.

Figure 4.23 shows the impact on the stresses of a node in the middle of the weak layer over time. The total stress, effective stress, and water pressure are plotted in a graph. The graph on the right shows the settlement of the same node. In both graphs, the moment of implementing the driver is

indicated with a dashed orange line.

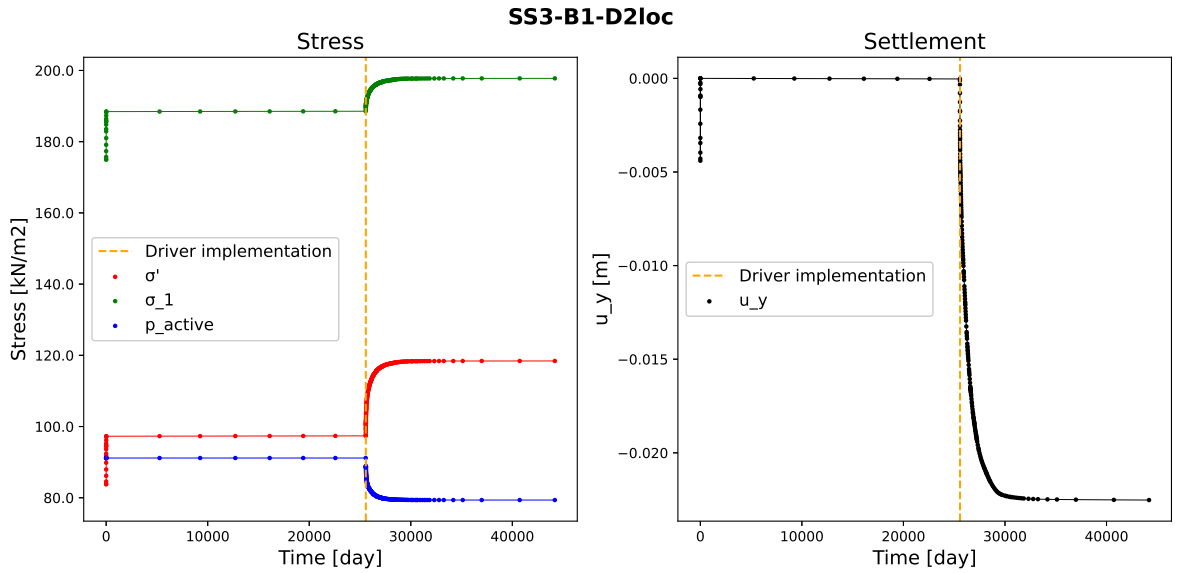

Figure 4.23: Left: Total stress, effective stress and the pore pressure over time for a node in the middle of the weak layer, Right: Settlement over time for the same the node in the middle of the weak layer. In both graphs, the moment of implementing the driver is indicated with a dashed orange line

From the graph, it is visible that the difference in pore pressure is smaller due to the implementation of the driver than is seen in figure 4.3 The vertical line at t=0 in the time-settlement graph is caused by the initiation of soil stresses in the initial phase. Immediately afterward, this settlement is reset to zero, so it does not affect the final result.

Figures 4.24,4.26 and 4.26 shows the excess pore pressure or phase 4, phase 5 and phase 6.

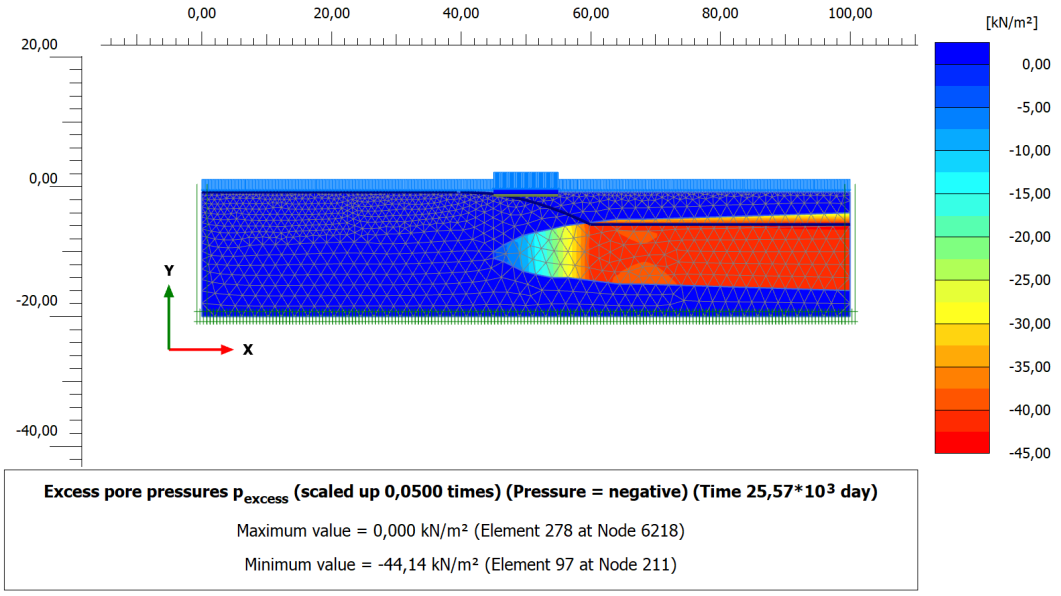

Figure 4.24: SS3-B1-D2loc: Excess pore pressure in phase 4, at the moment of implementing the driver, local water level lowering

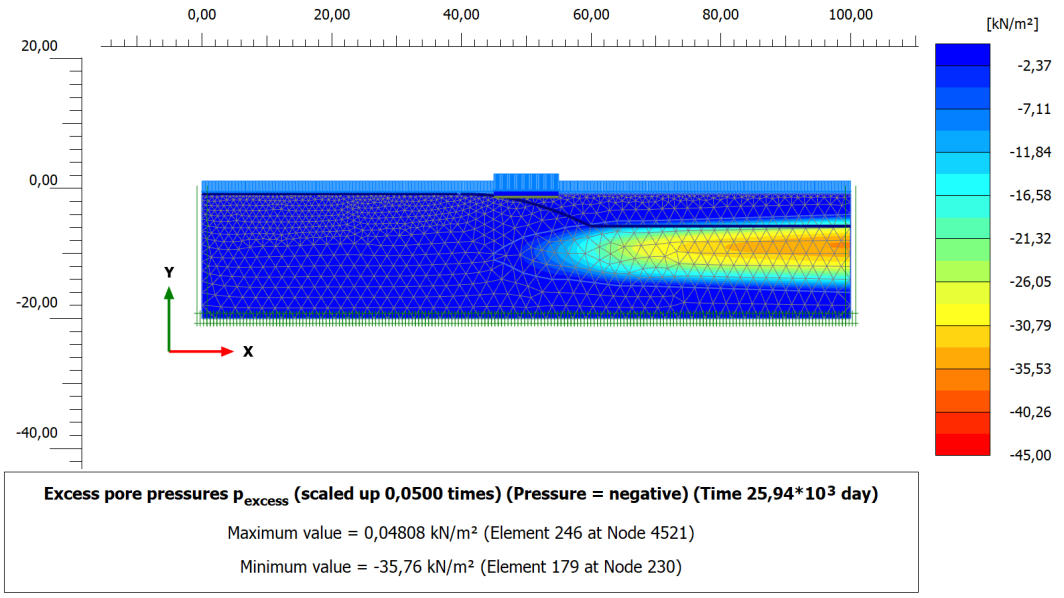

Figure 4.25: SS3-B1-D2loc: Excess pore pressure in phase 5, with a consolidation period of 1 year

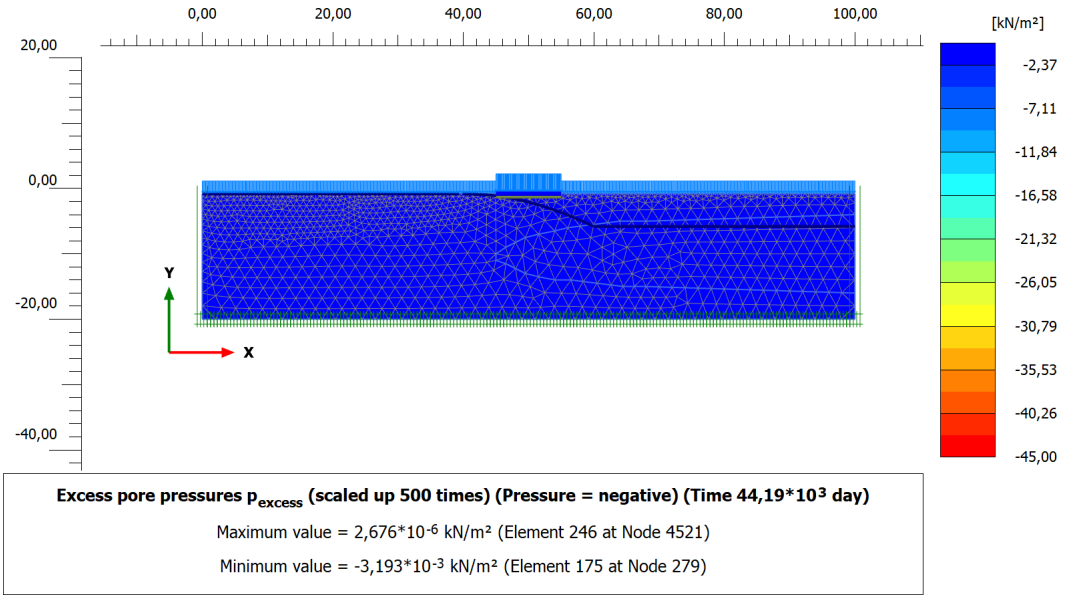

Figure 4.26: SS3-B1-D2loc: Excess pore pressure in phase 6, with a consolidation period of 50 years

The dissipation of excess pore pressure occurs, as expected, in the weak soil (clay layer). And again, a clear decrease in excess pore pressures is observed from the moment of implementing the driver until the final phase.

Figure 4.27 shows the settlement results for scenario SS3-B1-D2loc.

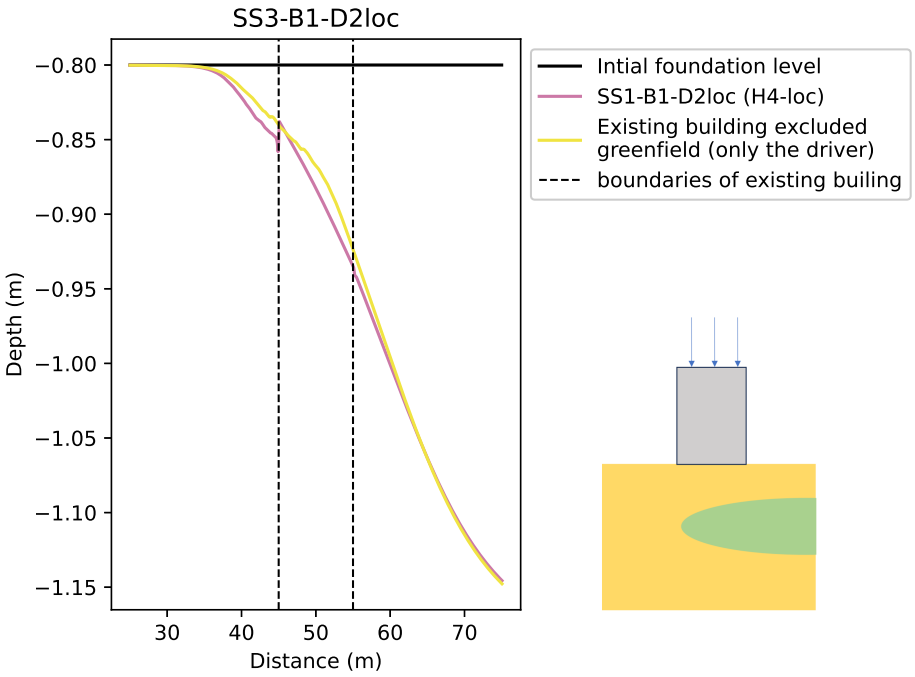

Figure 4.27: Settlement of the surface of scenario SS3-B1-D2loc

The settlement results of the greenfield situation naturally show a greater curvature than the situation with the building. What is notable is the deviation in the curvature of the greenfield situation on the left side of the building, which can be explained by the heterogeneous nature of the ground scenario SS3.

SS3-B1-D1
Figure 4.28 shows the settlement results for scenario SS3-B1-D1.

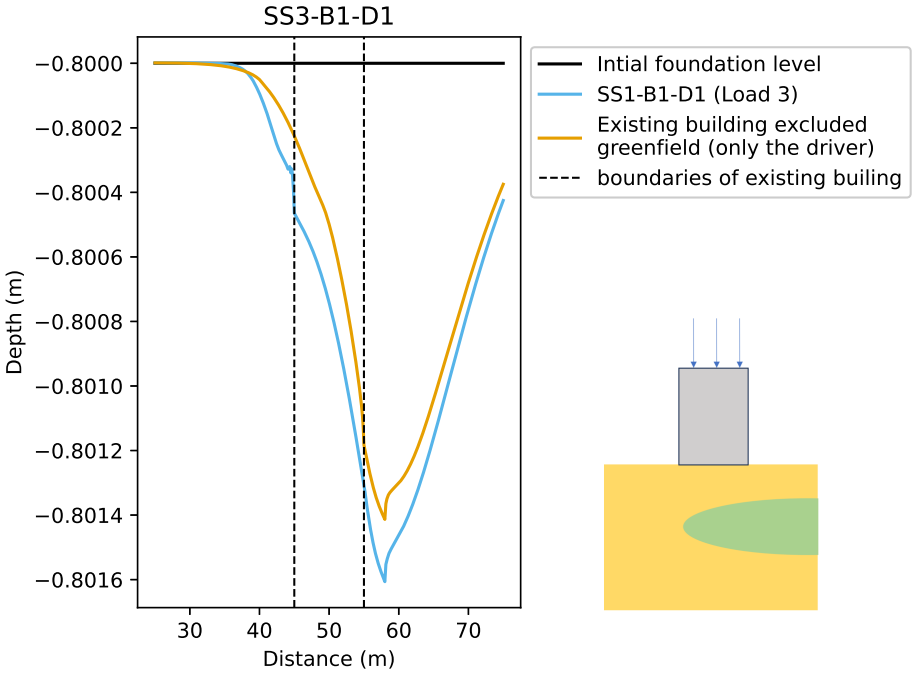

Figure 4.28: Settlement of the surface of scenario SS3-B1-D1

The settlement profile presents a different picture compared to the other drivers. This can be explained by the fact that the settlement in absolute terms is very small. This results in an exaggerated depiction of the profile when viewed along the vertical axis.

SS3-B1-D2glo
Figure 4.29 shows the settlement results for scenario SS3-B1-D2glo.

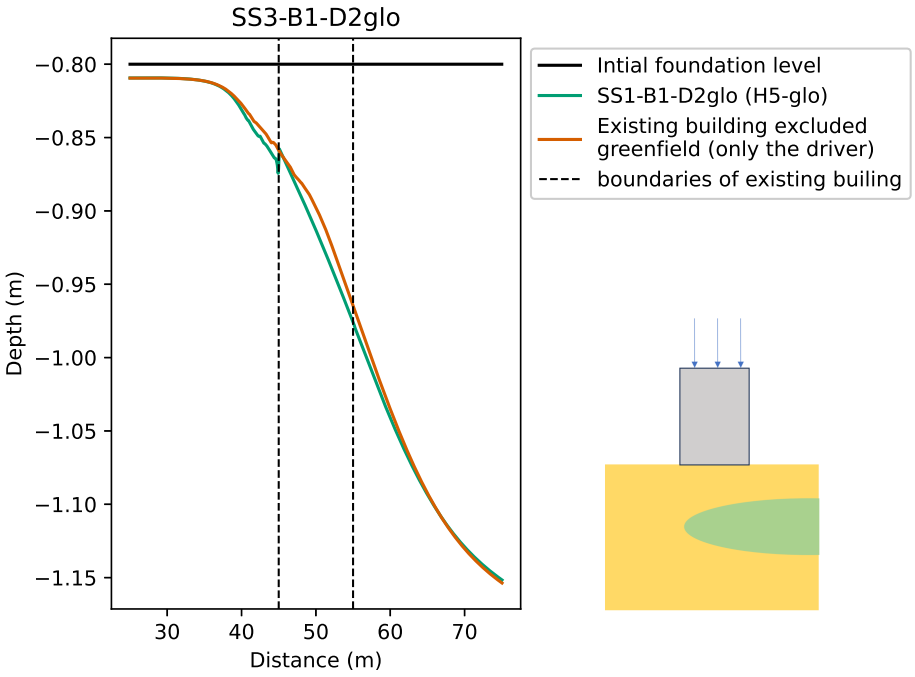

Figure 4.29: Settlement of the surface of scenario SS3-B1-D2glo

The settlement profile shows a corresponding result compared to driver D2loc.

SS3-B1-D1-D2glo-D2loc
In figure 4.30 the settlement for the situation with the existing building, caused by the different drivers, are again combined in one figure.

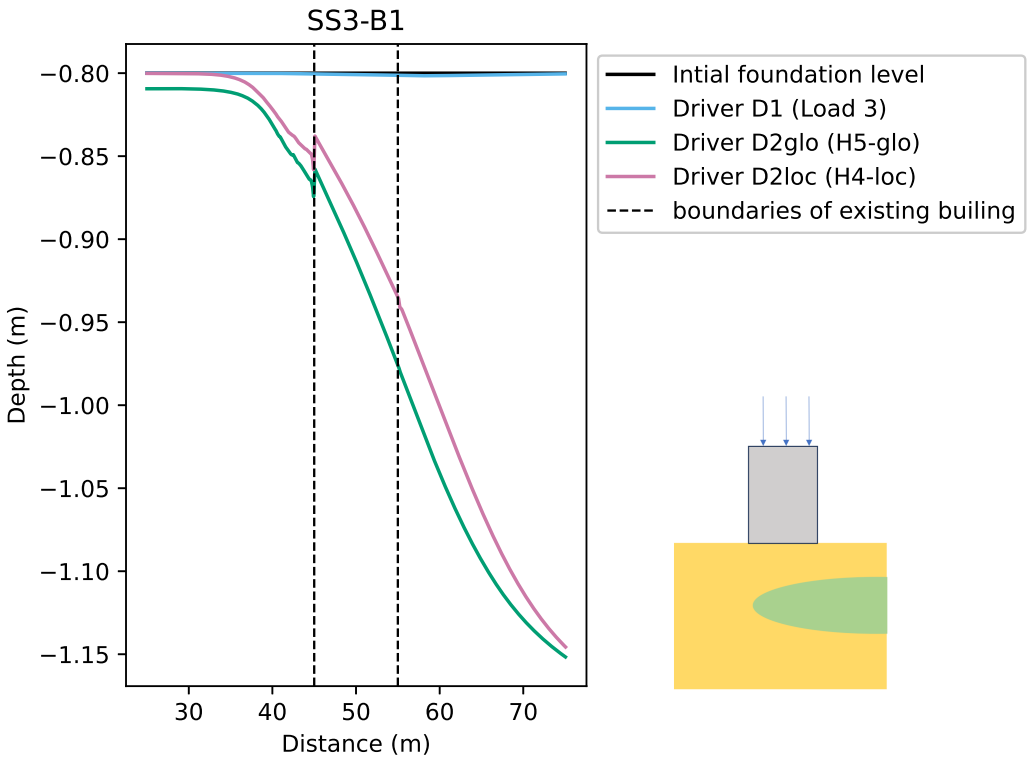

Figure 4.30: Surface settlement of Soil Scenario 3 (SS3)

From this figure, it can be deduced that drivers D2glo and D2loc show a similar pattern. Compared to the water-lowering drivers, driver D1 shows significantly less settlement.

4.1.4. Settlement computation: building scenarios with a basement (B2)

In this section, the results of the settlements for the different scenarios are presented. The same procedure as for the previous ground scenario has been applied. But unlike the previous sections, a building with a basement is now considered.

SS2-B2-D1

In this section, settlement results are presented for scenario SS2-B2-D1. This scenario is also selected as a scenario where the results of the finite element model are presented in more detail.

Figures 4.31 and 4.32 shows the deformed mesh for a situation with the existing building and the greenfield situation at the end of phase 6. The deformations are on an exaggerated scale, to make them more visible.

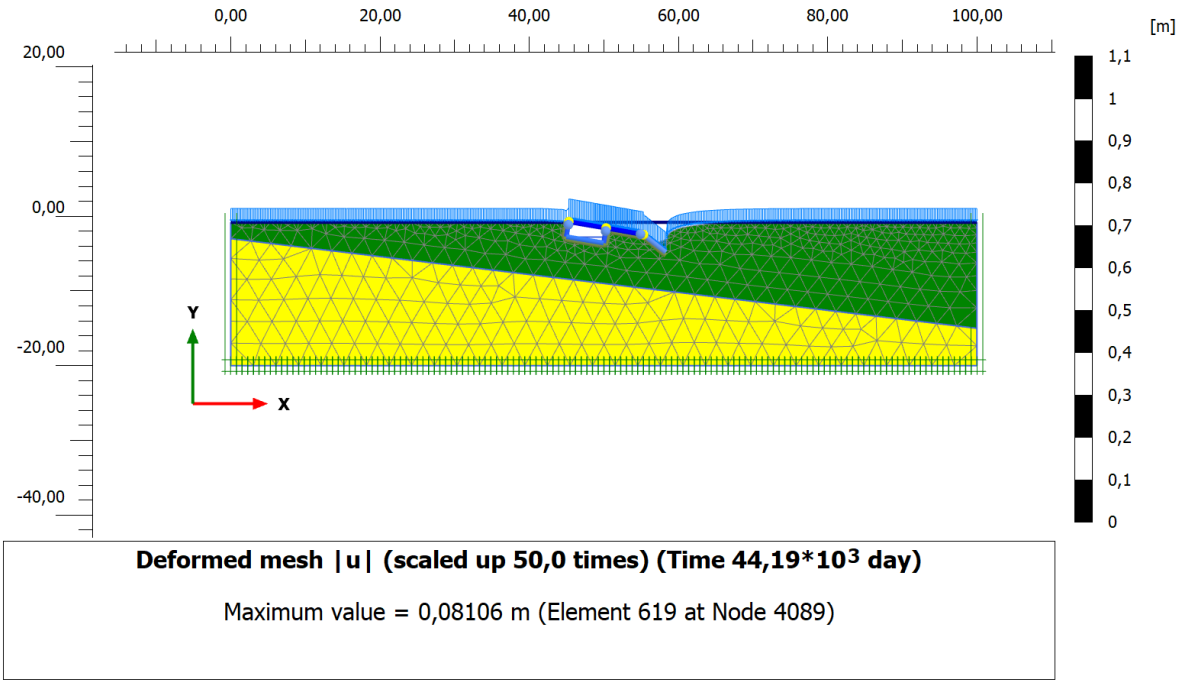

Figure 4.31: Deformed mesh scenario SS2-B2-D1

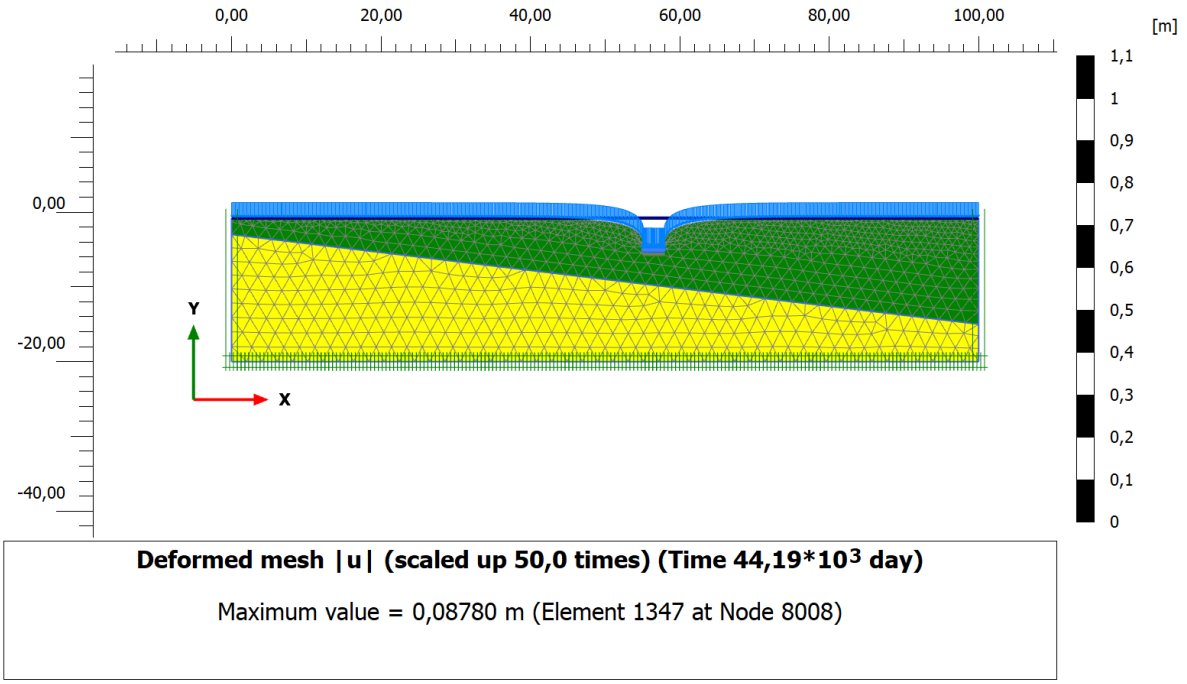

Figure 4.32: Deformed mesh scenario SS2-D1 (greenfield situation)

Figure 4.32 shows the result of the situation without the existing building, where only the driver, in this case an additional load (D1), is modelled. For consistency, this situation, like the groundwater-lowering drivers (D2glo and D2loc), is referred to as the greenfield situation. In reality, this is not a greenfield situation, but rather the situation where only the driver is acting.

Figure 4.31 shows that a coarser mesh is used for the situation with a basement compared to the greenfield situation, as seen in figure 4.32. Due to the long computation time in the situation of the basement, it was not possible to maintain the same mesh size.

Figure 4.33 shows the impact on the stresses of a node in the middle of the weak layer over time. The total stress, effective stress, and water pressure are plotted in a graph. The graph on the right shows the settlement of the same node. In both graphs, the moment of implementing the driver is indicated with a dashed orange line.

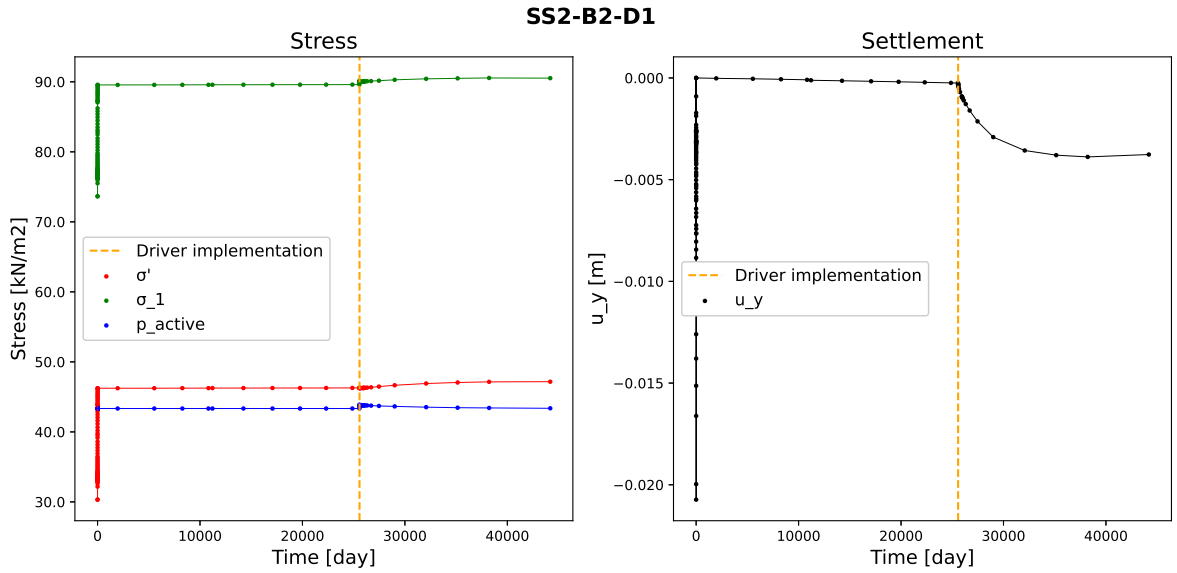

Figure 4.33: Left: Total stress, effective stress and the pore pressure over time for a node in the middle of the weak layer, Right: Settlement over time for the same the node in the middle of the weak layer. In both graphs, the moment of implementing the driver is indicated with a dashed orange line

When applying an additional load next to the existing building, a different distribution of stresses occurs compared to the drivers where groundwater is lowered. There is a clear difference in the behaviour of pore pressure, which naturally does not show such a significant decrease. Furthermore, it is noticeable that the stresses are relatively low in absolute terms for this scenario. The vertical line at t=0 in the time-settlement graph is caused by the initiation of soil stresses in the initial phase. Immediately afterward, this settlement is reset to zero, so it does not affect the final result.

Figures 4.34, 4.35 and 4.36 shows the excess pore pressure or phase 4, phase 5 and phase 6.

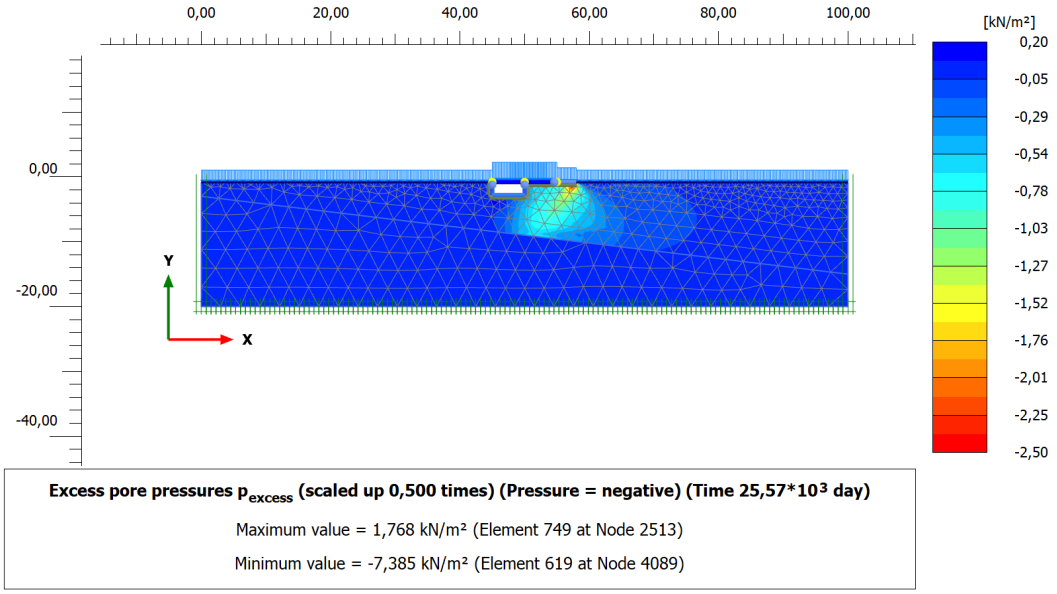

Figure 4.34: SS2-B2-D1: Excess pore pressure in phase 4, at the moment of implementing the driver, applying an additional load next to the existing building

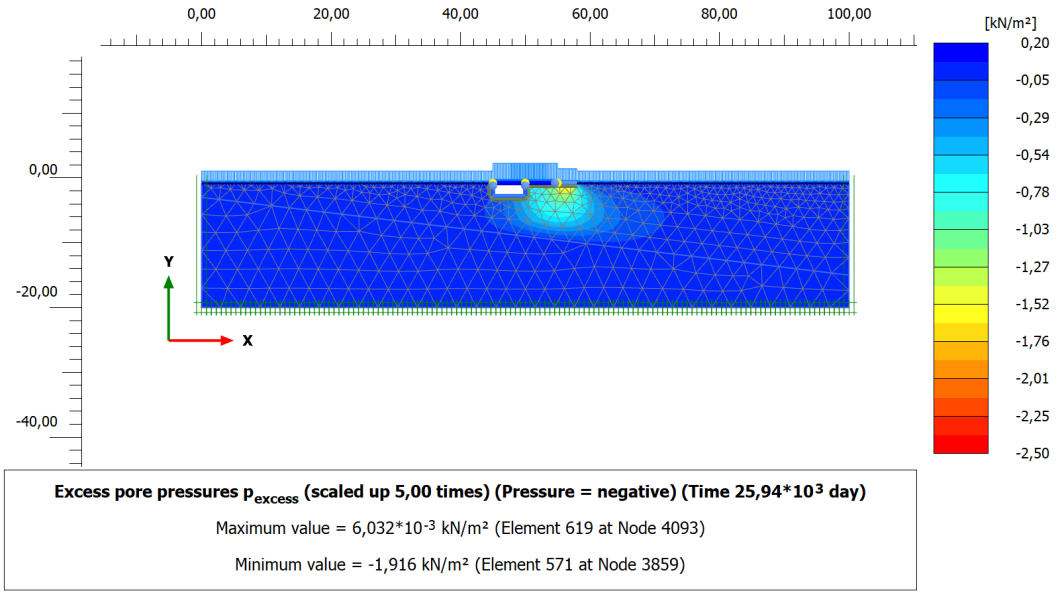

Figure 4.35: SS2-B2-D1: Excess pore pressure in phase 5, with a consolidation period of 1 year

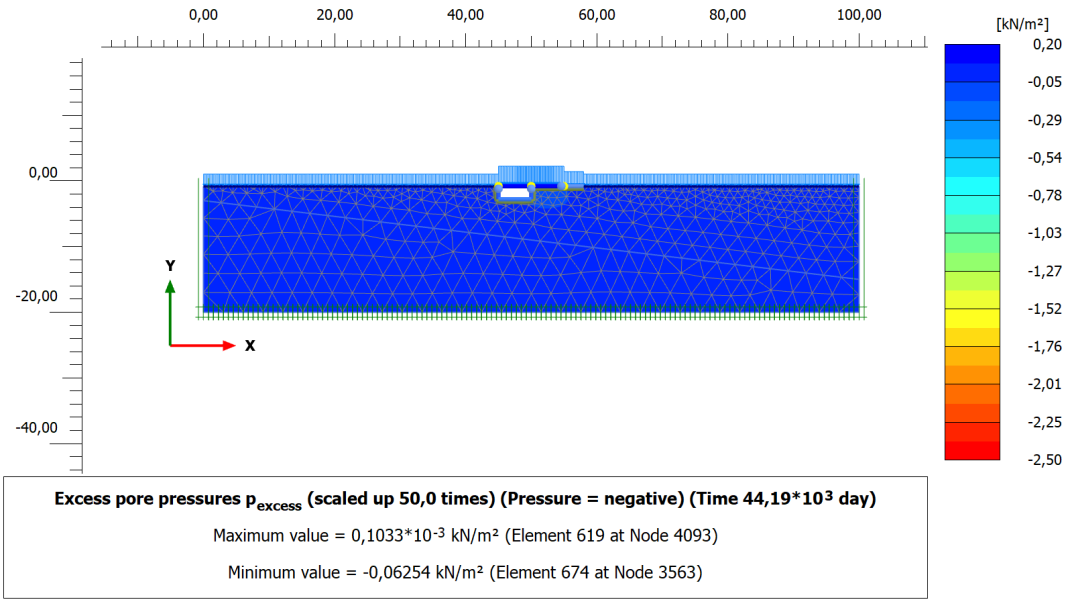

Figure 4.36: SS2-B2-D1: Excess pore pressure in phase 6, with a consolidation period of 50 years

The dissipation of excess pore pressure occurs, as expected, in the weak soil (clay layer). Despite the scale of the legends not being the same, it can be inferred from the values that the excess pore pressures decrease from the implementation of the driver to the final phase.

Figures 4.37, 4.38, and 4.39 present the results of surface settlements for soil scenarios SS1, SS2, and SS3 for the different drivers for the situation with a basement

SS1-B2
In figure 4.37 the settlement results with the different drivers are shown for a building with a basement with soil scenario SS1.

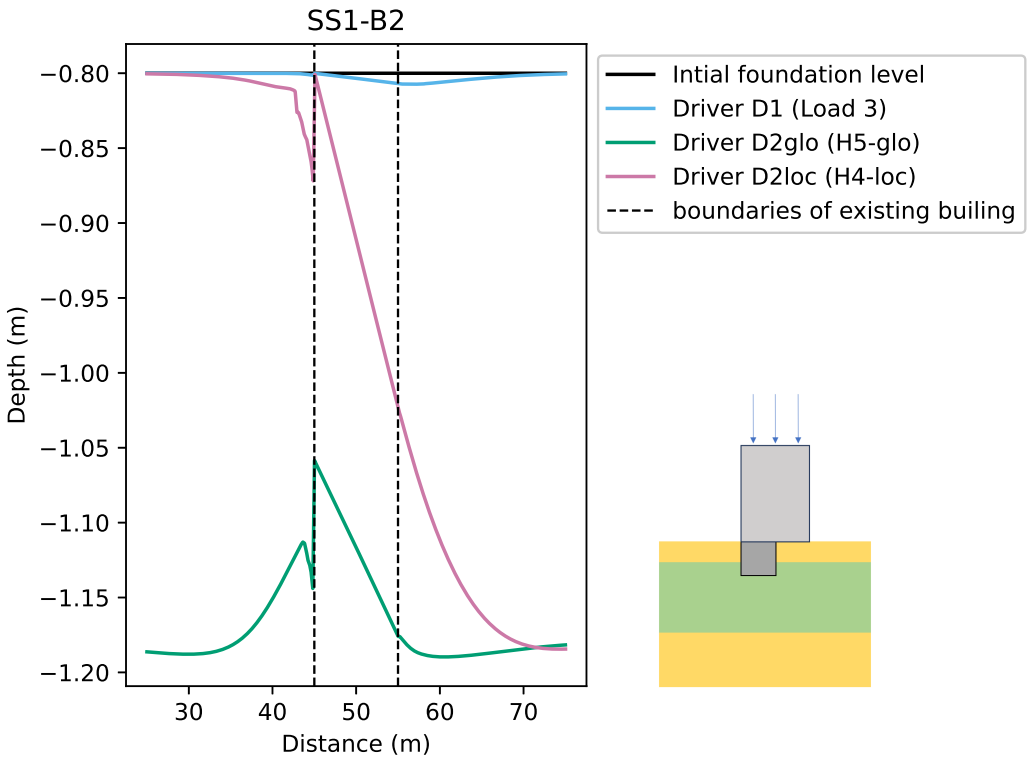

Figure 4.37: Settlement of the surface of scenario SS1-B2

SS2-B2
In figure 4.38 the settlement results with the different drivers are shown for a building with a basement with soil scenario SS2.

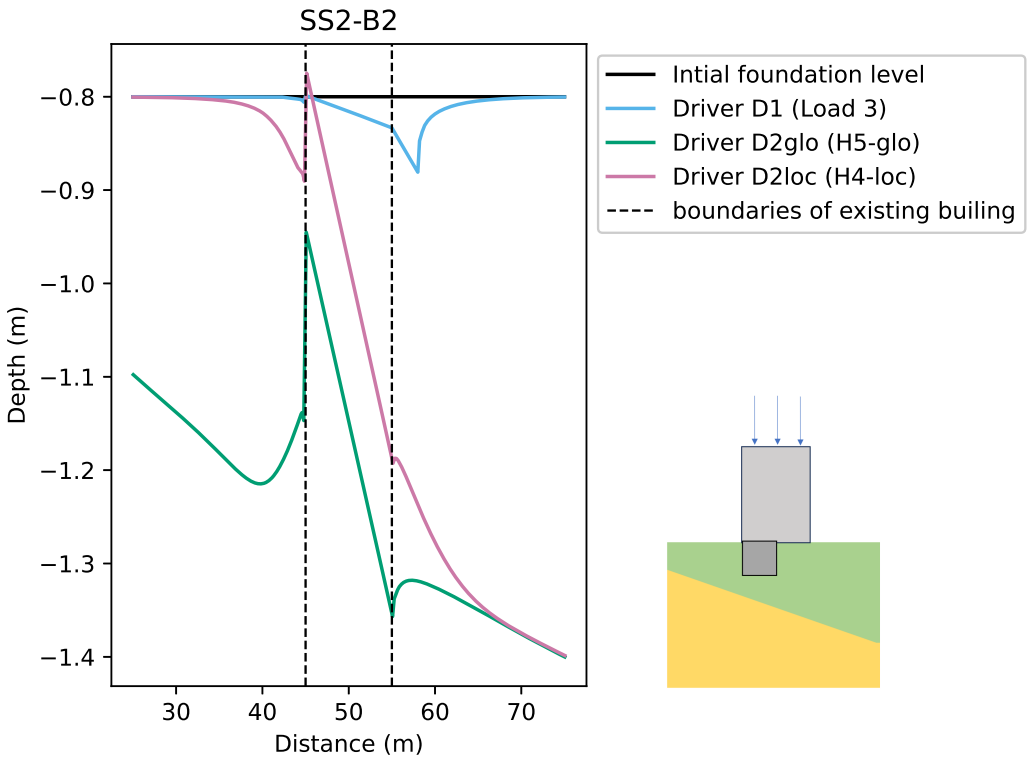

Figure 4.38: Settlement of the surface of scenario SS2-B2

SS3-B2
In figure 4.39 the settlement results with the different drivers are shown for a building with a basement with soil scenario SS3.

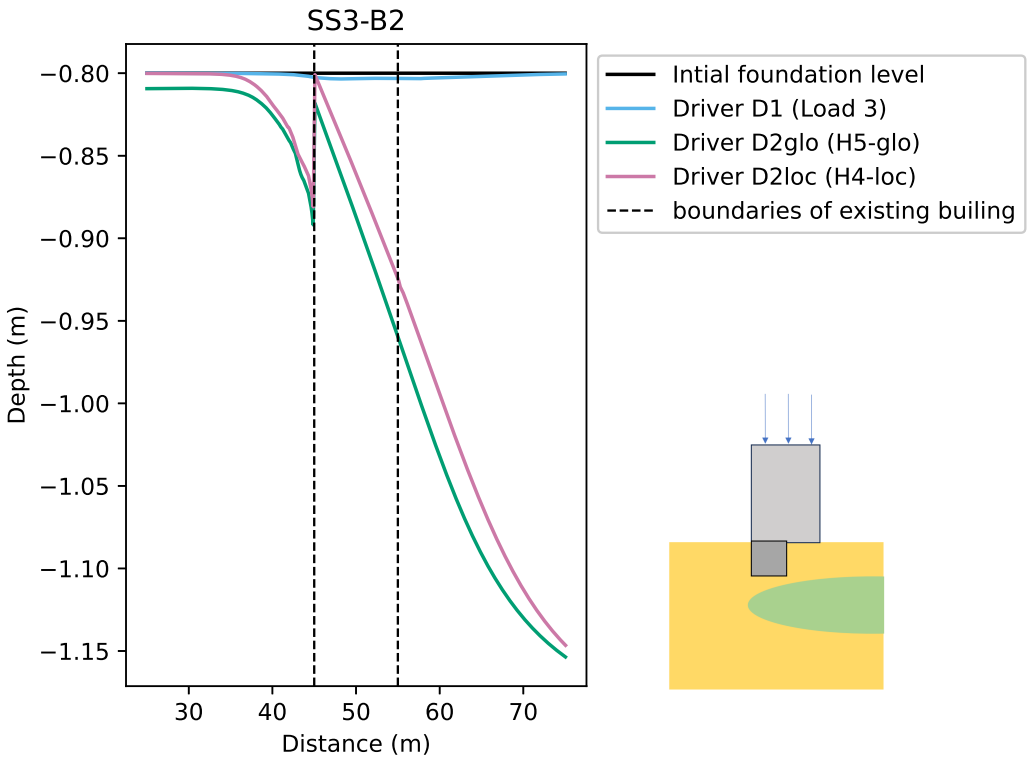

Figure 4.39: Settlement of the surface of scenario SS3-B2

From the graphs mentioned above, it is evident that there is a significantly greater differential settlement compared to the situation without a basement. Additionally, it is visible in these graphs that driver D1 results in relatively little settlement in absolute terms.

4.1.5. Internal forces structure

In this section, the internal forces of the structural elements are considered. Only scenario SS3-B1-D2loc (without basement) and SS3-B2-D2loc (with basement) are examined here because it is expected that the greatest forces in the structural element will occur in these scenarios. In figures 4.40 and 4.41, the total displacements, axial forces, bending moments, and shear forces are shown for these scenarios. This is only presented for the structural element that simulates the existing building. For both scenarios, these are provided for the final phase with the highest driver intensity. The results in the graph are scaled for a better visualization. The scale is indicated in the different figures. The scale is not the same for all graphs.

Total displacements |u| (scaled up 10,0 times) (Time 44,19*10³ day)

Maximum value = 0,1605 m (Element 20 at Node 5286)

(a) Total displacements SS3-B1-D2loc

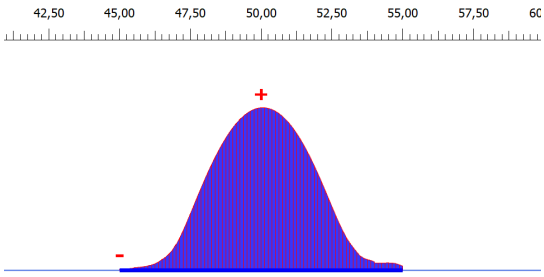

Axial forces N (scaled up 0,200 times) (Time 44,19*10³ day)

Maximum value = 28,71 kN/m (Element 11 at Node 5323)

Minimum value = 0,2320 kN/m (Element 1 at Node 5360)

(b) Axial forces SS3-B1-D2loc

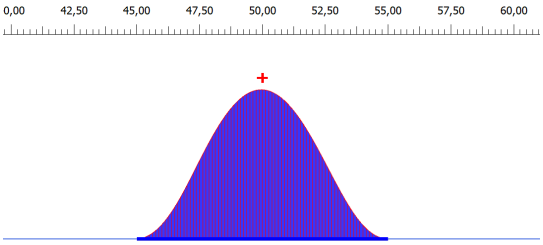

Bending moments M (scaled up 0,0500 times) (Time 44,19*10³ day)

Maximum value = 118,7 kN m/m (Element 10 at Node 5323)

Minimum value = -0,02198*10^{-12} kN m/m (Element 20 at Node 5286)

(c) Bending moments SS3-B1-D2loc

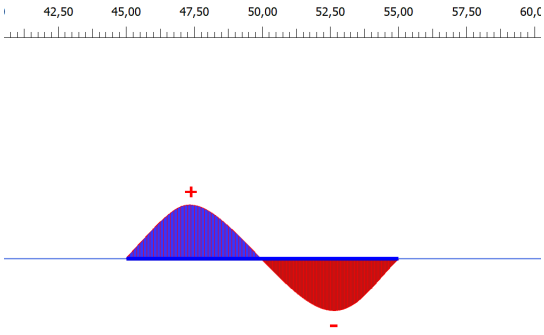

Shear forces Q (scaled up 0,0500 times) (Time 44,19*10³ day)

Maximum value = 39,60 kN/m (Element 5 at Node 5346)

Minimum value = -38,23 kN/m (Element 16 at Node 5300)

(d) Shear forces SS3-B1-D2loc

Figure 4.40: Internal forces and total displacements for scenario SS3-B1-D2loc

Figure 4.40b shows the axial forces in the structural element for scenario SS3-B1-D2loc. A positive sign denotes tension, whereas a negative sign denotes compression. The building is subjected to tension, with the maximum tensile force occurring at the centre of the structure. The maximum bending moments also occur at the centre of the building for this situation, see figure 4.40c.

(a) Total displacements SS3-B2-D2loc

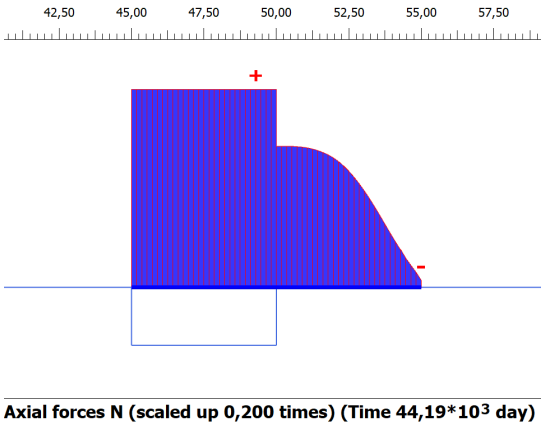

(b) Axial forces SS3-B2-D2loc

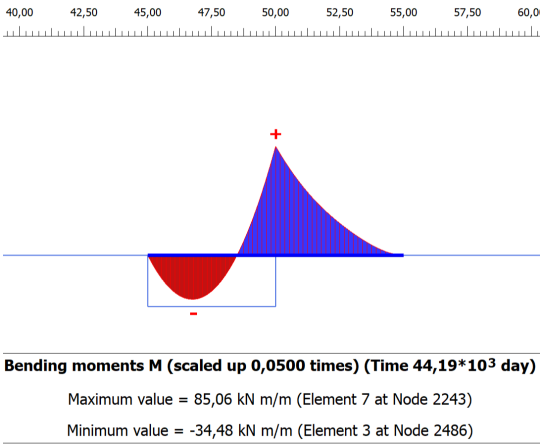

(c) Bending moments SS3-B2-D2loc

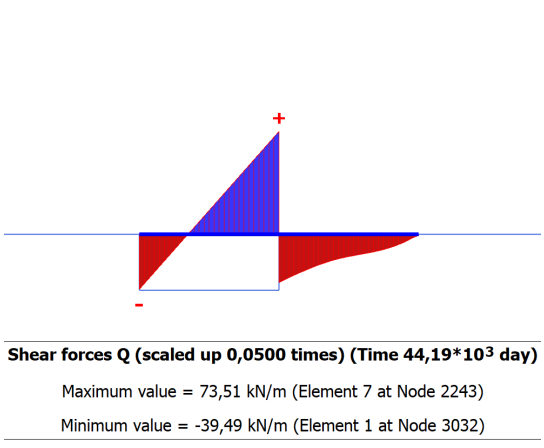

(d) Shear forces SS3-B2-D2loc

Figure 4.41: Internal forces and displacements for scenario SS3-B2-D2loc

While the total displacement between the scenario without a basement compared to the scenario with a basement does not differ significantly, the graphs depicting the internal forces do.

Figure 4.41b shows that the largest axial forces occur within the boundaries of the basement. Additionally, figure 4.41c shows that the maximum bending moment occurs at the boundary between the section with a basement and the section without a basement of the existing building.

4.2. Damage Assessment

In this section, a damage assessment is conducted with the aim of providing a measure of the different drivers on the resulting damage to the existing building.

In the first part of this section, the scenario is considered for a building without a basement, followed by a sensitivity analysis examining the influence of stiffness of the building on the damage. Finally, the damage is assessed in the scenario of a building with a basement.

Different damage parameters are considered here, which can be related to the extent of damage to a building.

$$\delta\rho_{max} = u_{y,max} - u_{y,min} \tag{4.1}$$

$$\epsilon_{hor} = \frac{\Delta L}{L} \tag{4.2}$$

$$\beta_{max} = \frac{\Delta u_y}{\Delta u_x} - \omega \tag{4.3}$$

- Formula 4.1: $\delta\rho_{\text{max}}$ represents the maximum differential settlement, calculated as the difference between $u_{y,\text{max}}$ and $u_{y,\text{min}}$, where u_y denotes vertical displacement.
- Formula 4.2: ϵ_{hor} denotes the horizontal strain, calculated as the change in length ΔL relative to the original length L.
- Formula 4.3: β_{max} represents the maximum angular distortion, calculated as the ratio between the change in vertical displacement Δu_y and the change in horizontal displacement Δu_x, subtracted by the tilt ω.

To determine the maximum differential settlement, formula 4.1 and the maximum angular distortion, formula 4.3, the calculation was iterated over each node. The horizontal strain, formula 4.2 was determined based on the horizontal strain of the endpoints. For a complete overview of the calculations, see Appendix C.

4.2.1. Damage Assessment: Building without a basement (B1)

In this section, the damage has been assessed for an existing building without a basement. The damage parameters, maximum angular distortion and horizontal strain, have been determined as described in the previous section. The damage is then assessed using the Boscardin and Cording graph (Boscardin and Cording, 1989). The Boscardin and Cording graph is plotted as a watermark to allow for an easy comparison with the results. Figures 4.42, 4.43 and 4.44 present the results.

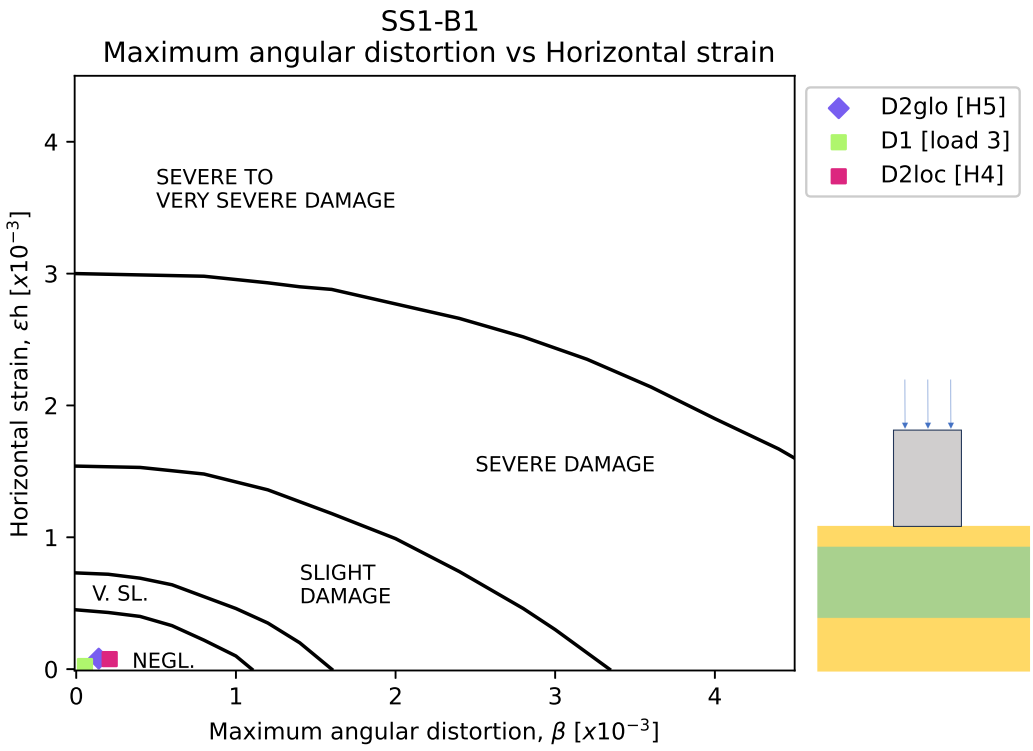

Figure 4.42: Damage assessment SS1-B1: The maximum angular distortion is plotted against the horizontal strain. This is done for the different drivers with the highest intensity. The Boscardin and Cording graph is plotted in the background as a watermark.

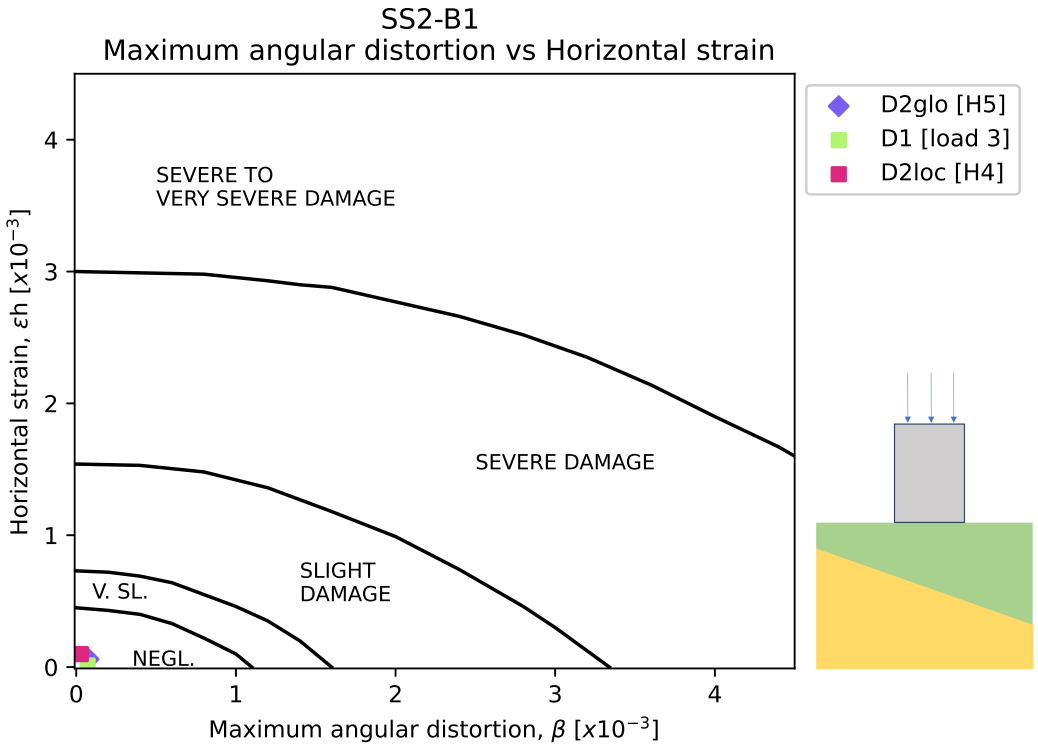

Figure 4.43: Damage assessment SS2-B1: The maximum angular distortion is plotted against the horizontal strain. This is done for the different drivers with the highest intensity. The Boscardin and Cording graph is plotted in the background as a watermark.

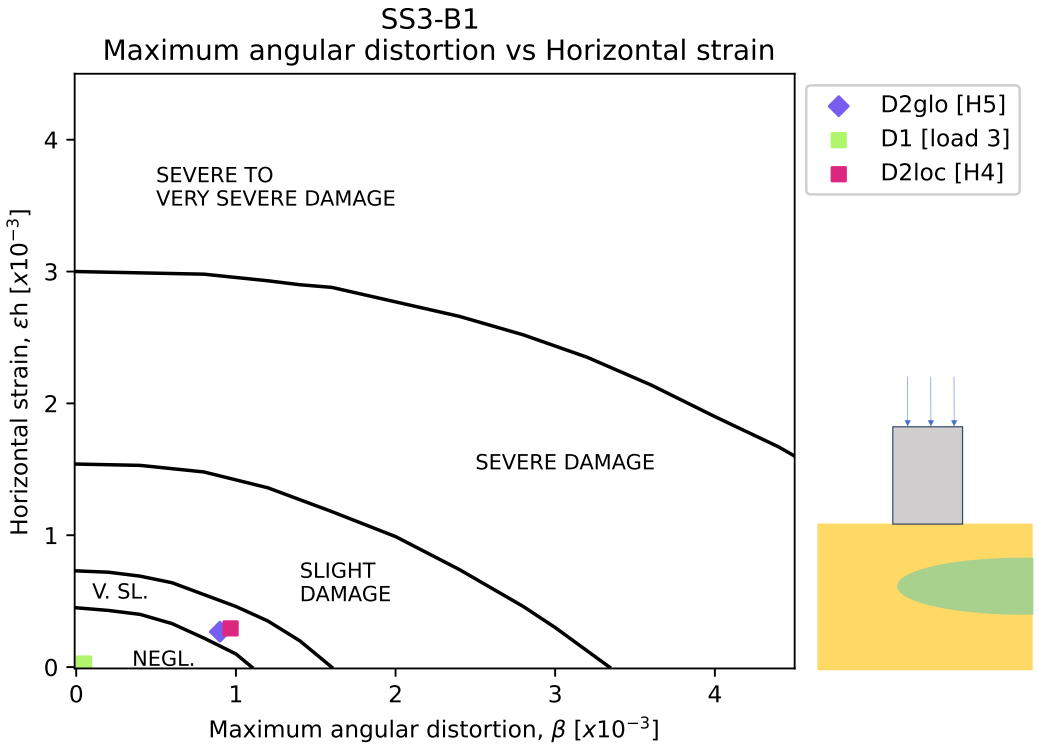

Figure 4.44: Damage assessment SS3-B1: The maximum angular distortion is plotted against the horizontal strain. This is done for the different drivers with the highest intensity. The Boscardin and Cording graph is plotted in the background as a watermark.

In the above figures, it is visible that in all scenarios the damage is negligible, except in the case of soil scenario SS3 with global and local groundwater lowering, where a very small amount of damage occurs.

4.2.2. Influence of building stiffness

The stiffness of a building is a significant factor in the extent of damage caused by settlements. A sensitivity analysis has been conducted to evaluate the impact of the axial stiffness and the bending stiffness on the damage parameters. This is executed for the different drivers of scenario SS3-B1. The variations in stiffness for the building are applied as shown in table 3.12. The results are shown in figure 4.47, considering the angular distortion against horizontal strain. So that these results can be compared with the graph Boscardin and Cording (Boscardin and Cording, 1989).

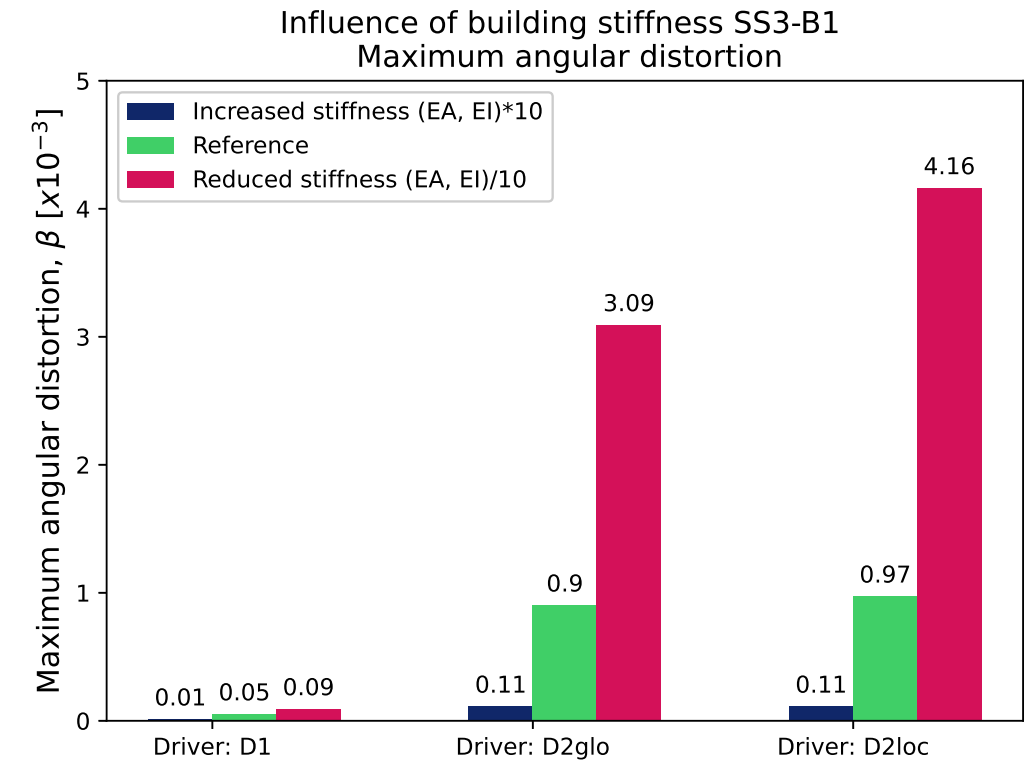

Figure 4.45: Sensitivity analysis: Influence of the building stiffness on the angular distortion using scenario SS3-B1 as example

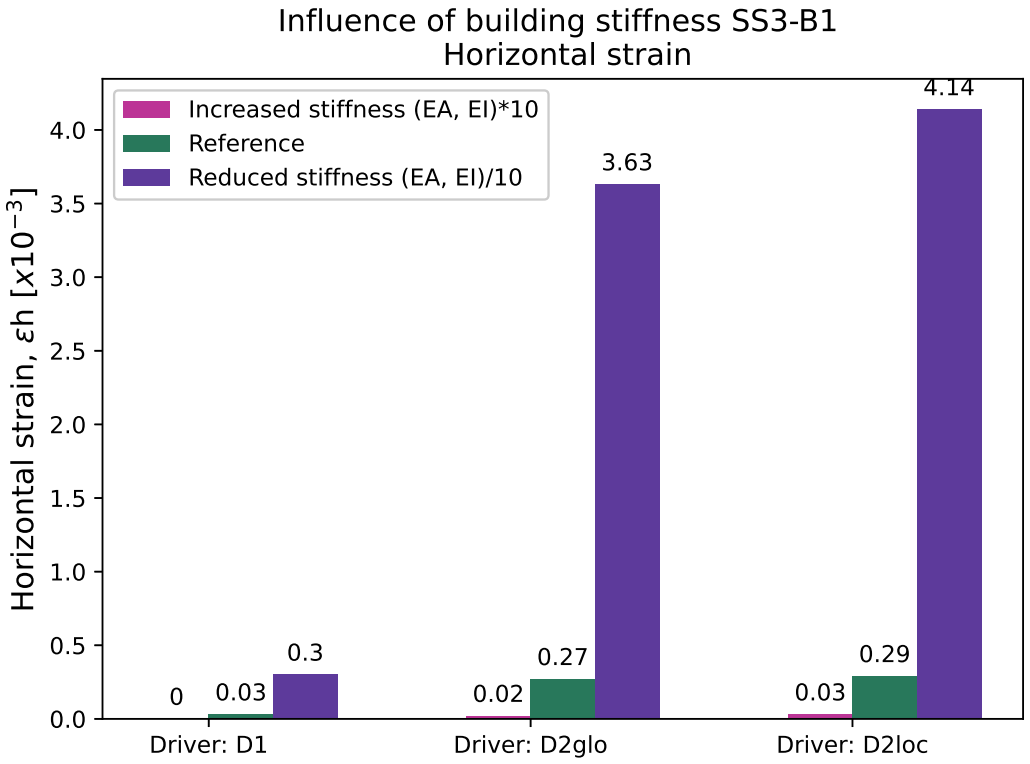

Figure 4.46: Sensitivity analysis: Influence of the building stiffness on the horizontal strain using scenario SS3-B1 as example

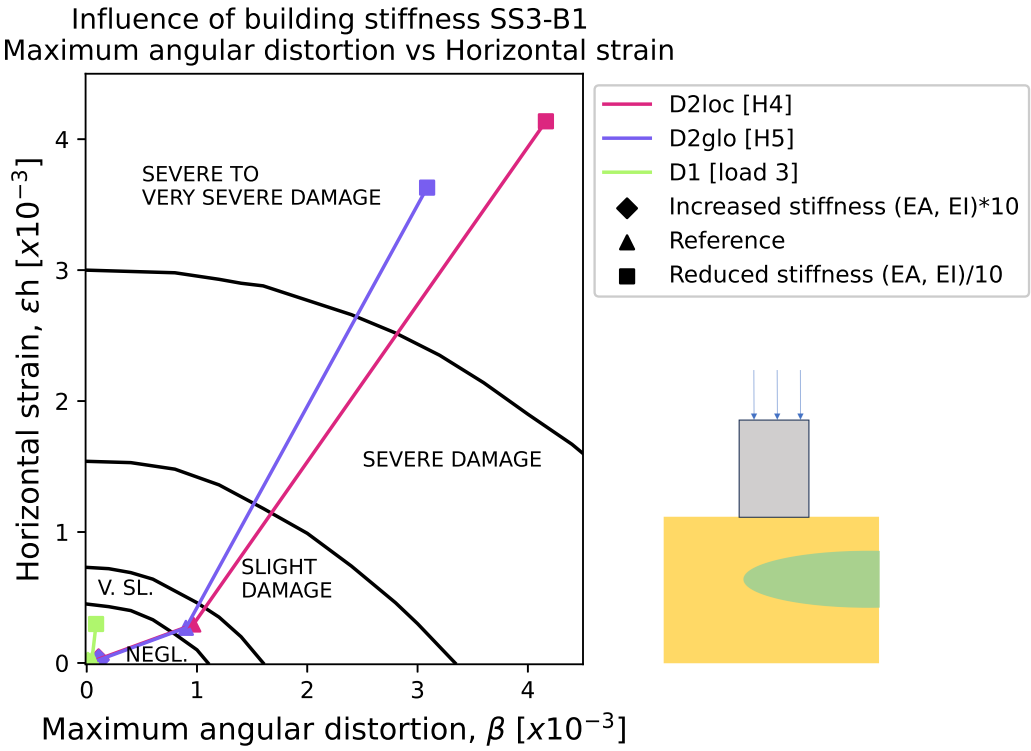

Figure 4.47: Influence of building stiffness of scenario SS3-B1: The maximum angular distortion is plotted against the horizontal strain. This is done for the different drivers with the highest intensity, where the stiffness of the building has been varied The Boscardin and Cording graph is plotted in the background as a watermark.

Figures 4.45 and 4.46 show the results of a sensitivity analysis of the influence of building stiffness on angular distortion and horizontal strain. Stiffness was varied by increasing it by a factor of 10 and decreasing it by a factor of 0.1. These factors were applied to both axial stiffness and bending stiffness. What is noticeable is that both the maximum angular distortion and the maximum horizontal strain significantly increase with decreasing stiffness.

When comparing the results in figure 4.47, it is noticeable that the horizontal strains are relatively low for the reference stiffness. For a building with the reference stiffness, all damage parameters are relative low, resulting in a very slightly amount of damage in the case of a global and a local water level lowering. When the stiffness of the existing building is reduced, the damage parameters increase, as expected. But what stands out is that the occurring damage in the case of driver D1 is negligible even for the reduced stiffness.

To compare the stiffness of the existing building with the actual stiffness values from literature, the relative bending stiffness is plotted against the modification factor. Using the results presented in figure 4.48, the bending stiffness of the building can be compared with that of Potts and Addenbrooke, 1997. The formulas used for this purpose are presented below. It should be noted that, unlike Potts and Addenbrooke where the deflection ratio is used, the maximum angular distortion has been used to determine the modification factor. For the soil stiffness, an average was taken over the height of the acting driver.

$$\rho^* = \frac{EI_{building}}{E_{soil}\frac{B}{2}^4} \tag{4.4}$$

$$M = \frac{\beta}{\beta_{greenfield}} \tag{4.5}$$

- ρ^* = Relative bending stiffness [-]

- EI_{building} = Bending stiffness of the building
- E_{soil} = Young's modulus of the soil
- B = Width of the building

- M = Modification factor [-]
- β = Angular distortion for the specific scenario
- $\beta_{\text{greenfield}}$ = Angular distortion for the greenfield scenario for a specific driver

In the graph, the results are displayed for the scenarios with the reference stiffness. Additionally, the results are also shown for soil scenario SS3, with a reduced and an increased stiffness, as determined in section 4.2.2

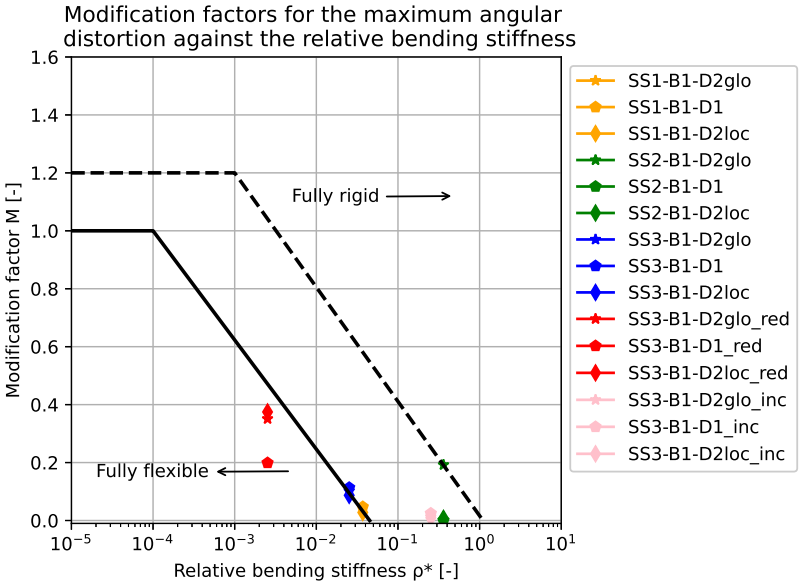

Figure 4.48: Modification factors for the angular distortion against the relative bending stiffness

When the results are located in the bottom right corner of the graph, the bending stiffness of the building is relatively high compared to the findings of Potts and Addenbrooke.

4.2.3. Damage Assessment: Building with a basement (B2)

In addition to the building without a basement, the damage was also assessed for the situation where the building does have a basement. The same procedure was followed as in section 4.2.1.

In figures 4.49, 4.50, and 4.51, the angular distortions are plotted against the horizontal strain for the different scenarios with a basement. The results are again compared with the graph of Boscardin and Cording (Boscardin and Cording, 1989).

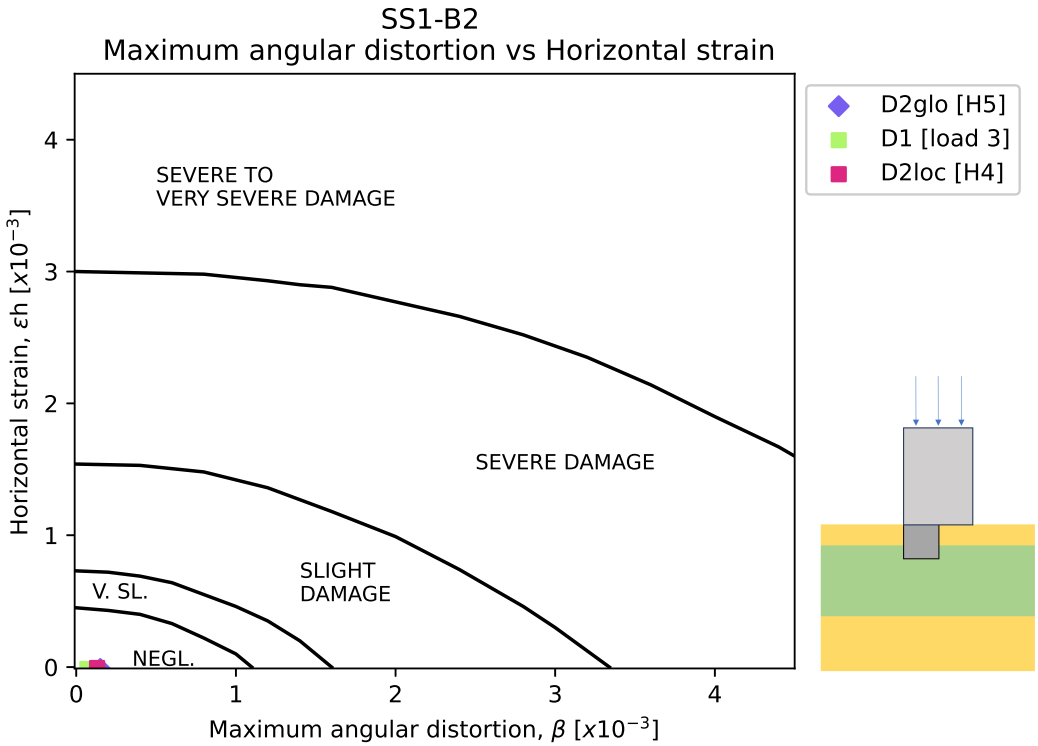

Figure 4.49: Damage assessment SS1-B2: The maximum angular distortion is plotted against the horizontal strain. This is done for the different drivers with the highest intensity. The Boscardin and Cording graph is plotted in the background as a watermark.

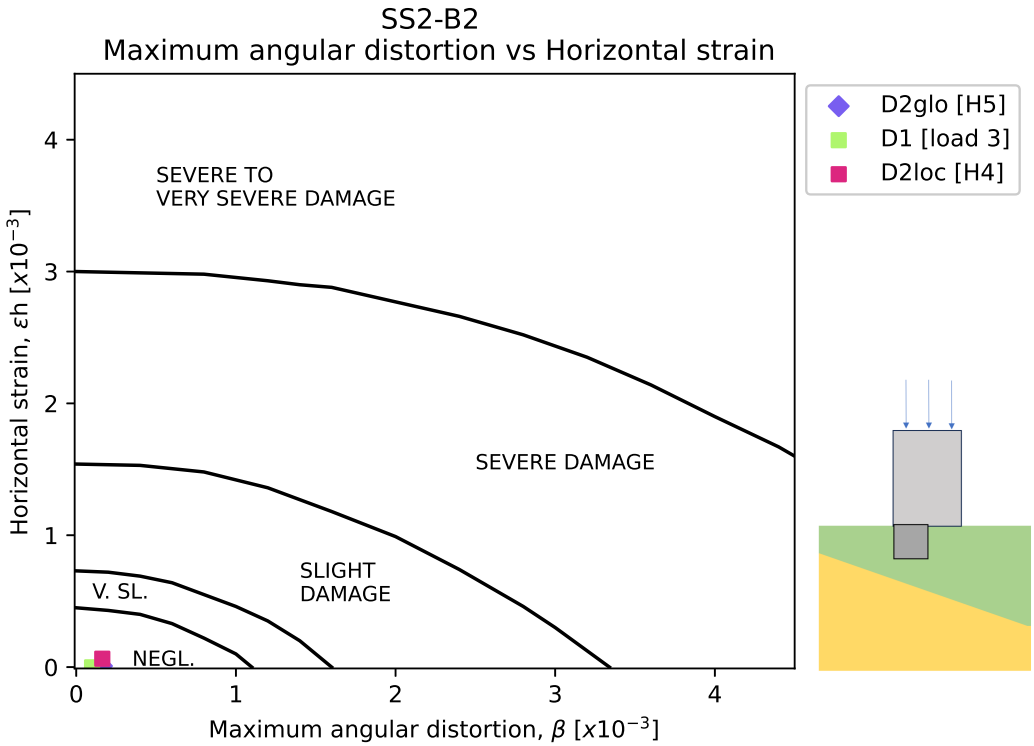

Figure 4.50: Damage assessment SS2-B2:The maximum angular distortion is plotted against the horizontal strain. This is done for the different drivers with the highest intensity. The Boscardin and Cording graph is plotted in the background as a watermark.

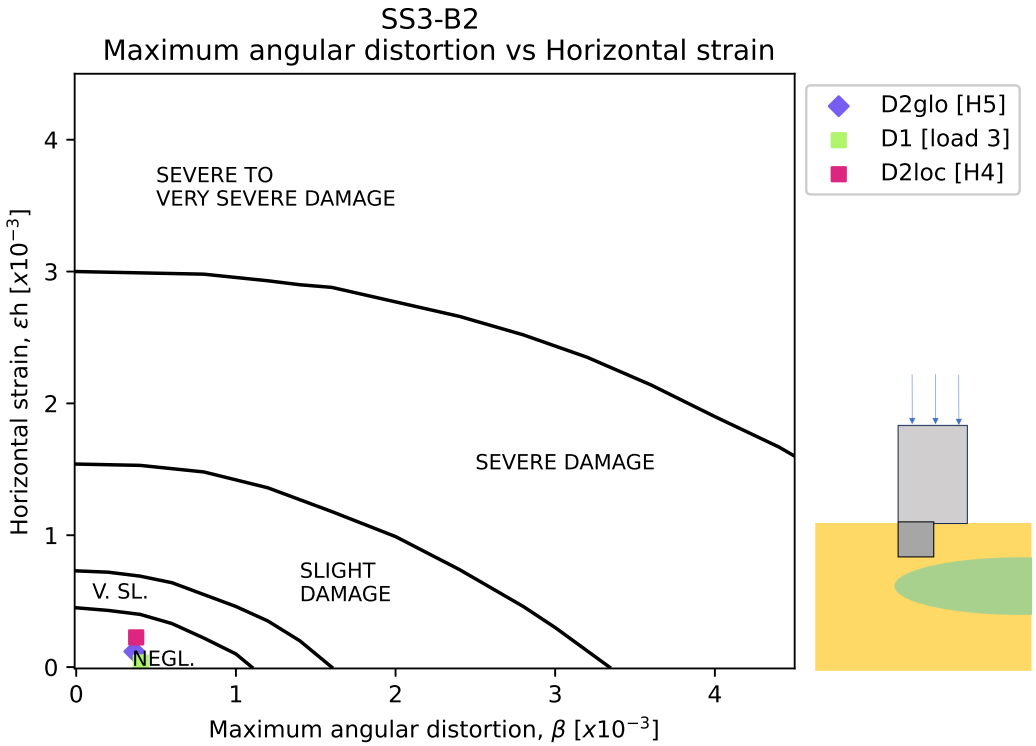

Figure 4.51: Damage assessment SS3-B2: The maximum angular distortion is plotted against the horizontal strain. This is done for the different drivers with the highest intensity. The Boscardin and Cording graph is plotted in the background as a watermark.

As shown in above figures, the damage for each scenario is negligible. Compared to the situation where the building has no basement, the occurring damage for the scenario with a basement is smaller.

4.3. Driver severity

To consider the influence of the different drivers, the values of the damage parameters from the situation with the existing building have been compared to those from the greenfield situations. This was done for different intensities of the drivers. The considered parameters are the maximum angular distortion, the maximum settlement and the maximum differential settlement. In the upcoming graphs, a dashed line also indicates where the value of the damage parameters for the situation with the existing building and the greenfield situation are equal. The steeper the slope of the graph, the greater the relative influence of the driver on the existing building, which potentially will cause more damage. The terms 'Unfavourable' and 'Favourable' refer to the influence of the building on the driver. This is indicated in the graphs with the text 'unfavourable,' or when the slope of the graph is less steep, 'favourable.'

In the first sections, only a building without a basement (B1) is considered. From section 4.3.6 onwards, the influence of the basement is taken into account.

4.3.1. Angular distortion

First, the results of the driver severity for the angular distortions were determined In figures 4.52, 4.53,4.54 the angular distortion of all drivers are plotted against the angular distortion for the situation where the load from the existing building is omitted, so the greenfield situation.

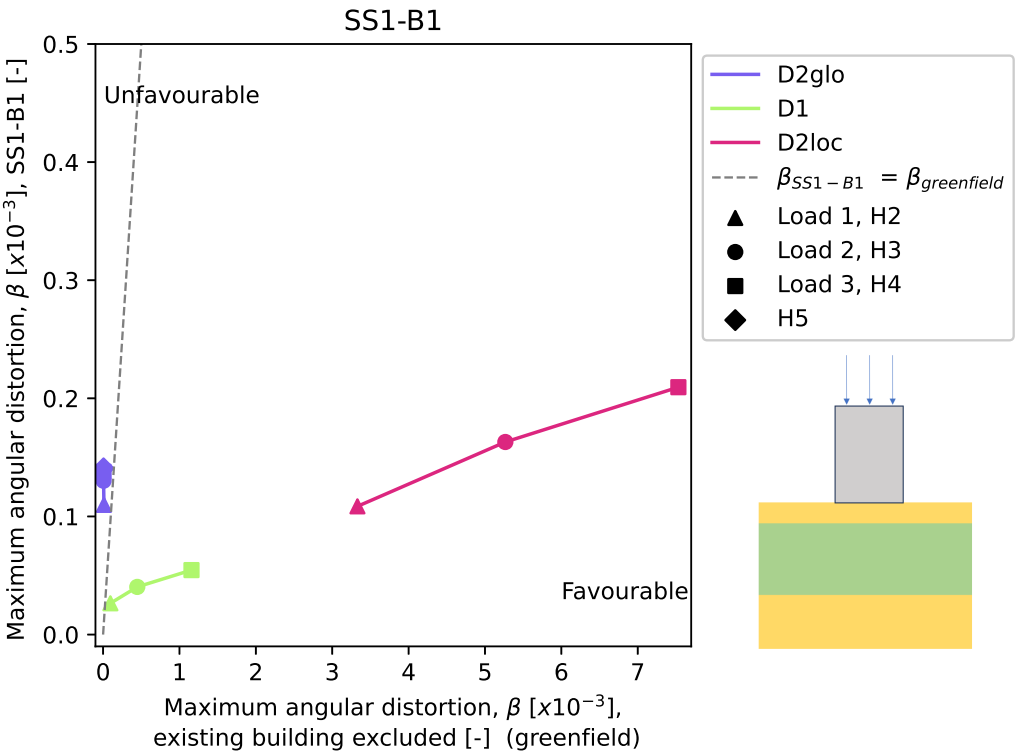

Figure 4.52: Angular distortion without building [-] vs angular distortion with building [-]

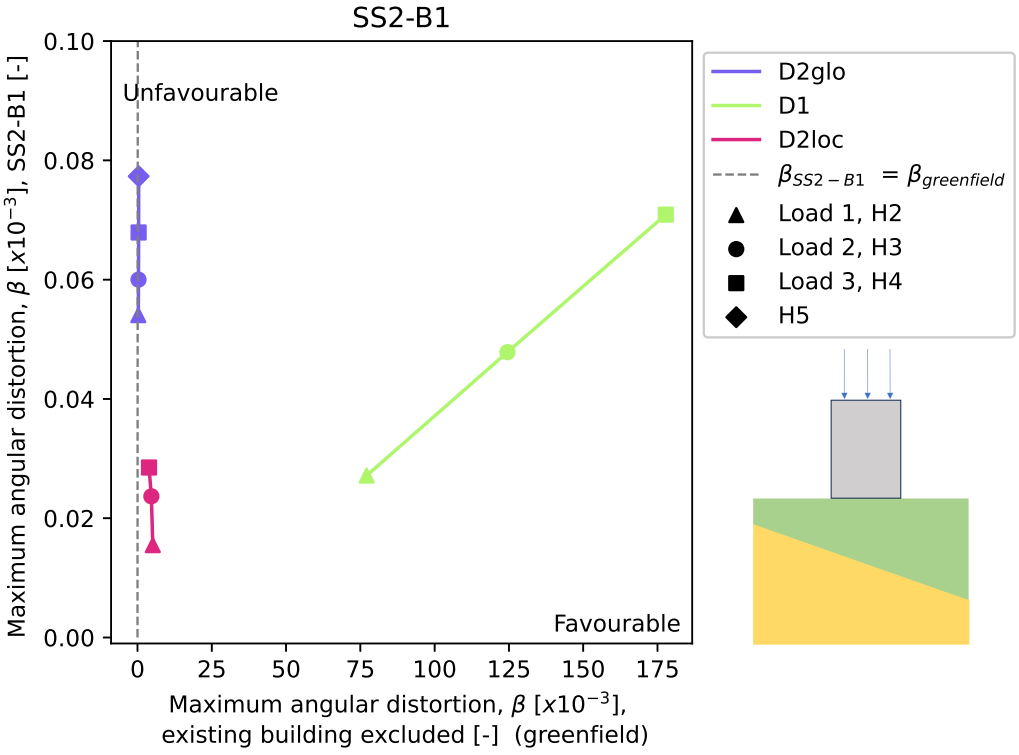

Figure 4.53: Angular distortion without building [-] vs angular distortion with building [-]

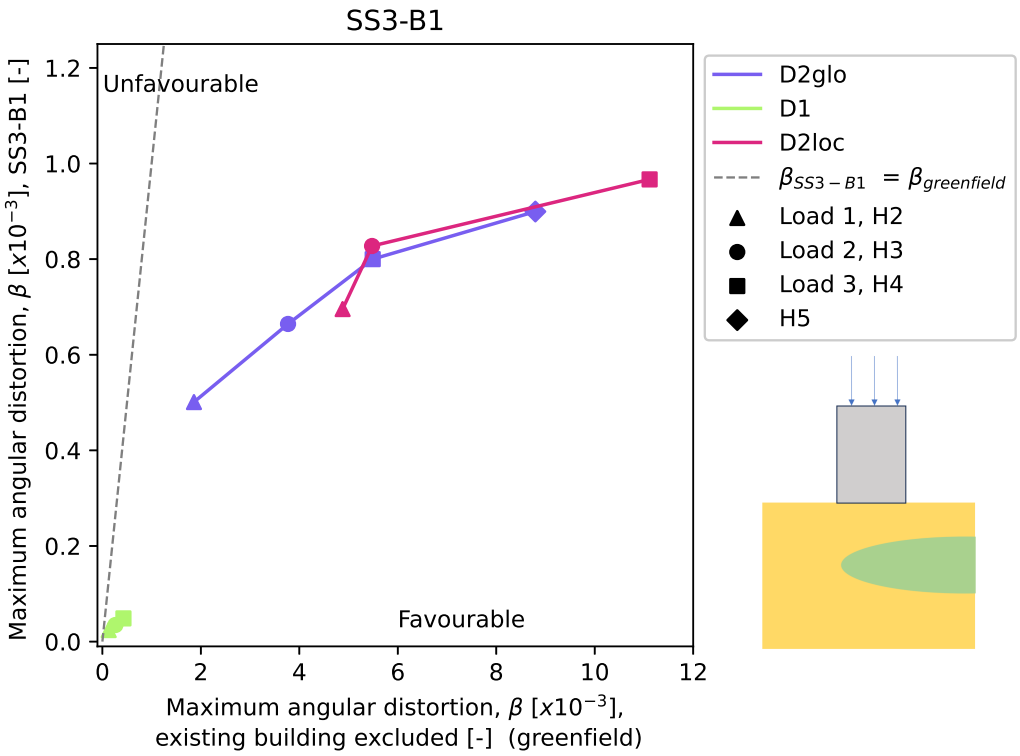

Figure 4.54: Angular distortion without building [-] vs angular distortion with building [-]

What can be observed from figures 4.52, 4.53,4.54 is that the angular distortions for the situation with the existing building are very small compared to the greenfield situation. This is especially the case for soil scenarios SS1 and SS2. Additionally, it is noticeable that the angular distortion for the greenfield situation in the case of ground scenario SS2 with driver D1 is very large compared to all other scenarios.

4.3.2. Maximum settlement

In figures 4.55, 4.56 and 4.57, the same procedure as in section 4.3.1 is applied, but for maximum settlement. The intensity of the different drivers has been varied again.

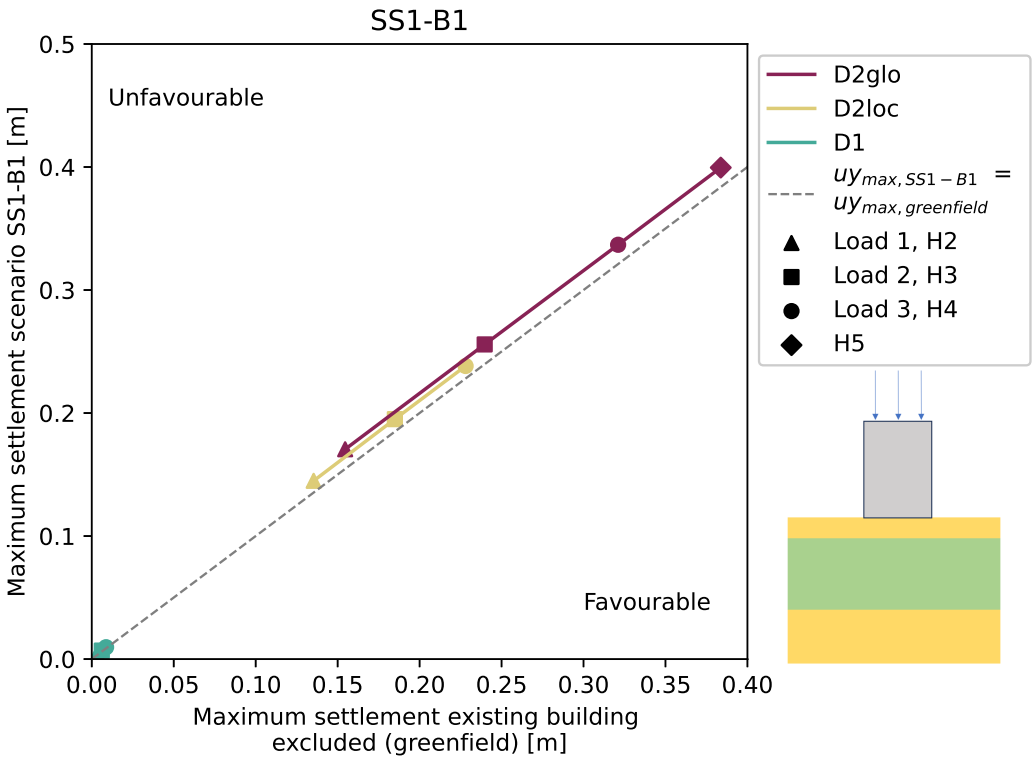

Figure 4.55: Maximum settlement without building [m] vs Maximum settlement with building [m]

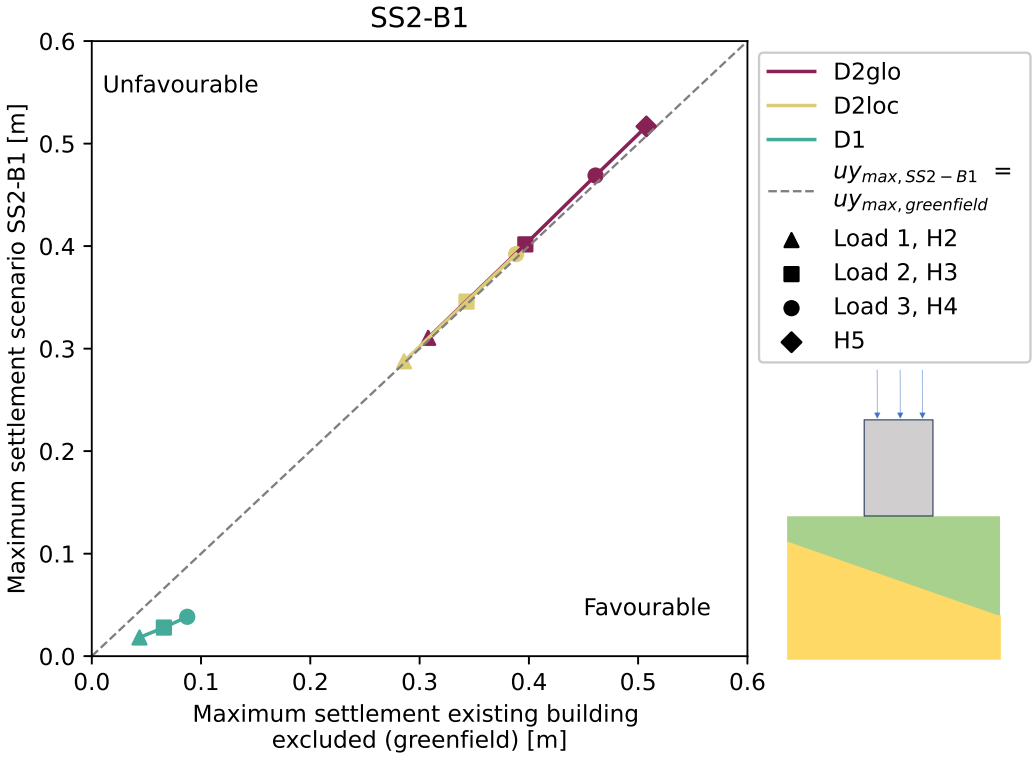

Figure 4.56: Maximum settlement without building [m] vs Maximum settlement with building [m]

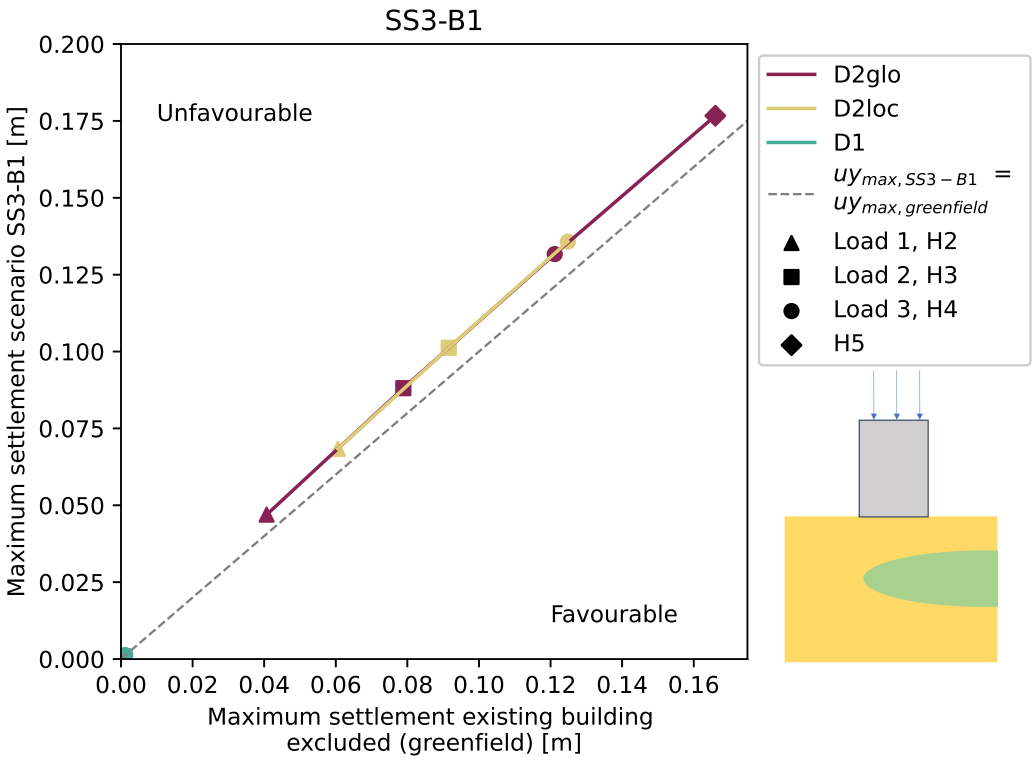

Figure 4.57: Maximum settlement without building [m] vs Maximum settlement with building [m]

The maximum settlements for the different drivers show an almost parallel pattern for the situation with the existing building compared to the greenfield situation. In all cases, there is slightly more maximum settlement in the situation with the existing building. An exception to this is driver D1 in the case of soil scenario SS2. Besides that, it is visible that the maximum settlements for soil scenario SS3 are relatively small compared to the other soil scenarios.

4.3.3. Differential settlement

In figures 4.58, 4.59 and 4.60, the same procedure as in section 4.3.1 and 4.3.2 is applied, but now for maximum differential settlement.

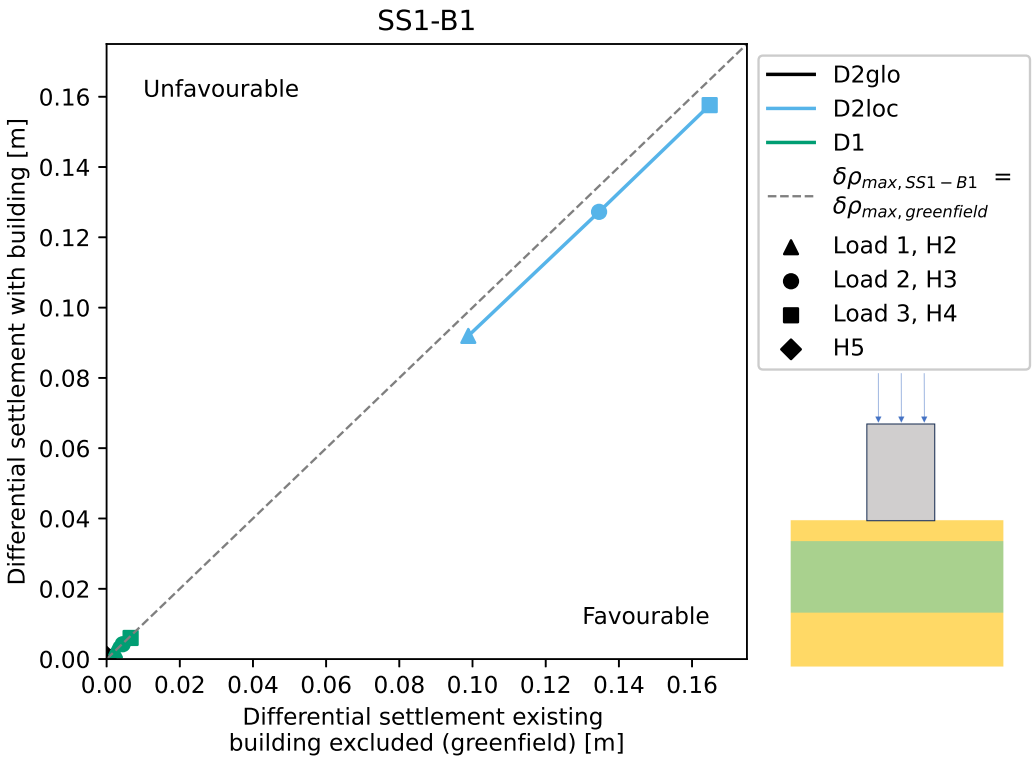

Figure 4.58: Differential settlement without building [m] vs Differential settlement with building [m] for SS1-B1

In the case of soil scenario SS1, it is visible that with a local groundwater lowering, the differential settlement is almost parallel in the situation with the existing building compared to the greenfield situation. The differential settlement in the case of drivers D1 and D2glo are very small for this soil scenario.

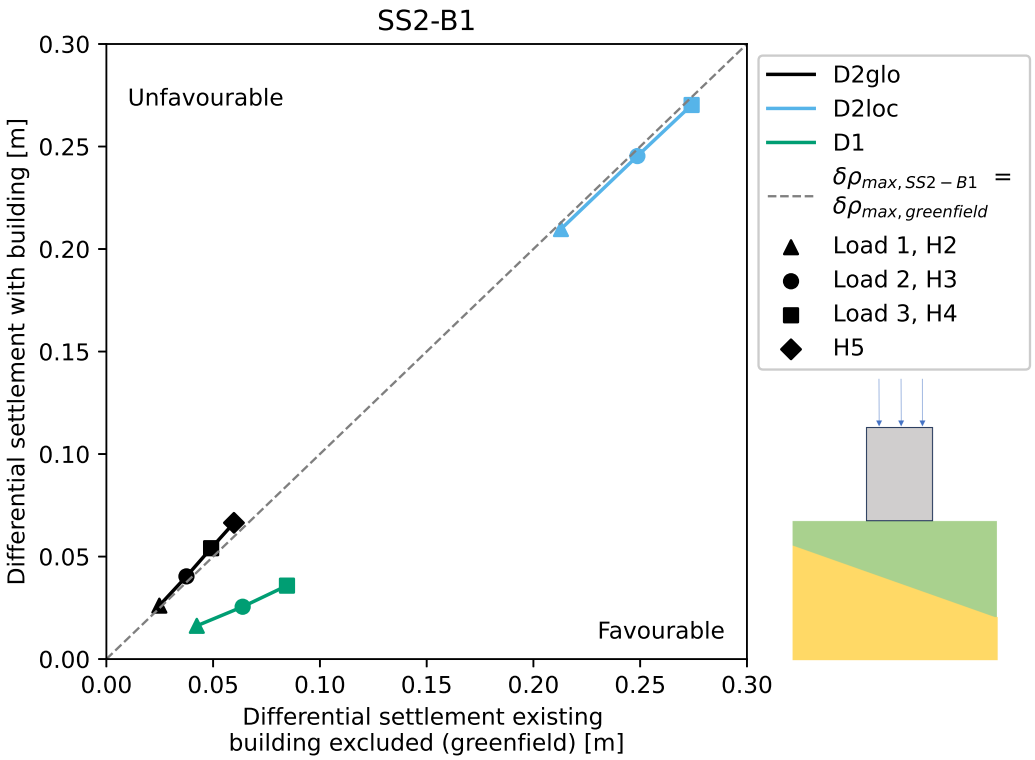

Figure 4.59: Differential settlement without building [m] vs Differential settlement with building [m] for SS2-B1

In the case of soil scenario SS2, it is visible that with a global and local groundwater lowering, the differential settlement is almost parallel in the situation with the existing building compared to the greenfield situation. The differential settlement in the case of driver D1 is lower in the greenfield situation.

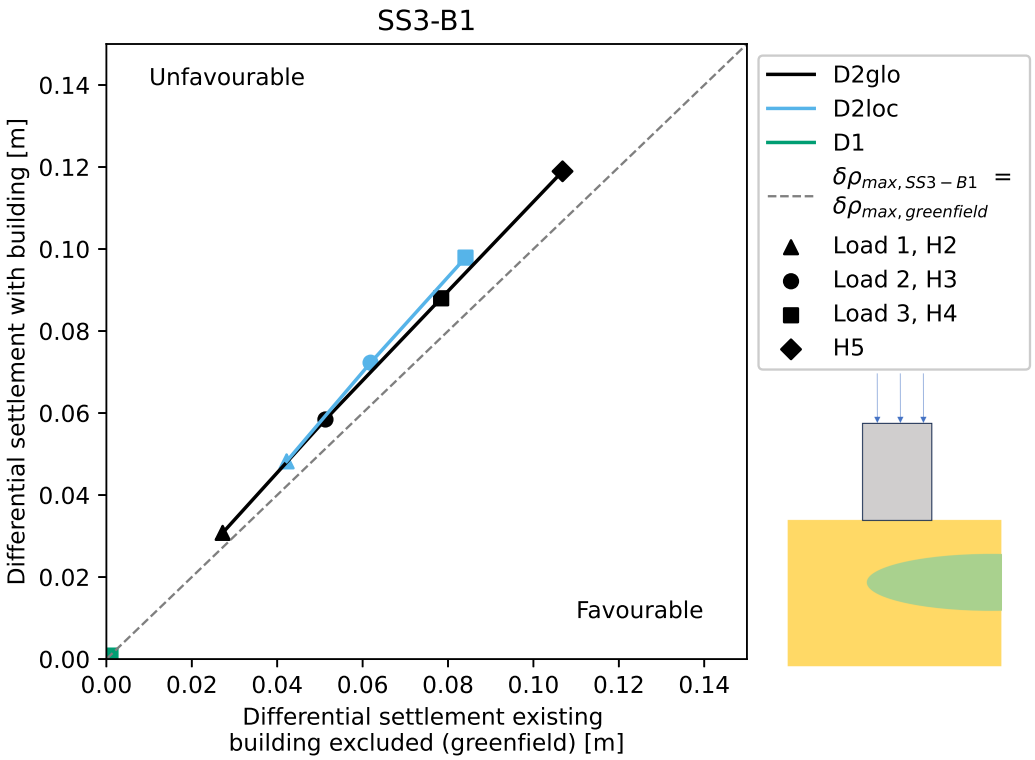

Figure 4.60: Differential settlement without building [m] vs Differential settlement with building [m] for SS3-B1

In the case of soil scenario SS3, it is visible that more differential settlement occurs with a global and local groundwater lowering in the situation with the existing building compared to the greenfield situation. The differential settlement in the case of driver D1 is very small.

4.3.4. Angular distortion vs maximum differential settlement

In figures 4.61,4.62 and 4.63 the maximum angular displacement against the differential settlement is plotted for each soil scenario. A trend line from the origin was then generated for each driver. The trend lines are also shown as found by Skempton and Macdonald. The upper limit is a slope with a coefficient of 550 and the lower limit is a slope with a coefficient of 350, corresponding to the findings of Skempton and Macdonald for foundations on clay and foundations on sand, respectively (Skempton and MacDonald, 1956).

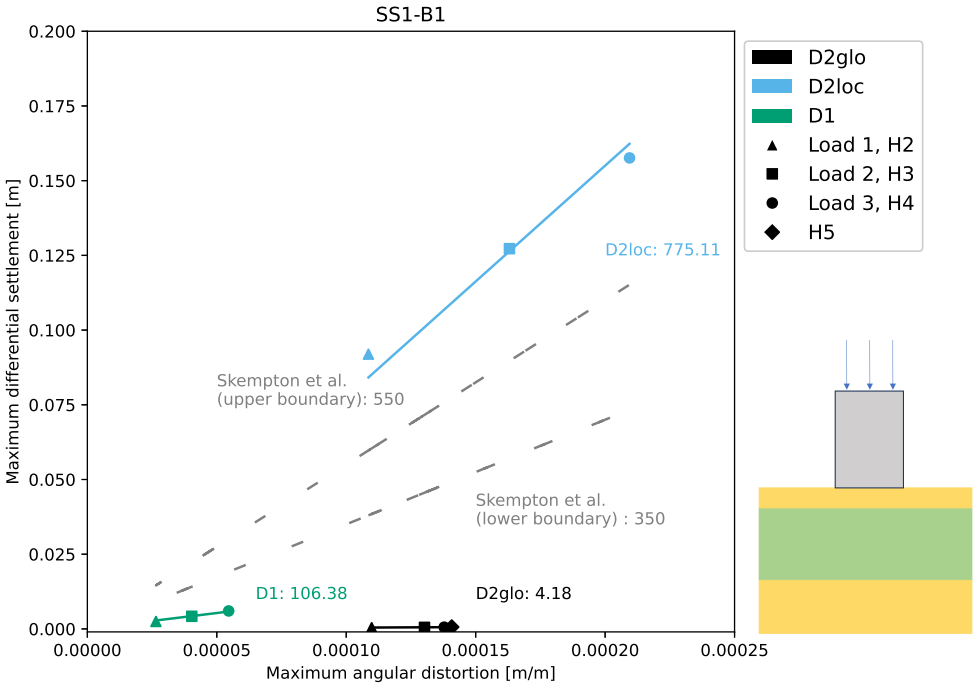

Figure 4.61: Maximum angular distortion [m/m] against maximum differential settlement[m], with the slope values for the different scenarios along with those from the findings of Skempton and MacDonald

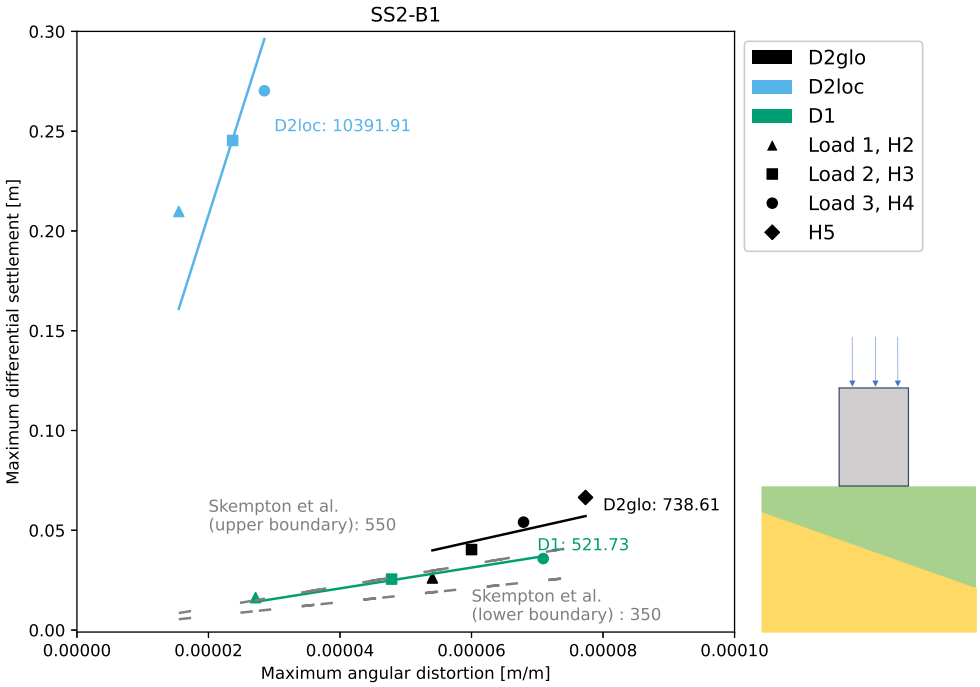

Figure 4.62: Maximum angular distortion [m/m] against maximum differential settlement[m], with the slope values for the different scenarios along with those from the findings of Skempton and MacDonald

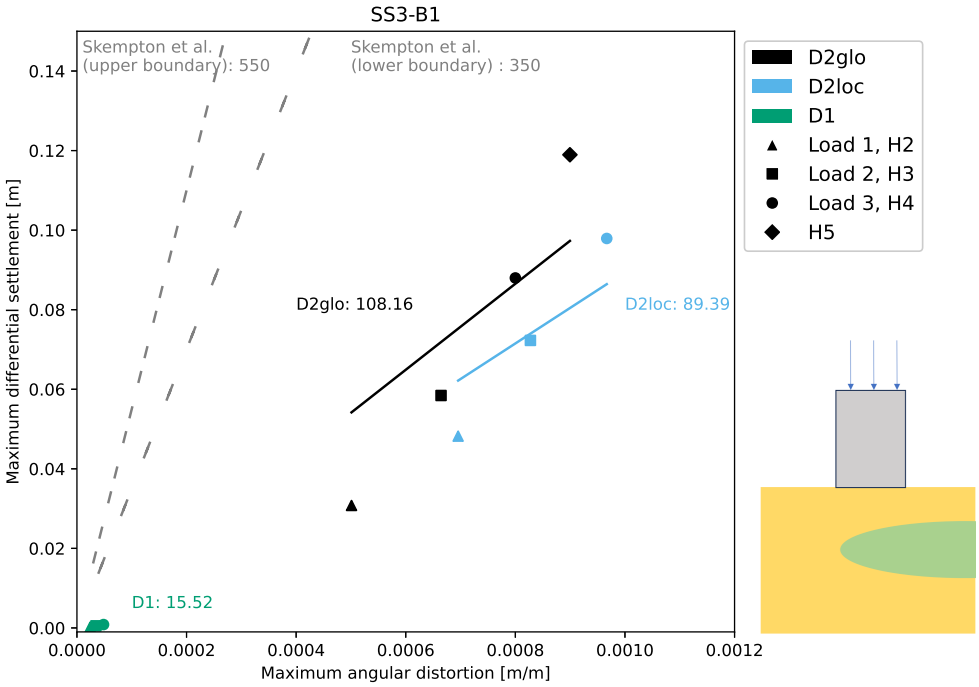

Figure 4.63: Maximum angular distortion [m/m] against maximum differential settlement[m], with the slope values for the different scenarios along with those from the findings of Skempton and MacDonald

The above graphs show that the ratio between the maximum angular distortion and the maximum differential settlement varies significantly between the different soil scenarios and drivers.

4.3.5. Angular distortion vs maximum settlement

The same procedure as for the maximum angular displacement against the maximum differential settlement has been used for the maximum angular displacement against the maximum settlement. The trend lines are also shown as found by Skempton and Macdonald. The upper limit is a slope with a coefficient of 1000 and the lower limit is a slope with a coefficient of 600, corresponding to the findings of Skempton and Macdonald for foundations on clay and foundations on sand, respectively (Skempton and MacDonald, 1956). The results are shown in figures 4.64,4.65 and 4.66

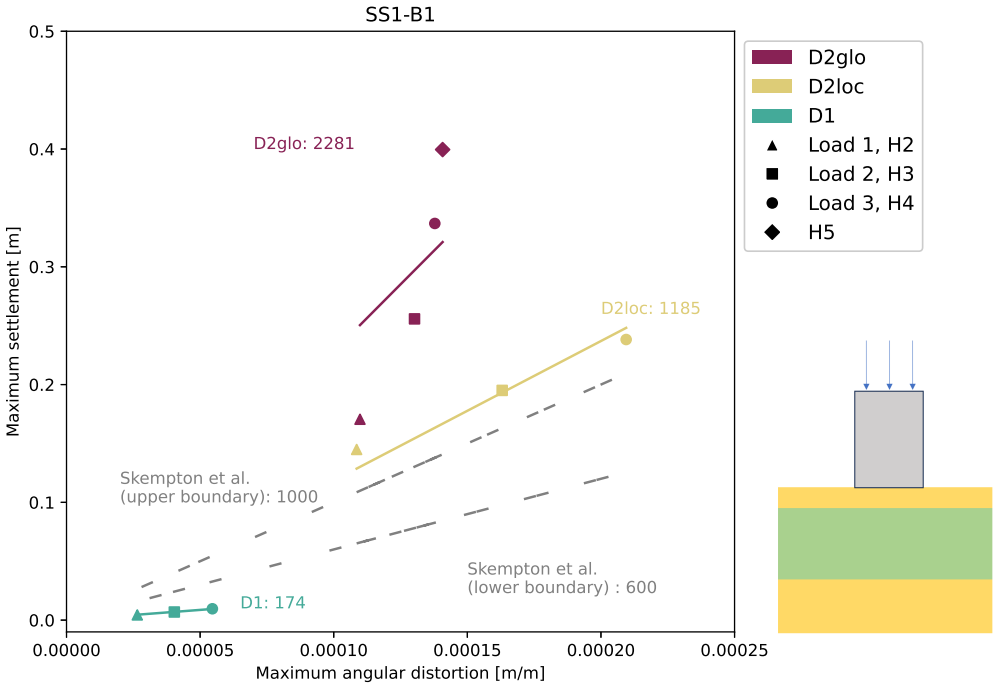

Figure 4.64: Maximum angular distortion [m/m] against maximum settlement[m], with the slope values for the different scenarios along with those from the findings of Skempton and MacDonald

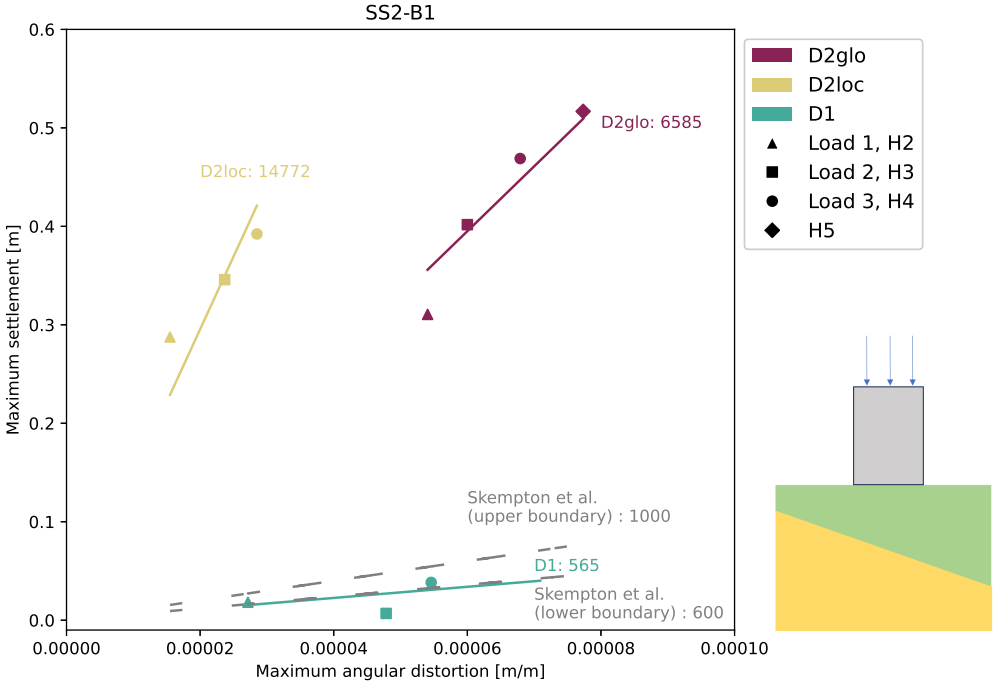

Figure 4.65: Maximum angular distortion [m/m] against maximum settlement[m], with the slope values for the different scenarios along with those from the findings of Skempton and MacDonald

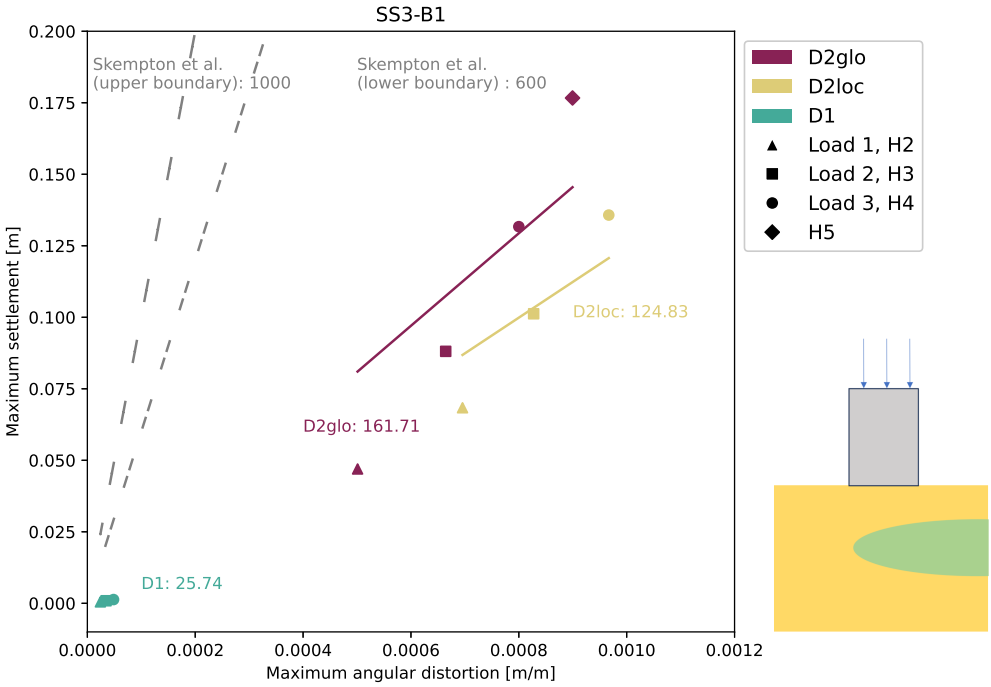

Figure 4.66: Maximum angular distortion [m/m] against maximum settlement[m], with the slope values for the different scenarios along with those from the findings of Skempton and MacDonald

The above graphs show that the ratio between the maximum angular distortion and the maximum settlement also varies significantly between the different soil scenarios and drivers.

4.3.6. Influence of the basement on the driver severity

In this section, the influence of a basement on the damage parameters is considered. This concerns a partial basement, as indicated in section 3.1.2. In particular, scenarios with a basement (building scenario: B2) are compared to the scenarios without a basement (building scenario: B1).

The graphs shown in this section are the same as those in section 4.3, with the difference that the results of the scenarios with a basement are also plotted in the graphs. The open markers show the results for the scenarios with a basement, while the closed markers show the results for the scenarios without a basement. This procedure was carried out for both the maximum angular distortions and the maximum differential settlement for soil scenarios SS1, SS2, and SS3, as shown in figures 4.67, 4.68 and 4.69

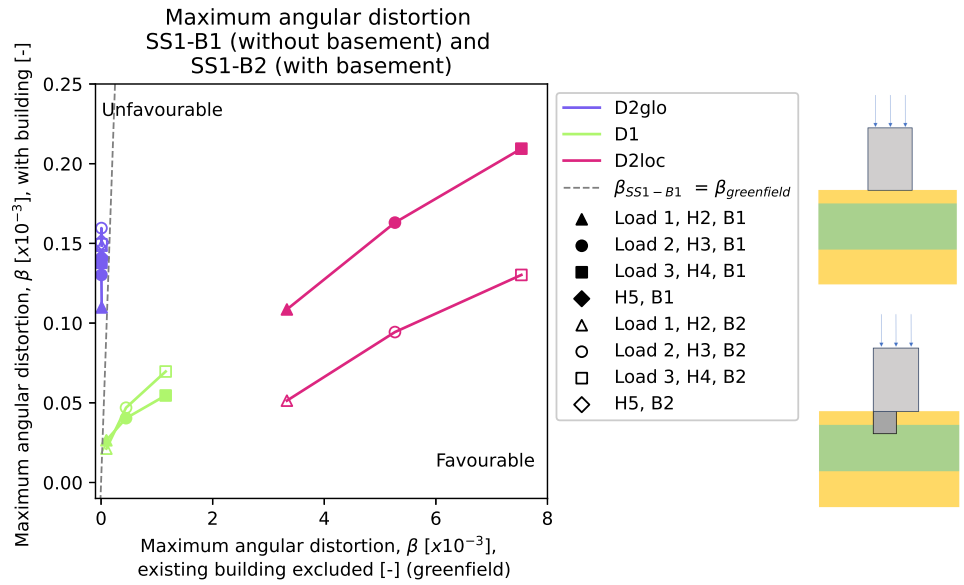

(a) Angular distortion for the greenfield situation against the angular distortion for the situation with the building: Where both the results for the situation without a basement and with a basement are presented

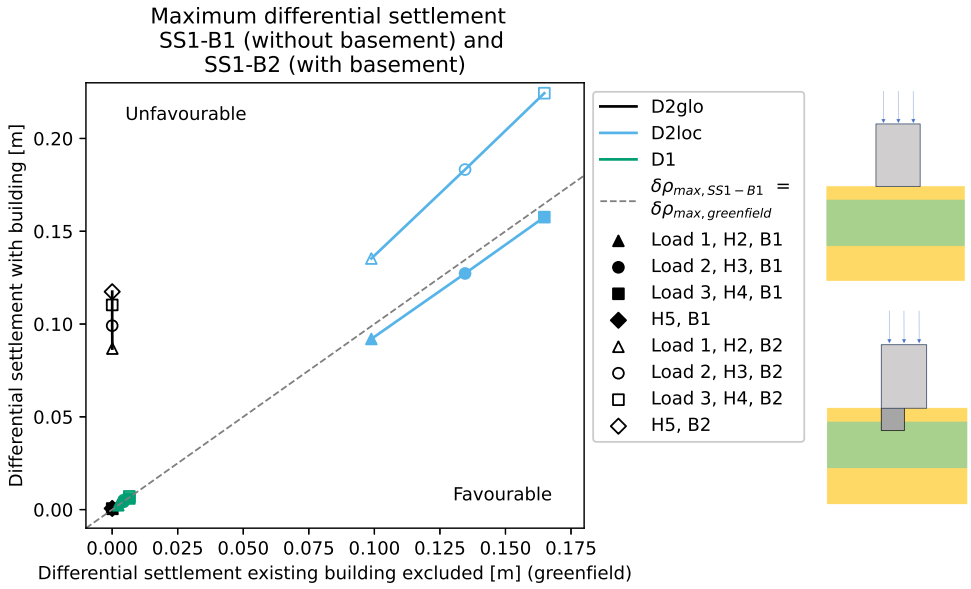

(b) Differential settlement for the greenfield situation against the differential settlement for the situation with the building: Where both the results for the situation without a basement and with a basement are presented

Figure 4.67: Soil scenario SS1 without basement, SS1-B1 vs soil scenario SS1 with basement, SS1-B2

Figure 4.67a shows higher angular distortions for driver D1 and driver D2glo for the situation with a basement, whereas driver D2loc shows the opposite. Additionally, in figure 4.67b, higher differential settlements are observed for driver D2glo and D2loc in the situation with a basement. For driver D1, the differences between the situation with and without a basement are very small.

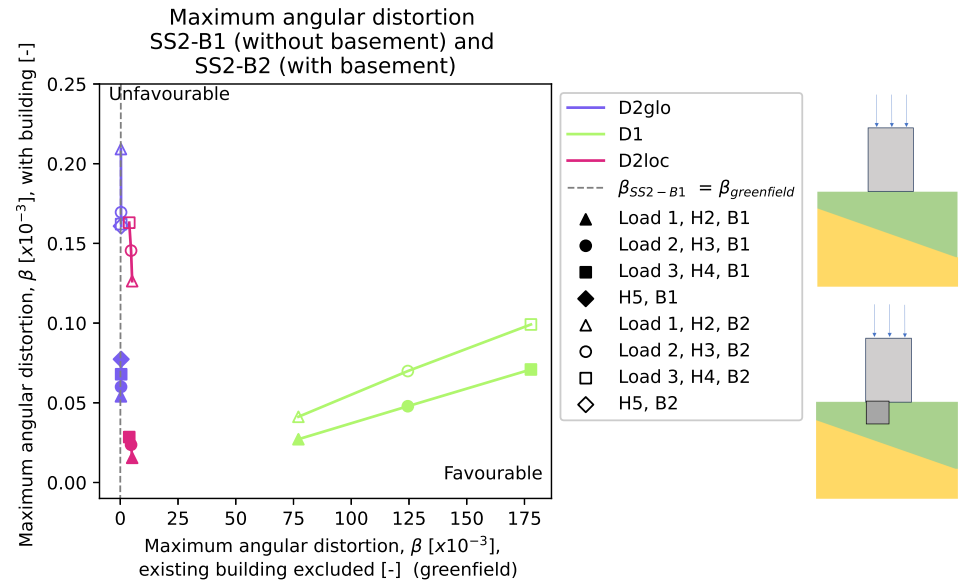

(a) Angular distortion for the greenfield situation against the angular distortion for the situation with the building: Where both the results for the situation without a basement and with a basement are presented

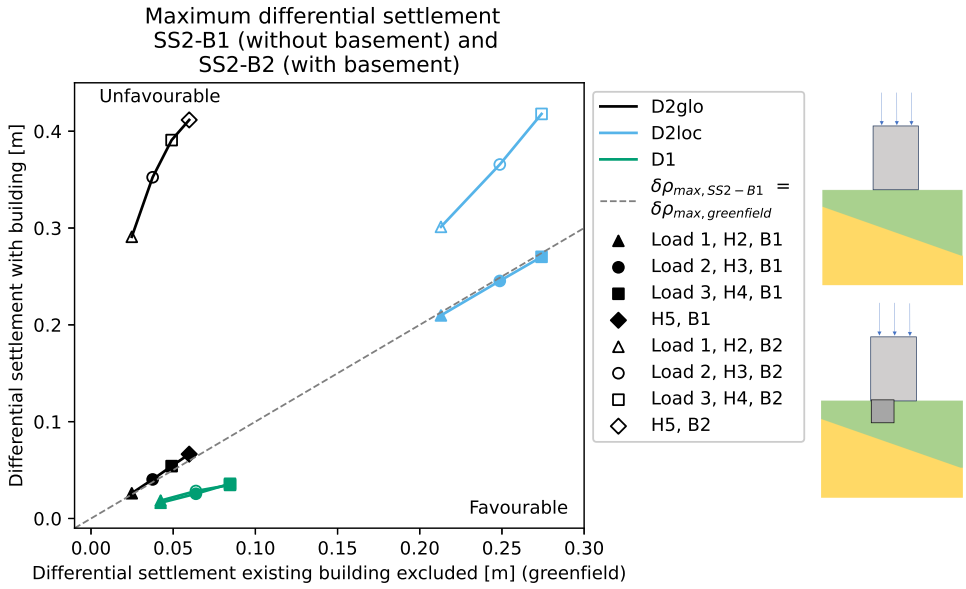

(b) Differential settlement for the greenfield situation against the differential settlement for the situation with the building: Where both the results for the situation without a basement and with a basement are presented

Figure 4.68: Soil scenario SS2 without basement, SS2-B1 vs soil scenario SS2 with basement, SS2-B2

Figure 4.68a shows higher angular distortions for drivers D1, D2glo and driver D2loc for the situation with a basement. Here, it can be observed again that the angular distortions for driver D1 are very high for the greenfield situation compared to the other drivers. Additionally, in figure 4.68b, higher differential settlements are observed for driver D2glo and D2loc in the situation with a basement. For driver D1, the differences between the situation with and without a basement are very small.

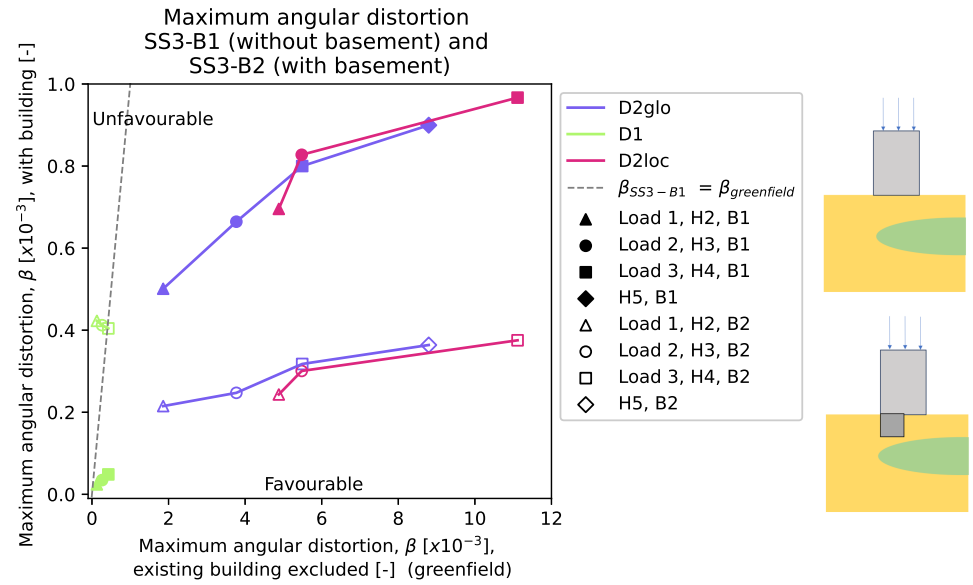

(a) Angular distortion for the greenfield situation against the angular distortion for the situation with the building: Where both the results for the situation without a basement and with a basement are presented

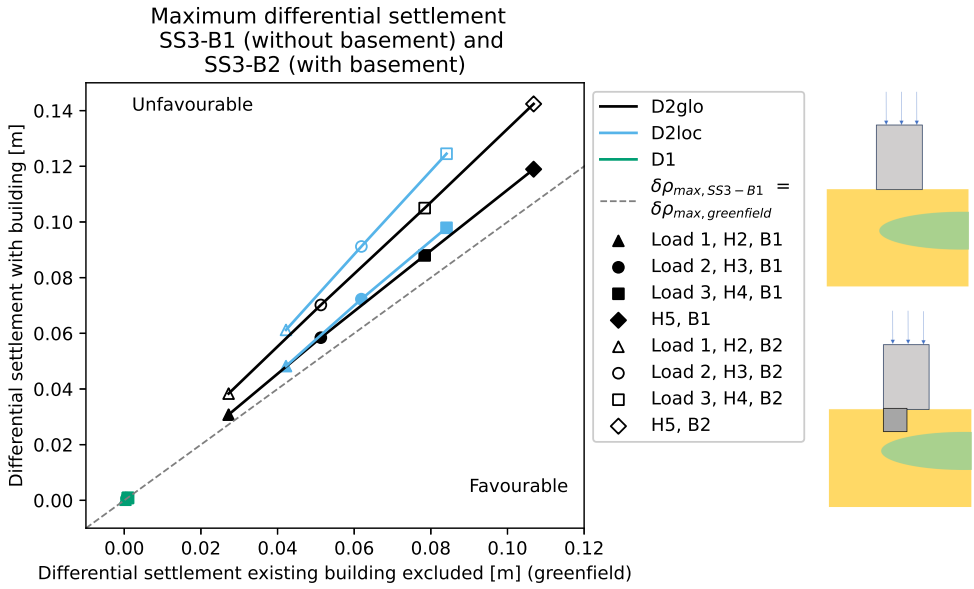

(b) Differential settlement for the greenfield situation against the differential settlement for the situation with the building: Where both the results for the situation without a basement and with a basement are presented

Figure 4.69: Soil scenario SS3 without basement, SS3-B1 vs soil scenario SS3 with basement, SS3-B2

Figure 4.69a shows higher angular distortions for driver D1 for the situation with a basement, whereas drivers D2glo and D2loc shows the opposite. Additionally, in figure 4.69b, higher differential settlements are observed for driver D2glo and D2loc in the situation with a basement. For driver D1, the differences between the situation with and without a basement are very small.

5

Discussion and Limitations

This chapter evaluates the results presented in the previous chapter, with the most important findings and their relevance to the research objectives. Additionally, it addresses the limitations encountered during the study.

This study aims to provide insights into the relative influence of different drivers on the damage to existing buildings with a shallow foundation. More specifically, it aims to understand how various conditions and factors influence the damage parameters associated with soil deformation. This approach allows for analysing the interactions between the soil and the structure, ultimately contributing to a better understanding of the relative influence of the different drivers.

5.1. Evaluation of the results

In the first section of this chapter, the results are evaluated.

5.1.1. Settlement computations

The different phases of the numerical models are presented in table 3.13. In the used soil models, the effect of creep is not considered. In the phases where no consolidation occurs, the process is time-independent. Nonetheless, it was decided to include a time interval for these phases as well, to provide a complete picture of the timeline.

The first four phases aim to generate maturity of the subsurface until the moment when the different drivers are implemented. This has been done both with and without the influence of the existing building. After implementing the different drivers, a consolidation period of a total of 51 years follows to allow the pore water pressures in the settlement-sensitive layers to fully dissipate. All results are based on the outcomes generated in the final phase (phase 6).

For all scenarios, settlement calculations were performed, serving as input for the damage assessment. For all scenarios, the highest occurring load from the drivers acts on the the building's right side. Additionally, the bearing capacity of the soil is the lowest on the right side of the building as well. Therefore, the settlement calculations for the selected scenarios consider the critical situations. As mentioned before, the calculations have been performed for both the situation with the existing building and the greenfield situation. The settlement results show, as expected, greater settlement on the right side of the existing building.

In this section, the settlement results are discussed and compared with the expectations outlined in section 3.1.5.

In the case of horizontal soil layers (SS1) and a uniform distributed load (D2glo), uniform settlement occurs as expected, see figure 4.7

Most differential settlement occurs in the case of inclined soil layers (SS2), but only in the for a local groundwater level lowering (D2loc), see figure 4.19. For a global groundwater lowering, the soil sce-

nario with a weak spot (SS3) is more susceptible to differential settlement, see figure 4.29. The reason is that soil scenario SS2 does not always cause the most differential settlement is that the building as a whole settles more due to being founded directly on soft soil, see figure 4.20.

When comparing the differential settlement caused by the different drivers alone, only the soil scenario with horizontal layers (SS1) is considered. Local groundwater lowering (D2loc) causes the most differential settlement in the case of horizontal soil layers (SS1), see figure 4.10. The addition of an extra load, such as an annex (D1), results in significantly less differential settlement in absolute terms.

The influence of the presence of a partial basement is discussed in section 5.1.6.
For all the situations discussed above, it applies that the occurring distortion is not visible in the graphs based on the settlement computations. The results will be discussed in the section on the driver severity, see section 5.1.4.

5.1.2. Damage Assessment

The occurring damage in this study has been determined by using the graph by Boscardin and Cording, which provides a graphical representation of the relationship between the angular distortion and the horizontal strain of the existing building, see figure 2.4. A damage class can be assigned based on the amount and ratio between the angular distortion and the horizontal strain (Boscardin and Cording, 1989). Because the focus of the numerical modelling is on the soil rather than on the structure itself, the damage effect has been considered, but in a simplified manner. A sensitivity analysis was performed to assess how stiffness affects the damage to the building, see section 5.1.3, but there has been no examination of the occurring stresses in the structural elements.

The damage assessment indicates that the occurring damage is negligible in all scenarios, except in the case of SS3-B1-D2glo and SS3-B1-loc, where the damage is very slight, see figures 4.42, 4.43 and 4.44. The main reason for this is that the building has been modelled as relatively rigid, as discussed further in section 5.1.3. The employed axial and bending stiffnesses are high enough to withstand the occurring ground deformations.

The damage assessment also reveals that the occurring damage in the case of the situation with the basement is negligible. In fact, the damage in the case with the basement is even smaller than the situation without the basement, see figures 4.49, 4.50 and 4.51. The way in which the partial basement and the existing building are modelled together contributes to a higher stiffness for the structure as a whole. Consequently, the expected damage resulting from the occurrence of more differential settlement is mitigated. The modelling strategy used to simulate a partial basement does not appear to align with expectations based on reality.

5.1.3. Influence of the building stiffness

A sensitivity analysis has been conducted for different stiffnesses of the existing building for soil scenarios SS3 for all the different drivers. In this analysis, both the axial stiffness and bending stiffness were multiplied by 0.1 and 10 to simulate a building ten times stiffer and a building ten times less stiff, respectively. Next, the angular distortions were plotted against the horizontal strains. This graph can be compared with the results of Boscardin and Cording (Boscardin and Cording, 1989) to evaluate the damage to the building. It can be observed that the building with the reference stiffness, under the influence of both global and local groundwater lowering (D2glo and D2loc), experiences very slightly damage. As for applied additional load next to the existing building (D1), the resulting damage is negligible.

In addition to the aforementioned sensitivity analysis, the modification factors and relative bending stiffness are determined using the method described by Potts and Addenbrooke (Potts and Addenbrooke, 1997). Relative bending stiffness is plotted against the modification factor along with the contours as described by Potts and Addenbrooke. This indicates that the determined ratio of modification factors and relative bending stiffness falls within the envelopes, but that the building for the reference bending stiffness is relatively stiff.

5.1.4. Driver severity

To analyse the relative influence of the different drivers on the resulting damage to an existing building, the damage parameters for the situation with the existing building were plotted against the greenfield situation. This was done for the damage parameters: maximum settlement, maximum differential settlement, and maximum angular distortion. In all cases, the calculations were performed for various driver intensities.

For all scenarios and drivers, the higher the intensity of the driver, the higher the value for the corresponding angular distortion. An exception to this is the soil scenario where the existing building is founded on an inclined clay layer (SS2). In this scenario, the settlement profile evolves from a sagging situation under low driver intensity to a hogging situation under high driver intensity. However, the final situation at high intensity is a structural element that exhibits less distortion than at low driver intensity, see figure 5.1

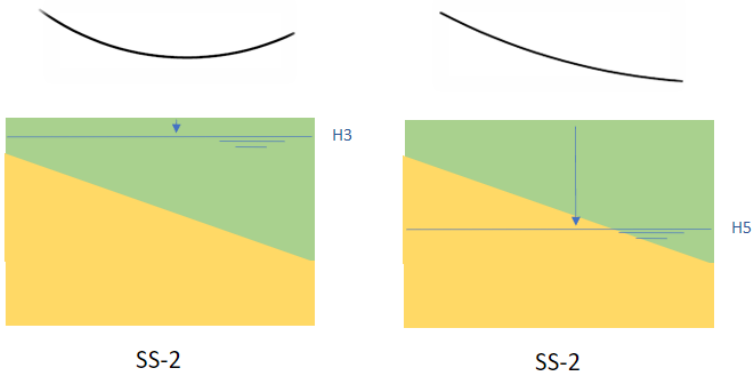

Figure 5.1: Illustration showing that higher driver intensity does not lead to greater angular distortion in every situation; the illustration is exaggerated

For soil scenario SS1, the angular distortions are too small to compare the relative influence of the different drivers with each other.

For soil scenario SS2, the angular distortions for the scenarios in the greenfield situation are greater than the angular distortions of for the situation with the existing building. It appears that for soil scenario SS2, the load from the existing building preloads the soil to such an extent that it has a reducing effect on the damage parameters, what explains the decreasing pink line in the graph 4.53

For all scenarios, there is more or an almost equal amount of differential settlement in the situation with the existing building compared to the greenfield situation. This is caused by the weight of the existing building. An exception is scenario SS2-B1-D1, see figure 4.59, the reason for this is also that a relatively high load is placed directly on soft soil.

The results regarding the angular distortion show that the angular distortion decreases for the situation with the existing building compared to the greenfield situation.The pressure from the building reduces the distortion of the building, see figure 5.2b for an example (SS3-B1). When this is compared for the same situations, but now for the differential settlement, it appears that this effect is not visible, see figure 5.2a for an example of the same scenario (SS3-B1). Whereas, the differential settlement for the situation with the existing building and the greenfield situation shows an almost parallel trend.

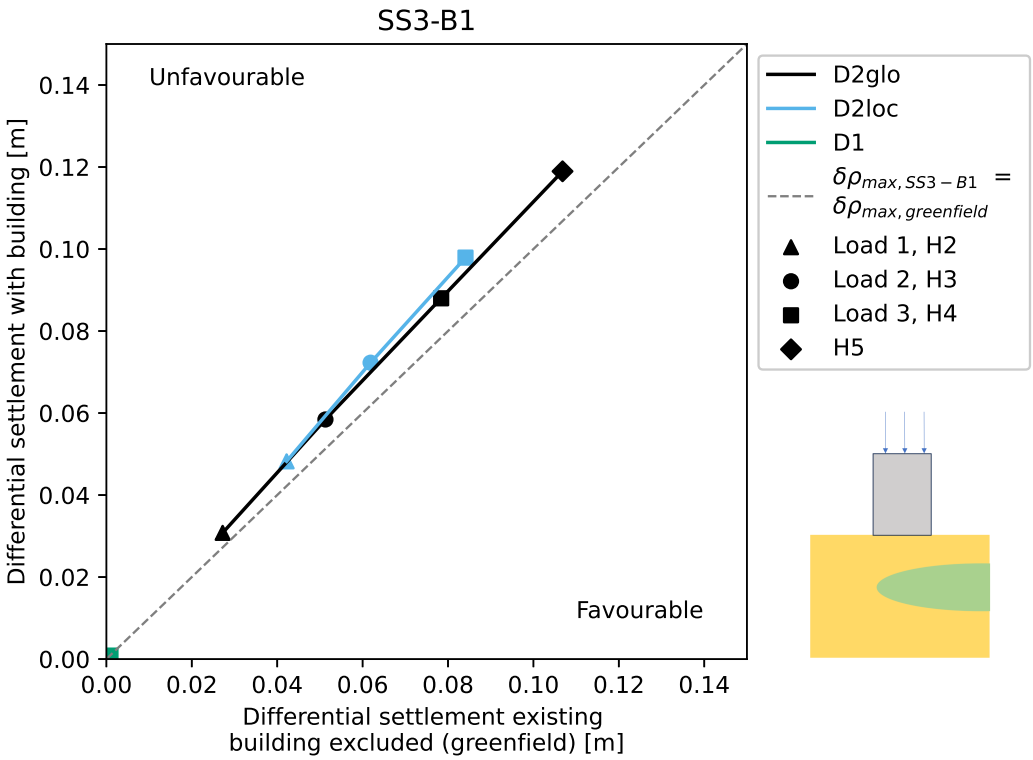

(a) Differential settlement without building [m] vs differential settlement with building [m] for scenario SS3-B1

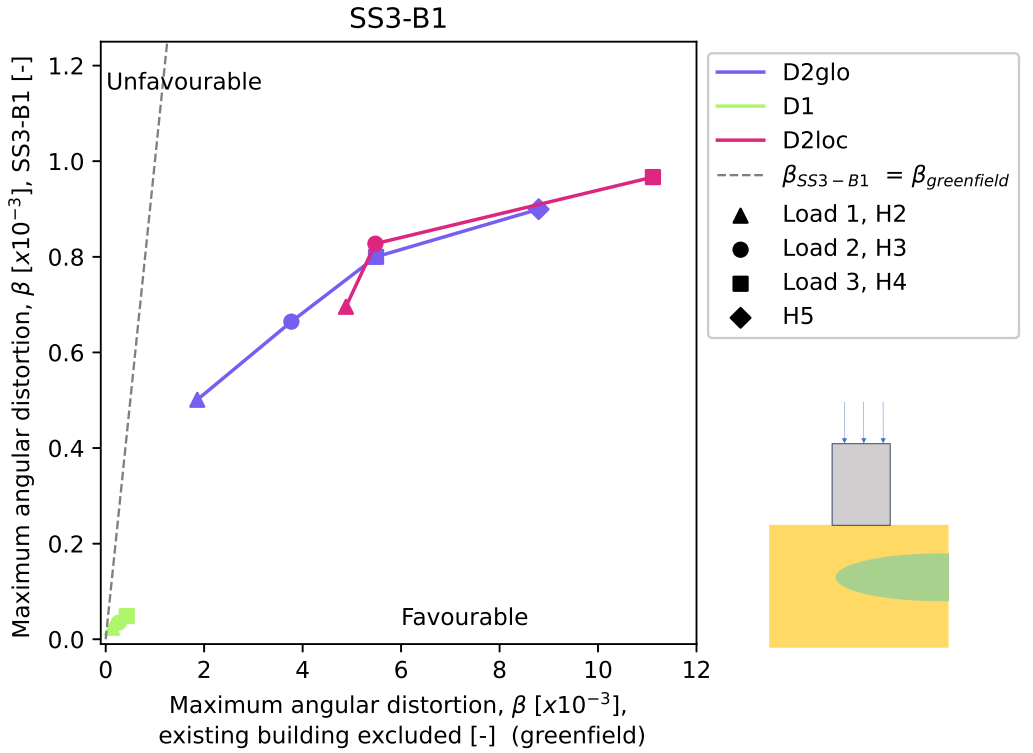

(b) Angular distortion without building [-] vs angular distortion with building [-] for scenario SS3-B1

Figure 5.2: Difference in the occurring effect between the differential settlement and the angular distortion, using scenario SS3-B1 as an example

An exception to this is the soil scenario where the existing building is founded on an inclined clay layer (SS2). In this scenario, the driver where an additional load is placed next to the existing building (D1) deviates from the parallel trend in terms of the differential settlements, see figure 4.59. The reason for this is that a relatively high load is placed directly on soft soil. This results in a relatively large differential settlement at surface level in the greenfield situation.

As shown in figures 4.55, 4.56 and 4.57, the maximum settlement for the greenfield situations are smaller than the situations with the existing building. This aligns with the expectations. The maximum settlements are all located at the far right side of the existing building (x = 55.0 m).

In the graphs where the angular distortion in the greenfield situation are plotted against the angular distortion in the existing building situation, the driver with the steepest observed line has relatively the greatest influence, see figures 4.52, 4.53,4.54. The relative influence of the different drivers on the occurrence of damage to existing buildings is highly dependent on the different scenarios. However, from the findings observed in this study, it can be inferred that a global groundwater level lowering is the driver with relatively the greatest influence on damage to an existing building, followed by a local groundwater level lowering and applying an additional load, for the scenarios considered in this study. The reason that the global groundwater level lowering has the most relative influence in the considered scenarios is that, compared to a local groundwater level lowering, there is a greater lowering of the water level under the building in absolute sense. The deepest level of the local groundwater level is not located under the building but 5.0 meters away from it, simulating the lowering caused by a waterway or the absorption by tree roots.

The largest applied groundwater level lowerings (H5-glo and H4-loc) are quite extreme, which is the reason why the resulting damage parameters are relatively high compared to driver D1, the driver where an additional load is placed next to the existing building. However, it should be noted that an annex, by its nature, is always limited in size, making this driver less unfavourable in absolute terms.

5.1.5. Relation between the maximum angular distortion and the maximum settlement/differential settlement

In this section, the relationship between the maximum angular distortion and the maximum (differential) settlement is considered. In addition, these results were compared with the findings of Skempton and MacDonald. It should be noted that the results have been converted to the metric system, unlike Skempton and MacDonald, which uses inches as the measure of length.

Figures 4.61, 4.62 and 4.63 show the maximum angular distortion against the maximum differential settlement for soil scenarios SS1 (horizontal stratification of the soil), SS2 (inclined stratification of the soil) and SS3 (soil scenario with a weak spot). And figures 4.64, 4.65 and 4.66 show the maximum angular distortion against the maximum settlement for these soil scenarios. The graphs also indicate the values of the slope coefficients for the trends of the different drivers and the extreme values from the literature. The higher the slope coefficient, the lower the resulting angular distortion relative to the maximum (differential) settlement.

According to the findings of Skempton and Macdonald, there is a relationship between the maximum angular distortion and the maximum (differential) settlement (Skempton and MacDonald, 1956). However, the results in this study show graphs with a lot of scatter for the different drivers and soil scenarios, see section 4.3.5.

The additional load next to the existing building (D1) seems to better align with the findings of Skempton and MacDonald. For soil scenario SS2, the values even fall within the extremes founded in this literature, see figures 4.62 and 4.65. A possible explanation for this is that driver D1 more closely matches to the observed case studies of Skempton and MacDonald. Additionally, the values for the maximum angular distortion and the maximum (differential) settlement for driver D1 are relatively low in absolute terms, which may affect the relationship between the maximum angular distortion and maximum (differential) settlement. Scenarios involving groundwater level lowering were not specifically considered in this literature.

For soil scenarios SS1 and SS2, the values for groundwater level lowering (D2glo and D2loc) show a significantly higher slope coefficient compared to the literature values. Except for the differential settlement in soil scenario SS1 for the global groundwater level lowering (D2glo). Here, hardly any differential settlement occurs due to the uniform nature of both the load from the driver and the resistance of the soil, see figure 4.61.

Figures 4.63 and 4.66 show significantly lower values for the slope coefficient compared to the values from the literature. So for this soil scenario (SS3), the maximum angular distortions for all drivers are relatively high compared to soil scenario SS1 and SS2. Which can be explained by the high degree of heterogeneity of this soil scenario.

5.1.6. Influence of a basement

An analysis on the relative influence of damage parameters was conducted for both the angular distortion and the differential settlement for the situation of a building with a basement together with the situation of a building without a basement.

A trend is visible indicating that a partial basement leads to more differential settlement compared to a building without a basement, which is consistent with expectations, see figures 4.67b, 4.68b and 4.69b

However, this trend is not visible for all scenarios and drivers in terms of angular distortions, which is contradictory to the expected outcomes, see figures 4.67a, 4.68a and 4.69a. In the case of a building with a partial basement, the part of the building where a basement is located settles less than the part of the building without a basement. The expectation is then that more distortion will occur in the building, resulting in more damage.

This reducing effect on the angular distortion in the case of a basement can be explained by that the stiffness for the section with the basement increases significantly. This halves the length of the building that is sensitive to distortion, resulting in less distortion. Nevertheless, the expectation remains that there should be more angular distortion in the case of a partial basement under an existing building, considering the significant increase in differential settlement. As previously mentioned, the modelling strategy used to simulate a partial basement does not appear to align with expectations based on reality.

5.2. Limitations

In this study, several assumptions have been made that lead to limitations. These are outlined in the following enumeration.

- the Soft Soil Model was used as the material model for the weak soil layers. So creep was not considered in the settlement calculations.

- For the lithology of the soil scenarios, moderately stiff clay was assumed as weak soil and moderately dense sand as strong soil. The calculations did not vary with different material properties of the soil.

- The driver, a local water level lowering (D2loc), simulates a water level reduction caused by, for example, a nearby waterway or the absorption of water by tree roots. It has been assumed that there is no distinction between the different causes of local water level lowering. Additionally, an assumption has been made regarding the amount of water bulging.

- The structural elements are modelled as beams using plate elements in PLAXIS. Then, an attempt was made to assign a stiffness to the plate elements that is representative of the real situation. This simplifies the representation of the structural elements but is considered suitable for the purpose of this study. Another method to simulate the building is by using polygons that

are assigned a material model to it. By doing this, more extensive material properties can be assigned to the structure. The difference between using polygons and using plate elements has been disregarded.

- A sensitivity analysis was conducted for different stiffnesses of the building. Both the axial stiffness and the bending stiffness were reduced and increased by a factor of 10. In reality, the axial stiffness and the bending stiffness do not relate to each other equally.

- It is common for an annex not to be attached to the existing building.Therefore, the extension must be freestanding. However, the foundation footings will overlap, affecting each other both vertically, and horizontally. It has been chosen to apply a hinge point as a connection, allowing rotation. As an alternative, a small gap, for example 0.01m, could be applied to simulate a dilatation. However, this results in a less well-fitting mesh generation, therefore, a hinge point has been chosen.

- For the considered scenarios with a basement, it has been assumed that the basement has half the width of the building above it. A basement with smaller dimensions could potentially result in greater damage effects.

- The occurring stresses in the structural elements were not examined. Here, an analysis could be conducted to determine if the tensile strength of masonry is exceeded, potentially causing cracking in a façade. Additionally, the weakening of the building over time could also be considered.

- In the literature of Skempton and MacDonald, a distinction is made between buildings founded on clay and buildings founded on sand. However, in this study, the soil consists of neither only sand nor only clay. To enable a comparison of the results with the findings of Skempton and MacDonald, the highest and lowest values from the literature were considered as extremes, after which a comparison was made.

6

Conclusions and Recommendations

6.1. Conclusions

In this chapter, the main conclusions of this study are presented. Subsequently, some recommendations for future research are provided.

In this study, the primary focus of the numerical modelling is on the soil rather than on the structure itself. The aim is to employ graphical techniques to evaluate the potential effects on the building resulting from the settlement computed through numerical models.

This study aims to provide insights into the relative influence of different drivers on the damage to existing buildings with a shallow foundation. More specifically, it aims to understand how various conditions and factors influence the damage parameters associated with soil deformation. This approach allows for analysing the interactions between the soil and the structure, ultimately contributing to a better understanding of the relative influence of the different drivers.

6.1.1. Research questions

Sub-question 1

What are the existing modelling strategies to compare the influence of different subsidence drivers?

Sub-question 1 aims to explore the existing modelling strategies for different subsidence drivers.

In the current state of the art, the focus is primarily on the effect of a specific subsidence driver. In the literature, no modelling strategy has been found that directly compares the influence of different drivers with each other.

To consider the influence of the building's presence on the settlements, the settlements in the situation with the existing building can be compared to the settlements in the situation without the existing building (greenfield settlements). This can then be done by including different implemented drivers in the calculation. This approach allows the relative influence of different drivers to be examined.

Sub-question 2

Which are the most relevant subsidence drivers for urban areas in the Netherlands?

In order to answer this question, a literature study has been conducted.

- The most common causes of subsidence are compiled in table 2.1 and categorized by scale, area, type, depth, and the resulting effect.
- Most subsidence-related damage cases to buildings in the Netherlands involve buildings with shallow foundations.
- Due to climate change, drier summers will occur more frequently in the future, causing groundwater levels to reach increasingly deeper levels.

Based on a lack of research and recent frequent occurrences, a global and local groundwater level lowering and the addition of extra load next to an existing building have been selected as drivers.

Sub-question 3
What are the causes of differential settlement?

Sub-question 3 delves into the causes of differential settlement, aiming to investigating the factors contributing to this phenomenon. This question can be partially answered based on the literature review and partially by the generated results.

- Subsidence can occur due to the consolidation and the oxidation of organic material in the subsoil. Heterogeneity in the subsoil can lead to differential settlements.

- An unevenly distributed load from a building can locally generate more ground pressure, which can lead to differential settlements.

- A driver can locally generate more stress in the subsurface, which can lead to differential settlements. In the case of groundwater-lowering drivers, the upward pressure generated by the water decreases due to the lowering of the water level. As a result, the effective stress increases. In the case of an additional load adjacent to the existing building, an extra loading is applied to the subsurface, resulting in an increase in effective stress.

- The degree of differential settlement is highly dependent on the soil conditions. For the soil scenarios with horizontal layering (SS1) and the inclined clay layer (SS2), it is visible that a local groundwater level lowering results in the most significant differential settlement, as shown in figures 4.58 and 4.59, while in the case of the soil scenario with a weak spot (SS3), this applies to a global groundwater lowering, see figure 4.60.

The occurrence of differential settlements is determined by a combination of soil conditions, building weight, and the intensity of the drivers. It is not straightforward to identify the worst combination of soil, drivers, and building based on differential settlement, indicating that the occurrence of differential settlements is case-specific.

Sub-question 4
Which are the most suitable modelling strategies to compute the settlement due to different subsidence drivers and their effect on existing buildings?

Sub-question 4 focuses on identifying the most suitable modelling strategies for computing settlements resulting from different subsidence drivers and assessing their impact on existing buildings.

In this study, settlements for various scenarios were calculated using the finite element method. In this study, a direct modelling approach was chosen. The structure, the building, is represented in a simplified manner, where the building is modelled as a beam. The reason for this is that the focus of this study is more on the soil than on the structure. For each scenario, the calculation was done for both the greenfield situation and the situation with the existing building. Based on the settlements, damage parameters were determined. Subsequently, a damage assessment was conducted, and the relative influence of the different drivers is compared with each other.

In the reviewed literature, no other modelling strategies were found that compare different subsidence drivers. Therefore, it is concluded the adopted strategy represents the best effort at the current stage.

Sub-question 5
How can the damage response of existing buildings due to differential settlements be determined?

The focus of sub-question 5 is on determining the damage response of existing buildings based on the numerically determined settlement results.

Based on these calculated settlements, various damage parameters have been determined: maximum settlement, differential settlement, angular distortion and the horizontal strain

- The literature review indicates that angular distortion is one of the most reliable predictors of damage to buildings. In combination with the horizontal strain, the angular distortion can be used to determine the resulting damage by comparing the results with findings from literature (Boscardin and Cording, 1989).

- Based on soil investigation, an accurate prediction of ground settlement can be made. By staying within the limits of the maximum allowable (differential) settlement, the deformation of a building can be limited. When plotting the maximum angular distortion against the maximum (differential) settlement, it appears that there is a significant difference between the various drivers. The relationship between the maximum angular distortion and the maximum (differential) settlement strongly depends on the driver.

- There is a visible trend of a decreasing angular distortion of the situation with the building compared to the greenfield situation. So the angular distortion is affected by the pressure of the existing building. When this phenomenon is compared with the damage parameter differential settlement, it appears that the differential settlement is not significantly affected by the pressure from the existing building. The soil-structure interaction plays a role in the distortion, but not in the differential settlement. From this, it can be concluded that differential settlement is not the most suitable damage parameter to estimate the damage to existing buildings caused by subsidence.

Sub-question 6
What is the impact of an partial basement under a building on the occurrence of differential settlement and the resulting damage?

To answer this question, an analysis on the relative influence of damage parameters was conducted for both the angular distortion and the differential settlement for the situation of a building with a basement together with the situation of a building without a basement.

- The differential settlements for the building with a basement are higher than the differential settlements for the building without a basement.

- There is no trend visible between the angular distortions for the building with a basement and without a basement.

Due to the partial basement of the existing building, less settlement occurs on the side of the basement. Based on the higher differential settlements of the situation with a basement, it can be concluded that an existing building with partial basement is more sensitive to damage caused by settlement than an existing building without a basement. The expectation is that a similar pattern will be visible for the angular distortion. So that the situation with a basement will result in larger maximum angular distortions than the situation without a basement, which is not the case. Consequently, it can be concluded that the adopted modelling strategy used to simulate a partial basement does not appear to align with expectations based on reality and that this modelling strategy is not appropriate for considering the impact of a partial basement on the damage to an existing building.

Main question
What is the relative influence of different subsidence-related drivers on damage to existing buildings on shallow foundations?

Several aspects related to settlement occurrence and its impact on buildings were investigated. The study provides multiple outcomes regarding the interaction between soil scenarios, different drivers of subsidence, and the presence of an existing building with and without a partial basement. This was achieved by considering the influence of each of these variables on the damage parameters, with emphasis placed on the relative influence of the different drivers. The approach includes a method that

compares the influence of the situation with the existing building and the situation without the existing building (greenfield situation). This comparison shows the settlement behaviour caused by the presence of the building load and its interaction with the soil.
Additionally, the combined effects of the soil scenarios, different drivers, and building scenarios on the resulting damage to an existing building are considered.

- Based on a comparison with findings from the literature, it can be concluded that negligible to very slightly damage occurs in the considered scenarios. Very slightly damage occurs in the case of the drivers where the groundwater level is lowered, both globally and locally (D2glo and D2loc). This is only the case for a building without a basement, with a soil scenario with a weak spot (SS3-B1). In all other cases, the resulting damage is negligible. In the scenario where the building stiffness is drastically reduced, significantly more damage occurs.

- Based on the analysis of the relative influence of the damage parameters, it can be concluded that, as expected, that the presence of an existing building reduces the angular distortion compared to the greenfield situation. This analysis also shows that the resulting damage parameters of applying an additional load (D1) are, in absolute terms, significantly lower than those from the groundwater level lowering drivers (D2glo and D2loc).

- When a driver has a higher intensity, a higher angular distortion is visible in all cases, apart from the soil scenario with a weak spot in it. It can be concluded from this that increasing the intensity of the driver does not necessarily mean that there will be more damage to the existing building

- In the graphs where the angular distortion in the greenfield situation are plotted against the angular distortion in the situation with the existing building, the driver with the steepest observed line has relatively the greatest influence. The relative influence of the different drivers on the occurrence of damage to existing buildings is highly dependent on the different scenarios. However, according to the findings observed in this study, it can be concluded that a global groundwater level lowering (D2glo) is the driver with relatively the greatest influence on damage to an existing building, followed by a local groundwater level lowering (D2loc) and applying an additional load (D1), for the scenarios considered in this study.

- When considering the graphs where the maximum angular distortions are plotted against the maximum (differential) settlement, it applies that for all soil scenarios, except in case of the reference model, the angular distortions of lowering the groundwater level, both globally and locally, are lower than those of applying an additional load next to an existing building (D1). In the soil scenarios with a horizontal stratification of the soil (SS1) and an inclined stratification of the soil (SS2), lowering the groundwater level gives lower values for the angular distortion than the findings from the literature. It can be concluded from this that the findings from the literature do not apply to lowering the groundwater level.

- When considering the graphs where the maximum angular distortions are plotted against the maximum (differential) settlement, it can be observed that for the soil scenario with inclined stratification (SS2), the application of an additional load (D1) falls within the limits established in the literature.

- When considering the graphs where the maximum angular distortions are plotted against the maximum (differential)settlement, it applies that for the soil scenario with a weak spot (SS3) the maximum angular distortions for all drivers are relatively high compared to the soil scenario with a horizontal stratification (SS1) and an inclined stratification of the soil (SS2). From which it can be concluded that the results, in the case of a soil structure with a lot of heterogeneity, do not correspond to the findings from the literature.

To conclude, for the soil scenarios considered in this study, the soil scenario with a weak spot (SS3) has the most unfavourable effect on an existing building. For the drivers considered in this study, when

evaluating the relative influence of the different drivers, the global groundwater lowering (D2glo) has the most unfavourable effect. Considering the combined effect, the soil scenario exerts the greatest influence on the resulting settlements for the evaluated scenarios, followed by the type of driver and the building scenario.

6.2. Recommendations

This study aims to provide insights into the relative influence of different drivers on the damage to existing buildings with a shallow foundation. More specifically, it aims to understand how various conditions and factors influence the damage parameters associated with soil deformation. This approach allows for analysing the interactions between the soil and the structure, ultimately contributing to a better understanding of the relative influence of the different drivers.

By determining various damage parameters across different soil scenarios, drivers, and building scenarios, insights into the soil-structure interaction can be obtained in multiple ways.

The occurring damage to the existing building can be determined using findings from the literature by plotting the maximum angular distortion against the horizontal strain.

Furthermore, the results can be compared with findings from the literature by plotting the maximum angular distortion against the maximum (differential) settlement.

Additionally, an approach is provided where the relative influence of different drivers can be determined by plotting the damage parameter results in the greenfield scenario against the scenario with the existing building.

Recommendations

- In this study, three different soil scenarios were considered. It is recommended to conduct further analyses with additional soil scenarios to improve the accuracy of predicting damage to existing buildings under different soil conditions. Additionally, a sensitivity analysis could be performed to assess the influence of soil parameters.

- More research could be conducted on local groundwater level lowering as a driver. This would allow for a more accurate analysis of the effect of water absorption by tree roots on groundwater levels and the resulting damage to buildings.

- Further research into possible modelling strategies to simulate a partial basement beneath an existing building and its influence on resulting damage is recommended

- The use of polygons in the structural elements, allowing for assignment of a more advanced material model, can be analysed.

- 3D analyses can provide a more representative depiction of the real effect of the building's stiffness and the drivers on settlement analysis.

- It is recommended to perform a more comprehensive damage assessment. For example, in a first model, settlements can be calculated using a simplified structure, and then in a separate model, using the deformations from the first model as input, a more detailed damage assessment can be conducted. For this purpose, a material model describing the behaviour of masonry could be selected, followed by an analysis of crack formation.

- It is recommended to pay more attention to the internal forces within the structure. Based on the maximum occurring bending moment and shear force in the beam, the normal and tangential stresses can be calculated. This can then be compared with the material properties of a masonry building/structure.

- There is not consistently a direct correlation between angular distortion and maximum (differential) settlement. Caution is advised when comparing the results with findings of Skempton and MacDonald regarding different subsidence related drivers. Further research into the relationship between maximum angular displacement and maximum (differential) settlement, particularly regarding groundwater level lowering, is recommended.

- The comparison of the results from numerical models with case studies would enhance the validation of the research.

- To minimize damage caused by a lowered groundwater level in buildings with shallow foundations, it is recommended to keep the groundwater level as high as possible near the buildings. It is important that the policies of the water boards are designed accordingly. Additionally, it is advisable to consider the risk of localized groundwater level lowering and, if possible, to keep the source of this local lowering at a sufficient distance from buildings. Water-retaining barriers in the subsurface may also be considered to reduce the risk.

References

Bagheri-Gavkosh, M., Hosseini, S. M., Ataie-Ashtiani, B., Sohani, Y., Ebrahimian, H., Morovat, F., & Ashrafi, S. (2021). Land subsidence: A global challenge. *Science of The Total Environment*, *778*, 146–193.

Bapir, B., Abrahamczyk, L., Wichtmann, T., & Prada-Sarmiento, L. F. (2023). Soil-structure interaction: A state-of-the-art review of modeling techniques and studies on seismic response of building structures. *Frontiers in Built Environment*, *9*, 1120351.

Blom, C., Van der Werf, K., Stuurman, R., & Kooi, H. (2022). Klimaatverandering klei en funderingsproblemen: Een case studie. *2*, 20–25.

Boscardin, M. D., & Cording, E. J. (1989). Building response to excavation-induced settlement. *Journal of Geotechnical Engineering*, *115*(1), 1–21.

Brinkgreve, R. B. J. (2020). *Reader of msc course cie4361 behaviour of soils and rocks*. TU Delft.

Brinkgreve, R. (n.d.). Materiaalmodellen voor grond en gesteente.

Bruna, M. (2020). Analyzing subsidence in the netherlands with attribute-enriched insar data. http://resolver.tudelft.nl/uuid:90970051-1c2c-4bfa-8862-051c4cdf3b5a

Burland, J., & Wroth, C. (1974). Settlement and associated damage, settlement of structures. *International proceedings of conference on settlement of structures*, 611–654.

Busschers, F. S., Kasse, C., van Balen, R. T., Vandenberghe, J., Cohen, K. M., Weerts, H. J. T., Wallinga, J., Johns, C., Cleveringa, P., & Bunnik, F. P. M. (2007). Late pleistocene evolution of the rhine-meuse system in the southern north sea basin: Imprints of climate change, sea-level oscillation and glacio-isostacy. *Quaternary Science Reviews*, *26*(25-28), 3216–3248. https://doi.org/10.1016/j.quascirev.2007.07.013

CBS. (2023, September). Hoeveel woningen zijn er? - Nederland in cijfers 2023. https://longreads.cbs.nl/nederland-in-cijfers-2023/hoeveel-woningen-zijn-er/#:~:text=De%20meeste%20huizen%20zijn%20rijtjeshuizen,Denk%20aan%20appartementen%20of%20bovenwoningen.

Costa, A. L., Kok, S., & Korff, M. (2020). Systematic assessment of damage to buildings due to groundwater lowering-induced subsidence: Methodology for large scale application in the netherlands. *Proc. IAHS*, *382*, 577–582. https://doi.org/10.5194/piahs-382-577-2020

Dufour, F. C., & Burrough-Boenisch, J. (2000). *Groundwater in the netherlands : Facts and figures*. Netherlands Institute of Applied Geoscience TNO.

Fellenius, B. H., & Eng, P. (1984). Negative skin friction and settlement of piles.

Figueroa-Miranda, S., Tuxpan-Vargas, J., Ramos-Leal, J. A., Hernández-Madrigal, V. M., & Villaseñor-Reyes, C. I. (2018). Land subsidence by groundwater over-exploitation from aquifers in tectonic valleys of central mexico: A review. *Engineering Geology*, *246*, 91–106. https://doi.org/https://doi.org/10.1016/j.enggeo.2018.09.023

Gaba, A., Simpson, B., Beadman, D., & Powrie, W. (2003). Embedded retaining walls: Guidance for economic design. *Proceedings-institution of civil engineers geotechnical engineering*, 13–16.

Geologische dienst nederland. (2024, January). https://www.geologischedienst.nl/

Giardina, G., van de Graaf, A. V., Hendriks, M. A. N., Rots, J. G., & Marini, A. (2013). Numerical analysis of a masonry façade subject to tunnelling-induced settlements. *Engineering Structures*, *54*, 234–247. https://doi.org/10.1016/j.engstruct.2013.03.055

KCAF. (2022). *Funderingen onder gebouwen*.

KNB. (2021). *VAN KLEI TOT BAKSTEEN*. Koninklijke Nederlandse Bouwkeramiek. https://www.knb-keramiek.nl/media/268957/bw_klei_tot_baksteen_def.pdf

Kok, S., & Angelova, L. (2020). *Impact droogte op funderingen*. Deltares. https://www.verzekeraars.nl/media/7875/20200930-rapport-impact-droogte-op-funderingen.pdf

Korff, M. (2013). *Response of piled buildings to the construction of deep excavations* (Vol. 13). IOS Press.

Koster, K., Stafleu, J., & Stouthamer, E. (2018). Differential subsidence in the urbanised coastal-deltaic plain of the netherlands. *Netherlands Journal of Geosciences*, *97*(4), 215–227. https://doi.org/10.1017/njg.2018.11

Lambe, T. W., & Whitman, R. V. (1969). *Soil mechanics*. Wiley. http://catdir.loc.gov/catdir/toc/onix05/68030915.html%20http://www.gbv.de/dms/bowker/toc/9780471511922.pdf

Longo, M., Sousamli, M., Korswagen, P. A., van Staalduinen, P., & Rots, J. G. (2021). Sub-structure-based 'three-tiered'finite element approach to soil-masonry-wall interaction for light seismic motion. *Engineering Structures*, *245*, 112847.

Lourenco, P. (1997). Computational strategies for masonry structures. http://resolver.tudelft.nl/uuid:4f5a2c6c-d5b7-4043-9d06-8c0b7b9f1f6f

Mercer, G., Reeves, A., & O'Callaghan, D. P. (2011). THE RELATIONSHIP BETWEEN TREES, DISTANCE TO BUILDINGS AND SUBSIDENCE EVENTS ON SHRINKABLE CLAY SOIL. *Arboricultural Journal*, *33*(4), 229–245. https://doi.org/10.1080/03071375.2011.9747615

Minderhoud, P. S. J., Erkens, G., Pham, V. H., Vuong, B. T., & Stouthamer, E. (2015). Assessing the potential of the multi-aquifer subsurface of the mekong delta (vietnam) for land subsidence due to groundwater extraction. *Proceedings of the International Association of Hydrological Sciences*, *372*, 73–76. https://doi.org/10.5194/piahs-372-73-2015

Peduto, D., Prosperi, A., Nicodemo, G., & Korff, M. (2022). District-scale numerical analysis of settlements related to groundwater lowering in variable soil conditions. *Canadian Geotechnical Journal*, *59*(6), 978–993.

Plaxis. (2023a). *2d reference manual*. https://bentleysystems.service-now.com/community?id=kb_article&sysparm_article=KB0107989

Plaxis. (2023b). *2d tutorial manual*. https://communities.bentley.com/cfs-file/__key/communityserver-wikis-components-files/00-00-00-05-58/PLAXIS_5F00_2D_5F00_2023.2_5F00_2D_5F00_1_5F00_Tutorial.pdf

Plaxis. (2024). *Material models manual 2d*. https://communities.bentley.com/cfs-file/__key/communityserver-wikis-components-files/00-00-00-05-58/PLAXIS_5F00_2D_5F00_2024.1_5F00_2D_5F00_3_5F00_Material-Models-Manual.pdf

Potts, D., & Addenbrooke, T. (1997). A structure's influence on tunnelling-induced ground movements. *Proceedings of the Institution of Civil Engineers-Geotechnical Engineering*, *125*(2), 109–125.

Prosperi, A., Korswagen, P. A., Korff, M., Schipper, R., & Rots, J. G. (2023). Empirical fragility and roc curves for masonry buildings subjected to settlements. *Journal of Building Engineering*, *68*. https://doi.org/10.1016/j.jobe.2023.106094

Prosperi, A., Longo, M., Korswagen, P. A., Korff, M., & Rots, J. G. (2023). Sensitivity modelling with objective damage assessment of unreinforced masonry façades undergoing different subsidence settlement patterns. *Engineering Structures*, *286*. https://doi.org/10.1016/j.engstruct.2023.116113

Raad voor de leefomgeving en infrastructuur. (2024). *GOED GEFUNDEERD ADVIES OM TE KOMEN TOT EEN NATIONALE AANPAK VAN FUNDERINGSPROBLEMATIEK*. Raad voor de leefomgeving en infrastructuur. https://www.rli.nl/sites/default/files/Rli%20advies%20Goed%20gefundeerd_Advies%20om%20te%20komen%20tot%20een%20nationale%20aanpak%20van%20funderingsproblematiek_2.pdf

Robertson, P. K. (2009). Interpretation of cone penetration tests — a unified approach. *Canadian Geotechnical Journal*, *46*(11), 1337–1355. https://doi.org/10.1139/t09-065

Rosenbaum, M. (2003). Characterisation of the shallow subsurface: Implications for urban infrastructure and environmental assessment. *New Paradigms in Subsurface Prediction*, 3–6.

Rots, J., Korswagen, P., & Longo, M. (2021). Computational modelling checks of masonry building damage due to deep subsidence. *Delft University of Technology*.

Skempton, A. W., & MacDonald, D. H. (1956). The allowable settlements of buildings. *Proceedings of the Institution of Civil Engineers*, *5*(6), 727–768.

Stewart, R. D., Abou Najm, M. R., Rupp, D. E., & Selker, J. S. (2016). Modeling multidomain hydraulic properties of shrink-swell soils. *Water Resources Research*, *52*(10), 7911–7930.

ten Brinke, W. (Ed.). (2016). *Dalende bodems, stijgende kosten: Mogelijke maatregelen tegen veenbodemdaling in het landelijk en stedelijk gebied: Beleidsstudie*. Planbureau voor de Leefomgeving.

Verruijt, A. (2018). An introduction to soil mechanics. https://doi.org/10.1007/978-3-319-61185-3

Zain, N. (2019). *Effect of oxidation on the compression behaviour of organic soils* [Doctoral dissertation, Delft University of Technology].

Zhang, X., & Briaud, J.-L. (2015). Three dimensional numerical simulation of residential building on shrink–swell soils in response to climatic conditions. *International Journal for Numerical and Analytical Methods in Geomechanics*, *39*(13), 1369–1409.

Zhou, Y. Y., Li, J., Ren, G., & Shi, X. S. (2011). Discussion of factors affecting tree root water absorption in expansive soil and their implications in numerical models. *Advanced Materials Research*, *255*, 3042–3046.

A

Input parameters

A.1. Geotechnical parameters

NEN 9997-1:2011
2.4.5.2

Tabel 2.b — Karakteristieke waarden van grondeigenschappen

Grondsoort			Karakteristieke waarde[a] van grondeigenschap																					
Hoofd-naam	Bijmengsel	Consis-tentie [b]	γ [c] kN/m³		γ_{sat} kN/m³		q_c [d] [g] MPa		C'_p [g]		C'_s		$C_c/(1+e_0)$ [g] CR [-]		C_o [f] [-]		$C_{sw}/(1+e_0)$ [g] RR [-]		E_{100} [g] [h] MPa		φ' [g] Graden		c' kPa		c_u kPa	
Grind	Zwak siltig	Los	17		19		15		500		∞		0,0046		0		0,0015		45		32,5		0			
		Matig	18		20		25		1000		∞		0,0023		0		0,0008		75		35,0		0		n.v.t.	
		Vast	19	20	21	22	30		1200	1400	∞		0,0019	0,0016	0		0,0006	0,0005	90	105	37,5	40,0	0			
	Sterk siltig	Los	18		20		10		400		∞		0,0058		0		0,0019		30		30,0		0			
		Matig	19		21		15		600		∞		0,0038		0		0,0013		45		32,5		0		n.v.t.	
		Vast	20	21	22	22,5	25		1000	1500	∞		0,0023	0,0015	0		0,0008	0,0005	75	110	35,0	40,0	0			
Zand	Schoon	Los	17		19		5		200		∞		0,0115		0		0,0038		15		30,0		0			
		Matig	18		20		15		600		∞		0,0038		0		0,0013		45		32,5		0		n.v.t.	
		Vast	19	20	21	22	25		1000	1500	∞		0,0023	0,0015	0		0,0008	0,0005	75	110	35,0	40,0	0			
	Zwak siltig, kleiig		18	19	20	21	12		450	650	∞		0,0051	0,0035	0		0,0017	0,0012	35	50	27,0	32,5	0		n.v.t.	
	Sterk siltig, kleiig		18	19	20	21	8		200	400	∞		0,0115	0,0058	0		0,0038	0,0019	15	30	25,0	30,0	0		n.v.t.	
Leem [e]	Zwak zandig	Slap	19		19		1		25		650		0,0920		0,0037		0,0307		2		27,5	30,0	0		50	
		Matig	20		20		2		45		1300		0,0511		0,0020		0,0170		3		27,5	32,5	1		100	
		Vast	21	22	21	22	3		70	100	1900	2500	0,0329	0,0230	0,0013	0,0009	0,0110	0,0077	5	7	27,5	35,0	2,5	3,8	200	300
	Sterk zandig		19	20	19	20	2		45	70	1300	2000	0,0511	0,0329	0,0020	0,0013	0,0170	0,0110	3	5	27,5	35,0	0	1	50	100
Klei	Schoon	Slap	14		14		0,5		7		80		0,3286		0,0131		0,1095		1		17,5		0		25	
		Matig	17		17		1,0		15		160		0,1533		0,0061		0,0511		2		17,5		5		50	
		Vast	19	20	19	20	2,0		25	30	320	500	0,0920	0,0767	0,0037	0,0031	0,0307	0,0256	4	10	17,5	25,0	13	15	100	200
	Zwak zandig	Slap	15		15		0,7		10		110		0,2300		0,0092		0,0767		1,5		22,5		0		40	
		Matig	18		18		1,5		20		240		0,1150		0,0046		0,0383		3		22,5		5		80	
		Vast	20	21	20	21	2,5		30	50	400	600	0,0767	0,0460	0,0031	0,0018	0,0256	0,0153	5	10	22,5	27,5	13	15	120	170
	Sterk zandig	-	18	20	18	20	1,0		25	140	320	1680	0,0920	0,0164	0,0037	0,0007	0,0307	0,0055	2	5	27,5	32,5	0	1	0	10
	Organisch	Slap	13		13		0,2		7,5		30		0,3067		0,0153		0,1022		0,5		15,0		0	1	10	
		Matig	15	16	15	16	0,5		10	15	40	60	0,2300	0,1533	0,0115	0,0077	0,0767	0,0511	1,0	2,0	15,0		0	1	25	30
Veen	Niet voorbelast	Slap	10	12	10	12	0,1		5	7,5	20	30	0,4600	0,3067	0,0230	0,0153	0,1533	0,1022	0,2	0,5	15,0		1	2,5	10	20
	Matig voorbelast	Matig	12	13	12	13	0,2		7,5	10	30	40	0,3067	0,2300	0,0153	0,0115	0,1022	0,0767	0,5	1,0	15,0		2,5	5	20	30
Variatiecoëfficiënt v			0,05				–		0,25										0,10				0,20			

A.2. Structural parameters

The geometries of the various structural elements used in the calculations are shown in the figures below.

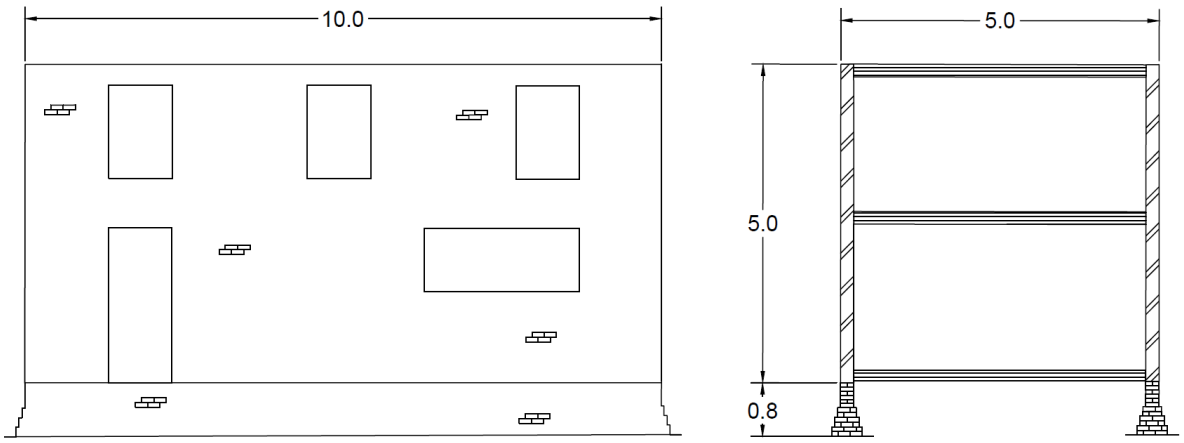

Figure A.1: Geometry of the different elements of the building in [m]

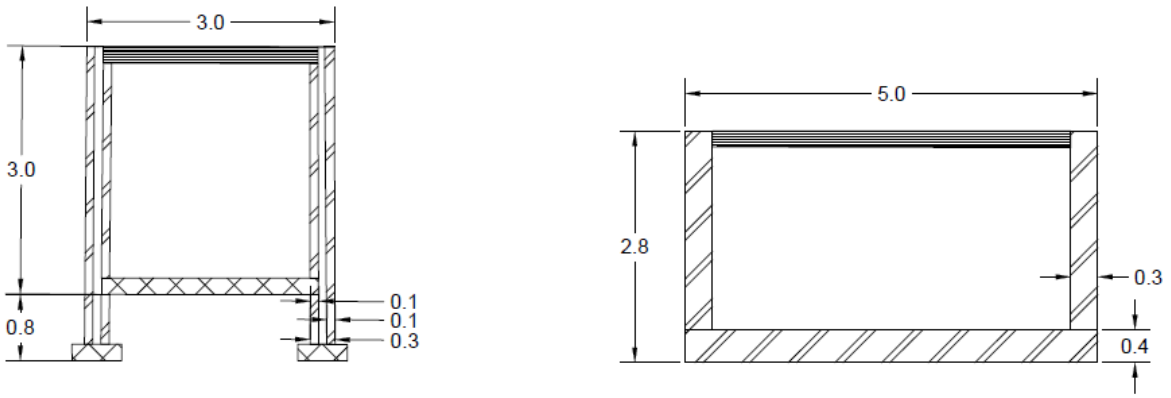

Figure A.2: Geometry of the annex and the basement in [m]

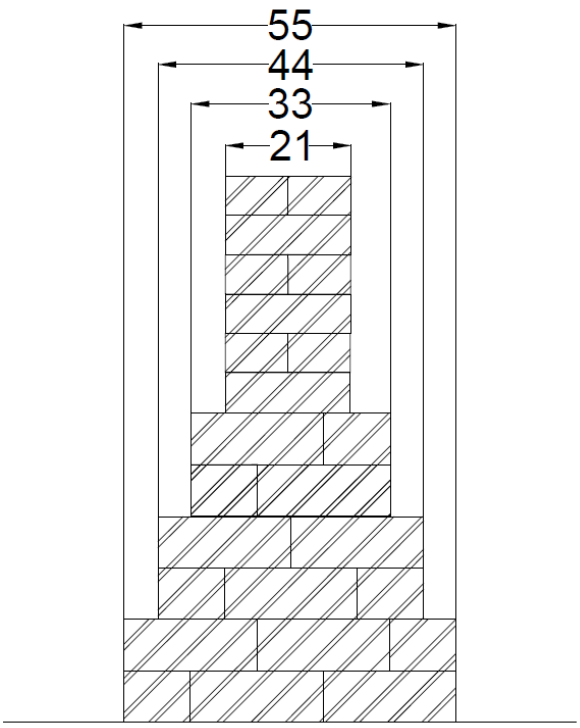

Figure A.3: Stepped brick footing, dimensions in [cm]

A.2.1. Building weight

In the Python script below, the calculation of the weight of the existing building and the annex is shown.

```
############################_Weight building_##########################

#Volumetric weight
m = 19                          #kN/m3 weight masonry
c = 24                          #kN/m3 weight concrete
w = 6                           #kN/m3 weight wood

#Dimensions
t = 0.21                            #thickness wall/floor
l1 =10                              #length wall
h1 = 5.4                            #height wall
b1 = 5

#Calculation
Am = l1 * h1 * t *4                 #m3 masonry
Aw = l1*b1 * t * 3                  #m3 wood 3 floors
Af = ((0.55*0.13+0.44*0.13+0.33*0.13) *
      0.4*(l1+l1+b1+b1))            #m3 foundation masonry strip

roof = 0.75*10 *5                   #kN/m2 dak

T = Am * m + Aw * w +Af * m +roof   #Total weight kN
L = T / l1 / b1                     # Plane strain
print('Total weight existing building [kN] =', T)
print("Lineload existing building [kN/m/m]", L)

wa = (( 6* 3.6 *t*m) + (8.6* t *c) + (2.6 * 2.6 * t*w)+
      (12 * 0.2 * 0.6 * c)) # walls + foundation strip + floor [kN]
print('Total weight annex [kN] == ', wa)
print('Lineload [kN/m/m] annex = ', wa/9)
```

The different elements and the total weight of the existing building and the annex are presented in table A.1 and A.2

Description	Value
Height building	5.0 m
Width building	10.0 m
No. of storeys	1 masonry strip foundation, 3 wooden floors/roof
Foundation	Masonry strip foundation 0.80 m
Walls	Masonry walls with a thickness of 0.21 m
Weight building	22.6 $kN/m/m$

Table A.1: Calculated weight of the building without basement

Description	Value
Height building	3 m
Width building	3 m
No. of storeys	1 concrete strip foundation,1 concrete floor, 1 wooden floor/roof
Foundation	Concrete strip foundation with a thickness of 0.20 m and a width of 0.60 m
Walls	Masonry cavity(0,1 m) walls (2 times 0.10 m) with a thickness of 0.30 m
Weight building	20.0 $kN/m/m$

Table A.2: Calculated weight of the annex

The weight of the basement is not considered. The weight of the removed soil exceeds that of the basement.

A.2.2. Building stiffness

The bending stiffness EI for a foundation can be calculated using formula A.1 in which the Young's modulus (E) is multiplied by the moment of inertia (I)

$$EI = E \cdot \frac{b \cdot h^3}{12} \tag{A.1}$$

The structural elements in the PLAXIS model are divided in three different parts, namely the existing building, a basement and an annex (driver D1) next to the existing building. When each of these elements is applied depends on the different scenarios, see subsection 3.1.4.

Condition of the building

In order to investigate the influence of the building's quality, two different stiffness variants have been considered. A variant where the building is so severely damaged that only the stiffness of the foundation is considered, and a variant where the stiffness of the building is taken into account.

Existing building

Description	Value
Young's modulus, E (masonry strip foundation)	6 GPa
Young's modulus, E (wooden floors) C24	11 GPa
Young's modulus, E (masonry walls)	6 GPa
Moment of inertia, I (masonry strip foundation)	$2 * 0.44/5 * 0.4^3/12 = 1.2 \cdot 10^{-4} m^4/m$
Moment of inertia, I (wooden floors)	$3 * 0.10^3/12 = 2.0 \cdot 10^{-3} m^4/m$
Moment of inertia, I (masonry walls)	$2 * 0.21/5 * 5.4^3/12 = 0.42 m^4/m$
Axial stiffness building, EA	$2.4 \cdot 10^7 kN/m$
Bending stiffness building, EI*	$3.2 \cdot 10^5 kNm^2/m$

Table A.3: Calculated bending stiffness for a negligible damaged existing building (* Including a reduction factor of 0.1 for the openings in the wall (Korff, 2013))

Basement

Description	Value
Young's modulus, E (masonry foundation slab)	6 GPa
Young's modulus, E (masonry walls)	6 GPa
Moment of inertia, I (foundation slab)	$0.4^3/12 = 5.33 \cdot 10^{-3} m^4/m$
Moment of inertia, I (masonry walls)	$2 * 0.33/5 * 2.8^3/12 + 2 * 2.8^3/12 = 44.1 m^4/m$
Axial stiffness, basement vert. plates, EA	$7.1 \cdot 10^6 kN/m$
Axial stiffness, basement hor. plates, EA	$2.4 \cdot 10^7 kN/m$
Bending stiffness basement (walls), EI	$2.3 \cdot 10^7 kNm^2/m$
Bending stiffness basement (footing), EI	$3.2 \cdot 10^5 kNm^2/m$

Table A.4: Calculated bending stiffness basement

Annex (driver D1)

Description	Value
Young's modulus, E (concrete strip foundation)	32 GPa
Young's modulus, E (masonry walls)	6 GPa
Moment of inertia, I (masonry walls)	$4 * 0.10/3 * 3.8^3/12 + 2 * 3.8^3/12 = 9.8 m^4/m$
Moment of inertia, I (concrete strip foundation)	$2 * 0.6/3 * 0.2^3/12 + 0.2^3/12 = 9.3 \cdot 10^{-4} m^4/m$
Axial stiffness annex, EA	$6.4 \cdot 10^6 kN/m$
Bending stiffness annex, EI	$2.1 \cdot 10^4 kNm^2/m$

Table A.5: Calculated bending stiffness annex (driver D1)

```
##############################Weight and Stiffnesses#####################
# Properties
Ec = 32000000   # Young modulus concrete [kPA]
Em = 6000000    # Young modulus masonry [kPA]
Ew = 11000000   #Young modulus masonry wood [kPA]
b = 1           # 1 m for plain strain calculations [m]
d = 0.2         # thickness masonry foundation strip [m]
dc =0.2         #thickness concrete foundation strip [m]
tw = 0.1        # thickness wooden floors [m]
tm = 0.10       # thickness masonry wall existing building [m]
ta = 0.10       # thickness masonry wall annex [m]
tb = 0.21       # thickness masonry wall basement [m]

A = b*d # Area [m2]
I = (b*d**3)/12 #moment of interia of a beam [m4/m]

############################stiffness calculation#################################
##################################################################################

# Bending stiffness existing building
If = (b * d**3)/12              #I4/m plane strain, 1 strip masonry
If2 = (2*0.44/5 * d**3)/12      #I4/m plane strain, 2 stripS masonry foundation
                                #average width strip 0.44m, height 0.40m

Iwo = (b * 2* tw**3)/12         #I4/m plane strain, 2 wooden floors

Iw = 2 * tm/5 * 5**3/12      #I4/m plane strain, 2 walls of 0.21m,
                                #width building 5m, height builing 5 m

print("moment of interia masonry strip [m4/m]", If2)
print("moment of interia masonry walls [m4/m]", Iw)
print("moment of interia woodenfloors [m4/m]", Iwo)

EIf = Em*If2
EImw = Em*Iw
EIwf = Ew*Iwo
print('Bending stiffness masonry strip foundation=',EIf)
print('Bending stiffness masonry walls=',EImw)
print('Bending stiffness wooden floors=',EIwf)

#total Bending stiffness existing building

TB = EIf + EImw + EIwf
#reduction openings one order of magnitude lower
TBr = TB/10
print('Total bending stiffness existing building [kN m2/m] = ', TBr)

# Axial stiffness existing building
Af = 0.55*0.13 +0.44*0.13 +0.33*0.13    # Area stepped brick footing [m2]
Amw = 2*5.4*tm                          # Area masonry walls [m2]
Awf = 3 * 5 * tw                        # Area wooden floors [m2]
TA= Af*Em + Amw*Em + Awf * Ew
print('Total axial stiffness existing building [kN/m] = ', TA)

##################################################################################
# Bending stiffness basement
Ifb = d**3/12
print('Ifb=',Ifb)
Imwb = 2*tb/5 * 2.0**3/12 + 2*2.0**3/12
print('Imwb=',Imwb)


#TBb = Ifb * Em + Imwb * Em
TBb1 = Ifb * Em
TBb2 = Imwb * Em
print('Bending stiffness basement slab [kN m2/m] = ', TBb1)
print('Bending stiffness basement masonry walls[kN m2/m] = ', TBb2)
#print('Total bending stiffness basement [kN m2/m] = ', TBb)

# Axial stiffness basement
Ab = d *b
```

```
Abw = 2 * tb * 2.0

EAb = Ab * Em
EAb2 =Abw *Em
EAbt = EAb + EAb2
print('Axial stiffness basement slab [kN/m] = ', EAb)
print('Axial stiffness basement walls [kN/m] = ', EAb2)
print('Total axial stiffness basement [kN/m] = ', EAbt)
################################################################################
# Bending stiffness annex
#Ifa = 2*0.6/3*dc**3/12 + b*dc**3/12
Ifa = 2*0.6/3*dc**3/12
print('Ifa=',Ifa)
Imwa = 4*ta/3 * 3.8**3/12 + 2*3.8**3/12
print('Imwa=',Imwa)

TBa = (Ifa * Ec + Imwa * Em)/10
print('Total bending stiffness annex [kN m2/m] = ', TBa)

# Axial stiffness annex
Aa = dc * b
Aaw = 2 * ta * 3.8
EAa = Ec * Aa + Em * Aaw
print('Axial stiffness annex [kN/m] = ', EAa)
```

B

Python Script PLAXIS

B.1. Example 1: Reference model

B.1.1. SS1-B1-D2glo.py

```python
from plxscripting.easy import *
import subprocess, time

PLAXIS_PATH = r'C:\Program␣Files\Seequent\PLAXIS␣2D␣2023.2\\Plaxis2DXInput.exe'  # Specify
    PLAXIS path on server.

PORT_i = 10000  # Define a port number.
PORT_o = 10001

PASSWORD = '############'  # Define a password (up to user choice).

subprocess.Popen([PLAXIS_PATH, f'--AppServerPassword={PASSWORD}', f'--AppServerPort={PORT_i}'
    ], shell=False)  # Start the PLAXIS remote scripting service.
time.sleep(5) #Wait for Plaxis to boor before sending commands to the scripting sevice

s_i, g_i = new_server('localhost', PORT_i, password=PASSWORD)

#####Soil geometry###############

exec(open('SS1.py').read())

######Structures
g_i.gotostructures()
exec(open('B1.py').read())

######Mesh
g_i.gotomesh()
g_i.mesh(0.02)

##########################Stages##########################################
##########################################################################
g_i.gotostages()
exec(open('Stages.py').read())

#Activation plates
g_i.Plate_1.activate(g_i.Phases[2])

#Activation Loads
g_i.LineLoad_1.activate(g_i.Phases[0])       # setting initial load
g_i.LineLoad_2.activate(g_i.Phases[0])       # implementation of the driver.
g_i.LineLoad_3.activate(g_i.Phases[0])       # setting initial load
g_i.LineLoad_4.activate(g_i.Phases[0])

g_i.LineLoad_2_1.qy_start[g_i.Phases[2]] = -22.6### AAN of UITZETTEN

# Activation Interfaces
```

```
g_i.NegativeInterface_1.activate(g_i.Phases[2])

# activation of geogrid
g_i.Geogrids.activate(g_i.Phases[0])

############################################################################################
exec(open('D2glo.py').read())
############################################################################################
#Calculate
g_i.calculate()
g_i.view(g_i.Phases[-1])

g_i.save(r'\\SynologyDS220\Studie\Thesis\Engineering\Models\SS1-B1-D2glov2.0.p2dx') #save the program
#
# ##################################Getting results ###################################
# ############################################################################################
#
exec(open('Gathering_results.py').read())
```

B.1.2. SS1.py

```
#Soft Soil model (5)
material1= g_i.soilmat("Identification", "Clay", "SoilModel", 5,'DrainageType',1,
                       "gammaUnsat", 17,"gammaSat", 17,
                        "lambdaModified", 0.1069, "kappaModified",0.02911,
                        "cRef", 5,"phi", 17.5,"psi", 0,
                        'UndrainedNuDefinitionMethod',1,
                        'OCR', 1.3,'PermHorizontalPrimary', 0.0001,'PermVertical', 0.0001)

material2 = g_i.soilmat("Identification", "Sand", "SoilModel", 4,'DrainageType',0,
                        "gammaUnsat", 18,"gammaSat", 20,
                        "E50Ref", 35000,'EOedRef',35000,'EURRef',100000,
                        "cRef", 0.01,'G0Ref',122600,'gamma07',0.00013, "phi", 32.5,"psi", 2.5,
                        'PermHorizontalPrimary', 1, 'PermVertical', 1)


colours = g_i.Colours
material1.setcolour(colours.Green)
material2.setcolour(colours.Yellow)

#####################################################
g_i.gotostructures()

polygon_1 = g_i.polygon((0,-0.8),
                        (100,-0.8),
                        (100, -3.5),
                        (0, -3.5),
                        )
polygon_2 = g_i.polygon((0,-3.5),
                        (100,-3.5),
                        (100, -12),
                        (0, -12),
                        )
polygon_3 = g_i.polygon((0,-12),
                        (100,-12),
                        (100, -20),
                        (0, -20),
                        )

g_i.setmaterial(g_i.Polygon_1.Soil, g_i.Sand)
g_i.setmaterial(g_i.Polygon_2.Soil, g_i.Clay)
g_i.setmaterial(g_i.Polygon_3.Soil, g_i.Sand)

g_i.gotostages()
g_i.Soils.activate(g_i.Phases[0])

#Adding a lineload on surface level to represent the upper part of the soil
g_i.gotostructures()
```

```
lineload1 = g_i.lineload((0, -0.8), (45,-0.8), "qy_start", -14.4)
lineload2 = g_i.lineload((45, -0.8), (55.0,-0.8), "qy_start", -14.4)
lineload3 = g_i.lineload((55.0, -0.8), (58.0,-0.8), "qy_start", -14.4)
lineload4 = g_i.lineload((58.0, -0.8), (100,-0.8), "qy_start", -14.4)
```

B.1.3. B1.py

```
##Structure
line_b1=g_i.line((45,-0.8),(55,-0.8))[-1]

#Plate
material_i = g_i.platemat("Identification", "Footing",
                          "MaterialType", "Elastic",
                          "w",  0,
                          "EA1", 24009600,
                          "EI", 315766,
                            'StructNu',0.2)

plate_g1=g_i.plate(line_b1,'Material',material_i)
#
# #Interface
interface1=g_i.neginterface(line_b1)

#Geogrid

geogrid = g_i.geogridmat("Identification", "Geogrid",
                          "MaterialType", "Elastic",
                          "EA1", 0.1)

line_gg = g_i.geogrid((25,-0.8), (75,-0.8), "Material", geogrid)[-1]
```

B.1.4. Stages.py

```
###############################################################################
phase0_s = g_i.InitialPhase      # Soil geometry only
phase1_s = g_i.phase(phase0_s)   # creep of only the soil of 50 years
phase2_s = g_i.phase(phase1_s)   # constr. phase of the existing building
phase3_s = g_i.phase(phase2_s)   # Cons. phase of existing situation of 70 years
phase4_s = g_i.phase(phase3_s)   # driver implementation
phase5_s = g_i.phase(phase4_s)   # cons. after implem. of driver after 1 year
phase6_s = g_i.phase(phase5_s)   # cons.after implem. of driver after 50 years

#Names of phases
g_i.InitialPhase.Identification = 'Initial␣phase␣A'
g_i.Phase_1.Identification = 'Initial␣phase␣B'
g_i.Phase_2.Identification = 'Construction␣phase'
g_i.Phase_3.Identification= 'Consolidation␣phase␣1'
g_i.Phase_4.Identification = 'Driver␣implementaton'
g_i.Phase_5.Identification = 'Consolidation␣phase␣2'
g_i.Phase_6.Identification = 'Consolidation␣phase␣3'

#Time
g_i.Phase_1.TimeInterval = 1
g_i.Phase_2.TimeInterval = 10
g_i.Phase_3.TimeInterval = 25550
g_i.Phase_4.TimeInterval = 10
g_i.Phase_5.TimeInterval = 365
g_i.Phase_6.TimeInterval = 18250

#Calculation type
g_i.Phase_5.DeformCalcType = 'Consolidation'
g_i.Phase_6.DeformCalcType = 'Consolidation'

# Ignore undrained behaviour in the phases until the construction phase
# of the existing building

g_i.Phase_1.Deform.IgnoreUndrainedBehaviour= True
g_i.Phase_2.Deform.IgnoreUndrainedBehaviour = True
g_i.Phase_3.Deform.IgnoreUndrainedBehaviour = True
```

```

# Reset the displacements in the phases until the construction phase
# of the existing building

g_i.Phase_1.Deform.ResetDisplacementsToZero = True
g_i.Phase_2.Deform.ResetDisplacementsToZero = True
g_i.Phase_3.Deform.ResetDisplacementsToZero = True


#Boundary conditions
for i in range(0,len(g_i.Phases)):
    g_i.GroundwaterFlow.BoundaryXMin[g_i.Phases[i]] = "Closed"
    g_i.GroundwaterFlow.BoundaryXMax[g_i.Phases[i]] = "Closed"
    g_i.GroundwaterFlow.BoundaryYMin[g_i.Phases[i]] = "Open"
    g_i.GroundwaterFlow.BoundaryYMax[g_i.Phases[i]] = "Open"
```

B.1.5. D2glo.py

```
#implementing an global waterlevel lowering as driver
g_i.gotoflow()
waterlevel_s1 = g_i.waterlevel((0, -0.8), (100, -0.8))
#waterlevel_s2 = g_i.waterlevel((0, -2.8), (100, -2.8))
#waterlevel_s3 = g_i.waterlevel((0, -3.8), (100, -3.8))
#waterlevel_s4 = g_i.waterlevel((0, -4.8), (100, -4.8))
waterlevel_s5 = g_i.waterlevel((0, -5.8), (100, -5.8))

g_i.setglobalwaterlevel(waterlevel_s1, g_i.Phases[0])
#g_i.setglobalwaterlevel(waterlevel_s2, g_i.Phases[4])
#g_i.setglobalwaterlevel(waterlevel_s3, g_i.Phases[4])
#g_i.setglobalwaterlevel(waterlevel_s4, g_i.Phases[4])
g_i.setglobalwaterlevel(waterlevel_s5, g_i.Phases[4])
```

B.1.6. Gathering-results.py

```
def footing_end_points(x1, y1, x2, y2):

    p_1 = [x1, y1]
    p_2 = [x2, y2]

    l_dis = math.sqrt((p_1[0] - p_2[0]) ** 2 + (p_1[1] - p_2[1]) ** 2)

    return p_1, p_2, l_dis

def list_nodes(p_1, p_2, n):
    x_ = []
    y_ = []

    if p_1[0] == p_2[0] or p_1[1] == p_2[1]:
        for i in range(n + 1):
            if p_1[0] == p_2[0]:
                x_.append(p_1[0])
                pass

            else:
                x0 = p_1[0]
                x1 = p_2[0]

                # X coordinate of xi
                xi = x0 + i * (1 / n) * (x1 - x0)
                x_.append(xi)

            if p_1[1] == p_2[1]:
                y_.append(p_1[1])
                pass

            else:
                y0 = p_1[1]
                y1 = p_2[1]

```

```
                # Y coordinate of yi
                yi = y0 + i * 1 / n * (y1 - y0)
                y_.append(yi)
    else:
        print("Please␣re-enter␣coordinates")
    return x_, y_

def geogrid(x_, y_, phase, n):

    uy_geogrid=[]
    ux_geogrid=[]

    # Get phase for output
    phase_name = "Phase_" + str(phase)

    phase_out_put = []
    for phase in g_o.Phases:
        if phase_name == str(phase.Name):
            phase_out_put.append(phase)

    # Gives the result at specified coordinates
    for i in range(n + 1):

        uy_geogrid_i = g_o.getsingleresult(phase_out_put[0], g_o.ResultTypes.Geogrid.Uy, (x_[
            i], y_[i]))
        ux_geogrid_i = g_o.getsingleresult(phase_out_put[0], g_o.ResultTypes.Geogrid.Ux, (x_[
            i], y_[i]))

        uy_geogrid.append(uy_geogrid_i)
        ux_geogrid.append(ux_geogrid_i)
    return uy_geogrid, ux_geogrid

def transformation_footing_displacement_coordinates(x_, uy):

    l_dis = math.sqrt((x_[-1] - x_[0])**2 + (uy[-1] - uy[0])**2)

    h = x_[0]
    k = uy[0]

    u_ = []
    v_ = []

    for i in range(len(x_)):
        # Translation and Rotation of origin
        v_y = uy[-1] - uy[0]

        tan_alpha = v_y/l_dis

        alpha_rad = math.atan(tan_alpha)

        sin_alpha = math.sin(alpha_rad)
        cos_alpha = math.cos(alpha_rad)

        x_2 = (x_[i] - h) * cos_alpha + (uy[i] - k) * sin_alpha
        y_2 = - (x_[i] - h) * sin_alpha + (uy[i] - k) * cos_alpha

        u_.append(round(x_2, 8))
        v_.append(round(y_2, 8))

    return u_, v_, l_dis

def u_y_origin(n):
    u_y_origin = []

    for i in range(n + 1):
        uy_o = i * 0
        u_y_origin.append(uy_o)

    return u_y_origin
def print_uy(x_,uy_geogrid, ux_geogrid):
    filename = easygui.enterbox("Enter␣the␣name␣under␣which␣you␣want␣to␣save␣the␣file:␣")
```

```
105     filepath = (r'\\SynologyDS220\Studie\Thesis\Engineering\Results\Greenfield\SS1\{}.txt'.
            format(filename))
106 
107     with open(filepath, "w") as file:
108         # Iterate over the list of floats
109         for number in x_, uy_geogrid, ux_geogrid:
110             # Convert float to string and write to the file
111             file.write(str(number) + '\n')
112 
113 def main():
114     x1, y1, x2, y2, phase, n = 25, -0.8, 75, -0.8, 6, 1000
115     p_1, p_2, l_dis = footing_end_points(x1, y1, x2, y2)
116     x_, y_ = list_nodes(p_1, p_2, n)
117     uy_geogrid, ux_geogrid = geogrid(x_, y_, phase, n)
118     print_uy(x_,uy_geogrid, ux_geogrid)
119 main()
```

B.2. Example 2: Basement + Annex, SS1-B2-D1.py

B.2.1. SS1-B2-D1.py

```
from plxscripting.easy import *
import subprocess, time

PLAXIS_PATH = r'C:\Program␣Files\Seequent\PLAXIS␣2D␣2023.2\\Plaxis2DXInput.exe'

PORT_i = 10000  # Define a port number.
PORT_o = 10001

PASSWORD = '##########$'  # Define a password (up to user choice).

subprocess.Popen([PLAXIS_PATH, f'--AppServerPassword={PASSWORD}', f'--AppServerPort={PORT_i}'
    ], shell=False)
time.sleep(5) #Wait for Plaxis to boor before sending commands to the scripting sevice

s_i, g_i = new_server('localhost', PORT_i, password=PASSWORD)

#####Soil geometry###############

exec(open('SS1.py').read())

######Structures
g_i.gotostructures()
exec(open('B2.py').read())

#Driver
exec(open('D1_B.py').read())

######Mesh
g_i.gotomesh()
g_i.mesh(0.03)

##########################Stages##########################################
###########################################################################
g_i.gotostages()
exec(open('Stages.py').read())
###########################################################################
#Activation plates
g_i.Plate_1.activate(g_i.Phases[2])
g_i.Plate_2.activate(g_i.Phases[2])
g_i.Plate_3.activate(g_i.Phases[2])
g_i.Plate_4.activate(g_i.Phases[2])
g_i.Plate_5.activate(g_i.Phases[2])
g_i.Plate_6.activate(g_i.Phases[4])

#Activation Loads
g_i.LineLoad_1.activate(g_i.Phases[0])       # setting initial load
g_i.LineLoad_2.activate(g_i.Phases[0])       # implementation of the driver.
g_i.LineLoad_3.activate(g_i.Phases[0])       # setting initial load
g_i.LineLoad_4.activate(g_i.Phases[0])

g_i.LineLoad_2_1.qy_start[g_i.Phases[2]] = -22.6
g_i.LineLoad_2_2.qy_start[g_i.Phases[2]] = -22.6

g_i.Polygon_1_1.deactivate(g_i.Phases[2])

g_i.LineLoad_3_1.qy_start[g_i.Phases[4]] = -20#16.4, 18.2, 20
#Activation Interfaces
g_i.NegativeInterface_1.activate(g_i.Phases[2])
g_i.NegativeInterface_2.activate(g_i.Phases[2])
g_i.NegativeInterface_3.activate(g_i.Phases[2])
g_i.PositiveInterface_1.activate(g_i.Phases[2])
g_i.NegativeInterface_4.activate(g_i.Phases[4])

# activation of connection
g_i.Connection_1_1.activate(g_i.Phases[2])
g_i.Connection_2_1.activate(g_i.Phases[2])
g_i.Connection_3_1.activate(g_i.Phases[4])
```

```

# activation of geogrid
g_i.Geogrids.activate(g_i.Phases[0])

##############################################################################################
#Calculate
g_i.calculate()
g_i.view(g_i.Phases[-1])

g_i.save(r'\\SynologyDS220\Studie\Thesis\Engineering\Models\SS1-B2-D1v2.0.p2dx') #save the
    program

################################Getting results ##################################
###########################################################################
exec(open('Gathering_results.py').read())
```

B.2.2. B2.py

```
##Structure
line_b2_1=g_i.line((45,-2.8),(50,-2.8))[-1] #m i2
line_b2_2=g_i.line((45,-0.8),(45,-2.8))[-1] #m i2
line_b2_3=g_i.line((50,-0.8),(55,-0.8))[-1] #m i1
line_b2_4=g_i.line((50,-0.8),(50,-2.8))[-1] #m i2
line_b2_5=g_i.line((45,-0.8),(50,-0.8))[-1] #m i1

#Plate
material_i = g_i.platemat("Identification", "Footing",
                          "MaterialType", "Elastic",
                          "w",  0,
                          "EA1", 2.4E7,
                          "EI", 3.2E5,
                            'StructNu',0.2)

material_i2 = g_i.platemat("Identification", "Footing-basement", # Plates basement
                          "MaterialType", "Elastic",
                          "w", 0,
                          "EA1", 2.4E7, # 2400000
                          "EI",3.2E5, # 32000
                           'StructNu', 0.2)

material_i3 = g_i.platemat("Identification", "walls-basement", # Walls basement
                          "MaterialType", "Elastic",
                          "w", 0,
                          "EA1", 7056000, # 7056000
                          "EI",22873983, # 22873983
                           'StructNu', 0.2)

plate_g1=g_i.plate(line_b2_1,'Material',material_i2)
plate_g2=g_i.plate(line_b2_2,'Material',material_i3)
plate_g3=g_i.plate(line_b2_3,'Material',material_i)
plate_g4=g_i.plate(line_b2_4,'Material',material_i3)
plate_g5=g_i.plate(line_b2_5,'Material',material_i)

#Interface
interface1=g_i.neginterface(line_b2_1)
interface2=g_i.neginterface(line_b2_2)
interface3=g_i.neginterface(line_b2_3)
interface4=g_i.posinterface(line_b2_4)

#Connections
connection=g_i.connection(g_i.Plate_2,g_i.Plate_5)
g_i.Connection_1.Rotation = "Free"
connection=g_i.connection(g_i.Plate_4,g_i.Plate_5)
g_i.Connection_2.Rotation = "Free"


#Geogrid
geogrid = g_i.geogridmat("Identification", "Geogrid",
                          "MaterialType", "Elastic",
```

```
                            "EA1", 0.1)

line_gg = g_i.geogrid((25,-0.8), (75,-0.8), "Material", geogrid)[-1]
```

B.2.3. D1-B.py

```
#Additional load as driver#
line_d1=g_i.line((55.0,-0.8),(58.0,-0.8))[-1]

#Plate
material_i = g_i.platemat("Identification", "Footing",
                            "MaterialType", "Elastic",
                            "w", 0,
                            "EA1", 6400000,
                            "EI", 21333,
                            'StructNu',0.2)

plate_g2=g_i.plate(line_d1,'Material',material_i)


#Interface
interface6=g_i.neginterface(line_d1)

#Connections
connection=g_i.connection(g_i.Plate_3,g_i.Plate_6)
g_i.Connection_3.Rotation = "Free"

#Waterlevel
##Groundwater
g_i.gotoflow()
waterlevel_s1 = g_i.waterlevel((0, -0.8), (100, -0.8))

for i in range(0,len(g_i.Phases)):
    g_i.setglobalwaterlevel(waterlevel_s1, g_i.Phases[i])
```

C

Damage Analysis

The damage parameters have been determined based on the numerically calculated settlements in PLAXIS. The formulas used in the post-processing phase are presented in section C.1, C.2 and C.3. Figure C.1 provides a visual representation of the various damage parameters, including differential settlement ($\delta\rho_{max}$), horizontal strain(ϵ_{hor}), and angular distortion (β_{max}), which have been considered in this thesis.

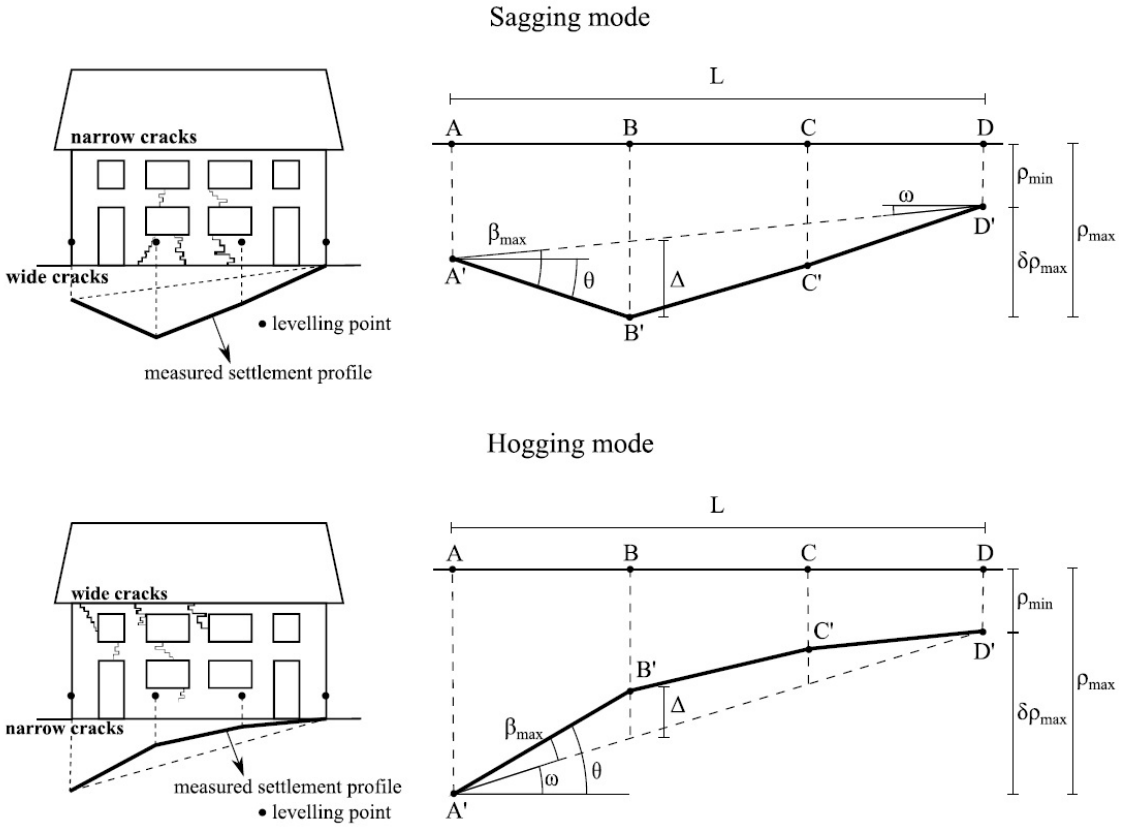

Figure C.1: Definitions for the deformation of foundations
(Prosperi, Korswagen, et al., 2023)

C.1. Differential settlement

See below for the formula and the script used in the post-processing phase for determining the differential settlement.

$$\delta\rho_{max} = u_{y,max} - u_{y,min} \tag{C.1}$$

```
def calculate_diff(uy_data_list):
    diffl = []
    for uy_data in uy_data_list:
        diff = abs(max(uy_data) - min(uy_data))
        diffl.append(diff)
    return diffl
```

C.2. Horizontal strain

See below for the formula and the script used in the post-processing phase for determining the horizontal strain.

$$\epsilon_{hor} = \frac{\Delta L}{L} \tag{C.2}$$

```
def horizontal_strain(ux_plate, x_plate):
    eps = []
    for i in range(len(x_plate)-1):
        eps_i = (ux_plate[i + 1] - ux_plate[i]) / abs((x_plate[i + 1] - x_plate[i]) / (len(
            x_plate)-1)) * 1000
        eps.append(eps_i)
    eps_max = max(eps)
    eps_h_ave = (ux_plate[-1] - ux_plate[0]) / (x_plate[-1] - x_plate[0]) * 1000

    return eps_max, eps_h_ave
```

C.3. Angular distortion

See below for the formula and the script used in the post-processing phase for determining the angular distortion.

$$\beta_{max} = \frac{\Delta u_y}{\Delta u_x} - \omega \tag{C.3}$$

```python
import matplotlib.pyplot as plt
import numpy as np

def calculate_beta(x, y, showplot=False):

    x = np.array(x).reshape(-1)
    y = np.array(y).reshape(-1)
    rot = np.diff(y) / np.diff(x)
    omega = (y[-1] - y[0]) / abs(x[-1] - x[0])
    y_omega = omega * x + y[0]

    ang = rot - omega
    ang_max = np.max(np.abs(ang))
    #print(ang_max)

    if showplot:
        fig, ax1 = plt.subplots()
        ax1.plot(x, y, color='black', label='Settlement contour')
        ax1.plot(x, y_omega, color='#5D3A9B', label='Tilt')
        ax2 = ax1.twinx()
        ax2.plot(x[1:], rot, color='#5B8081', label='Rotation')
        ax2.plot(x[1:], ang, color='#E66100', label='Angular distortion')
        ax1.legend(loc='upper left', bbox_to_anchor=(0.5, 1.15))
        ax2.legend(loc='upper right', bbox_to_anchor=(0.5, 1.15))

        plt.tight_layout(rect=[0, 0, 1, 1])
        plt.show()

    return ang_max
```